

“A Lysozyme and Magnetic Beads Based Method for Separation and Detection of Bacteria”

zur Erlangung des akademischen Grades eines

DOKTORS DER INGENIEURWISSENSCHAFTEN (Dr.-Ing.)

Fakultät für Chemieingenieurwesen und Verfahrenstechnik des
Karlsruher Institut für Technologie (KIT)

genehmigte

DISSERTATION

von

Dipl.-Biol. (t.o.) Ebru Diler

geboren am 28.04.1982 in Öhringen

Referent: Prof. Dr. Ursula Obst

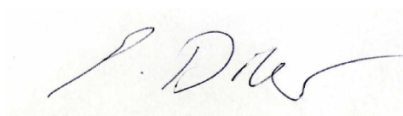
Korreferent: Prof. Dr. Christoph Syldatk

Tag der mündlichen Prüfung: 21.10.2013

Erklärung

Ich versichere, dass die hier vorliegende Dissertation mit dem eingereichten und genehmigten Prüfexemplar der Doktorarbeit übereinstimmt.

Homburg, den 13.11.2013

A handwritten signature in black ink, appearing to read 'E. Diler', written over a horizontal line.

(Ebru Diler)

Danksagung

Prof. Dr. Ursula Obst danke ich herzlich für die Übernahme des Gutachtens, Aufnahme in ihr Labor und für die konstruktiven Diskussionen.

Prof. Dr. Christoph Syldatk danke ich für die Begutachtung dieser Arbeit als Korreferent.

Dr. Thomas Schwartz danke ich für die Überlassung des Themas, für die Unterstützung, fachlichen Diskussionen und Ratschläge während der experimentellen Phase und für das Korrekturlesen der schriftlichen Ausarbeitung.

Prof. Dr. Katja Schmitz danke ich für die Unterstützung während der experimentellen Durchführung dieser Arbeit.

Caroline Bauch und Samuel Huber danke ich für ihre Beiträge zu dieser Arbeit, die sie während des Praxissemesters und im Rahmen der Studienarbeit geleistet haben.

Allen Mitarbeitern der Abteilungen Mikrobiologie an natürlichen und technischen Grenzflächen und Prozesstechnik partikelbasierter Grenzflächen danke ich für die schöne Arbeitsatmosphäre und für die Hilfsbereitschaft. Besonders Thomas Teutenberg, dem mein zusätzlicher Dank für Korrekturvorschläge zur schriftlichen Ausarbeitung dieser Arbeit gilt, Dana Wiese, Christine Müller, Mareike Marten, Silke Kirchen, Dr. Gerald Brenner-Weiß.

Dorothea Helmer, Miray Emreol und Hasan Arslan danke ich für ihre Freundschaft und Ermutigungen während fachlicher und privater Tiefpunkte.

Ingo Fischer danke ich für seine Unterstützung und für das Korrekturlesen.

Meinen Eltern Fatma Adali und Hüseyin Erdönmez, meiner Schwester Ahu Erdönmez, meiner Familie und Seref Diler danke ich für die liebevolle Unterstützung und Verständnis während des Studiums und während der Entstehung dieser Doktorarbeit.

Abstract

The control of contamination in food production and in drinking water conditioning is an essential task to maintain public health, especially considering that food and drinking water are possible targets for bioterrorism. Standard cultivation based pathogen detection methods fail in some circumstances, as it was the case in 2011 with EHEC outbreak in Germany. Therefore, techniques directly targeting the nucleic acids of pathogens and, thus, avoiding the disadvantages of conventional cultivation based detection methods came into focus. These methods require the concentration of bacteria present in tap water or their separation from food matrices without accumulation of components that would interfere with the detection system.

In the course of this project a method for the specific separation of bacteria from complex matrices or for their enrichment from liquids for a subsequent detection and quantification by quantitative PCR was developed. The separation method is based on μ -scaled magnetic beads, which are functionalized with recombinantly expressed wild-type or mutated lysozymes and can be easily separated by an external magnetic field. The recombinant proteins provide specific capture of bacteria based on their ability to bind to the peptidoglycan cell wall components. Using this set-up, the capture of a broad range of species is possible. Therefore, this method is superior to immunomagnetic separation (IMS), where only particular bacteria are separated based on surface antigen-antibody interactions.

In its native form, lysozyme causes bacteriolysis due to the catalytic amino acid glutamic acid 35, which is localized in the binding cleft. This undesired bacteriolytic property was eliminated by the exchange of glutamic acid 35 by glutamine (LysE35Q) and alanine (LysE35A) via site-directed overlap connection PCR. The mutated fragments were cloned into the *Pichia pastoris* expression vector pPic9. The subsequent expression of the recombinant lysozymes in *P. pastoris* strain GS115 yielded in the expression of up to 30 mg l⁻¹ mutated lysozyme and wild-type lysozyme.

The purification of the recombinant proteins from the expression broth was performed by adsorption of the lysozymes to nano-scaled magnetic cation exchange particles. The binding properties of the magnetic particles were determined by means of Langmuir

analysis: The maximum adsorption of commercial hen egg white lysozyme onto the ion exchanger particles was determined to 64.4 mg g^{-1} for single component adsorption from phosphate buffer with neutral pH, $254 \text{ } \mu\text{g g}^{-1}$ for the adsorption of recombinantly expressed wild-type lysozyme in alkaline expression broth, and $751 \text{ } \mu\text{g g}^{-1}$ for adsorption of mutated lysozyme in alkaline expression broth.

The residual bacteriolytic activity of the purified recombinant lysozymes was investigated by means of a turbidity assay. Using this assay it was shown that the lysis activity of the mutated lysozymes was diminished, while the recombinant wild-type lysozyme was still active. Lysozymes were immobilized on μ -scaled commercial streptavidin-functionalized magnetic beads. These beads were subsequently used for the capture of *Enterococcus faecalis* cells from bacteria suspension and from artificially contaminated food. Two analytical procedures for the investigation of the capture efficiency of the magnetic beads were compared: Real-Time PCR (RT-PCR) and cultivation based bacteria quantification. RT-PCR turned out to be more reliable, therefore, the capture efficiency of the beads was consequently determined in this way.

The standardisation of the capture procedure to $1 \text{ } \mu\text{g}$ magnetic beads revealed a capture of $2053 \text{ cells } \mu\text{g}^{-1} \text{ ml}^{-1}$ from bacteria suspension achieved with Dynabeads® Myone™ C1 Streptavidin, which was functionalized with mutated lysozyme (LysE35Q). The unfunctionalized beads did not capture bacteria.

Up to 70% of the initial *E. faecalis* were captured from a suspension with a concentration of 10 cells ml^{-1} . 86.6% of the bacteria were recovered from a suspension with an initial *E. faecalis* amount of $4.6 \times 10^4 \text{ cells ml}^{-1}$ using mutated lysozyme functionalized Dynabeads® Streptavidin M 270. The unspecific capture with unfunctionalized beads was 2.8%.

The bacteria recovery from artificially contaminated food with $5.5 \times 10^4 \text{ cells ml}^{-1}$ resulted in a maximum recovery of 94.6% with Dynabeads® MyOne™ C1 Streptavidin beads functionalized with mutated lysozyme, whereas the lysozyme-independent adsorption of bacteria onto unfunctionalized beads was 14.9%. The functionalized M-PVA SAV2 beads could capture 57.7% of the initial bacteria amount ($6.7 \text{ cells } \mu\text{g}^{-1} \text{ ml}^{-1}$), whereas unfunctionalized beads did not capture a detectable cell amount.

Abstract

In summary, the mutated lysozyme functionalized magnetic beads were successful in high and specific recovery of bacteria from *E. faecalis* suspensions and artificially contaminated food matrix.

Zusammenfassung

Um die Gesundheit der Bevölkerung nicht zu gefährden, ist die regelmäßige Kontaminationskontrolle der Lebensmittelproduktion und der Trinkwasseraufbereitung unverzichtbar, besonders, da Trinkwasser und Lebensmittel jederzeit ein Angriffsziel für Bioterror sein können. Die Detektion der Bakterien durch standardisierte Methoden basiert auf Kultivierung der Bakterien. In manchen Fällen erwiesen sich diese Methoden jedoch als ungenügend, beispielsweise beim EHEC Ausbruch im Jahr 2011 in Deutschland. Daher rücken kultivierungsunabhängige Methoden, die auf der Detektion der bakteriellen Nukleinsäuren basieren, immer mehr in den Fokus. Diese Methoden vermeiden die Nachteile, die kultivierungsbasierte Methoden mit sich bringen, erfordern aber eine Anreicherung der Bakterien aus dem Trinkwasser oder ihre Separation aus der Lebensmittelmatrix ohne dabei Komponenten zu konzentrieren, die die Detektionsmethoden inhibieren können.

In Rahmen dieses Projektes wurde eine Methode zur Separation von Bakterien aus komplexen Matrizen und zur Anreicherung aus Flüssigkeiten entwickelt, die eine anschließende Detektion durch Quantitative PCR ermöglicht. Die Methode basiert auf magnetischen Mikropartikeln, die mit rekombinantem Wildtyp- und Mutanten-Lysozym funktionalisiert sind und sich durch ein externes Magnetfeld leicht separieren lassen. Die rekombinanten Proteine ermöglichen eine spezifische, auf der Wechselwirkung von Lysozym und Peptidoglykan beruhende, Bindung der Partikel an die Bakterien. Durch die Verwendung von Lysozym als funktionellen Liganden ist die Erfassung einer breiteren Bakterienpopulation möglich. Demgegenüber basiert die Methode der Immunomagnetischen Separation (IMS) auf der Funktionalisierung mit Antikörpern, die gegen Oberflächenantigene bestimmter Spezies gerichtet sind. IMS ermöglicht somit nur eine Spezies-spezifische Separation.

In ihrer nativen Form katalysieren Lysozyme die Bakteriolyse, was durch die Aminosäure Glutaminsäure 35, die in der Bindungsstelle des Lysozyms lokalisiert ist, erfolgt. Ein Austausch dieser katalytischen Aminosäure durch Glutamin und Alanin mittels gerichteter, PCR basierender Mutagenese, führte zur Elimination dieser unerwünschten Eigenschaft. Die mutierten Proteine wurden in *Pichia pastoris* exprimiert, was nach Optimierung der Expressionsbedingungen eine Lysozymausbeute von bis zu 30 mg l⁻¹ führte.

Die Aufreinigung der rekombinant exprimierten Lysozyme aus dem Expressionsmedium erfolgte durch den Einsatz von magnetischen Kationenaustauscher Nanopartikel. Die Bindeeigenschaften wurden durch Lagmuiranalyse ermittelt: Einstoffadsorption von kommerziellem Wildtyp-Hühnereiweiß-Lysozym aus pH- neutralem Phosphatpuffer resultierte in einer maximalen Bindekapazität von $65,5 \text{ mg g}^{-1}$. Die Adsorption an die Partikel von rekombinant exprimiertem Wildtyp-Lysozym und mutiertem Lysozym in alkalischem Expressionsmedium ergab jeweils maximale Bindekapazitäten von $254 \text{ } \mu\text{g g}^{-1}$ und $751 \text{ } \mu\text{g g}^{-1}$.

Die bakteriolytische Aktivität der aufgereinigten Enzyme wurde durch einen turbidimetrischen Aktivitätstest bestimmt. Dieser zeigte, dass die mutierten Lysozyme, wie gewünscht, nicht mehr aktiv waren, während das rekombinante Wildtyp-Lysozym weiterhin bakteriolytisch aktiv war. Über Biotin-Streptavidin Bindungen wurden die Lysozyme auf kommerzielle, magnetische Mikropartikel immobilisiert. Die Partikel wurden für die Anreicherung von *Enterococcus faecalis* aus Suspensionen und zur Separation der Bakterien aus künstlich kontaminierten Lebensmitteln eingesetzt. Für die anschließende Analyse wurden zwei Quantifizierungsmethoden getestet: Real-Time PCR (RT-PCR) und Quantifizierung durch Kultivierung. Die Ergebnisse der RT-PCR erwiesen sich als zuverlässigere Methode und wurden aus diesem Grund zur Beurteilung der spezifischen Bakterienseparationseffizienz der magnetischen Partikel herangezogen.

Die Normierung der angereicherten Zellen aus Bakteriensuspension auf $1 \text{ } \mu\text{g}$ Magnetpartikel ergab, dass die höchste Anreicherungsrate mit $2053 \text{ Zellen } \mu\text{g}^{-1} \text{ ml}^{-1}$ von Dynabeads® Myone™ C1 Streptavidin Partikel erzielt wurde, die mit mutiertem Lysozym (LysE35Q) funktionalisiert wurden. Durch die reinen Basispartikel, ohne Lysozymfunktionalisierung, wurde hingegen keine detektierbare Menge an Zellen gebunden.

Von den eingesetzten magnetischen Partikeln konnten mittels Dynabeads® Streptavidin M270, die mit mutiertem Lysozym (LysE35Q) funktionalisiert wurden, 70% der Bakterien aus einer Suspension mit 10 Zellen pro ml und 86.6% der Zellen aus einer Suspension mit 4.6×10^4 Zellen pro ml angereichert werden. Durch unfunktionalisierte Partikel wurden hingegen 2.8% der Bakterien angereichert.

Durch Dynabeads® Myone™ C1 Streptavidin Partikel, die mit mutiertem Lysozym funktionalisiert wurden, konnten 94.6% (104 Zellen $\mu\text{g}^{-1} \text{ml}^{-1}$) aus einer mit $5,5 \times 10^4 \text{ml}^{-1}$ *E. faecalis* kontaminierten Lebensmittelprobe angereichert werden. Der Betrag der unspezifischen Separation ergab sich zu 14.9% (16 Zellen $\mu\text{g}^{-1} \text{ml}^{-1}$).

Mit M-PVA SAV2 Partikeln konnte eine spezifische Separation von 57.7% aus 5.8×10^3 Zellen ($6.7 \text{ Zellen } \mu\text{g}^{-1} \text{ml}^{-1}$) aus der Lebensmittelmatrix erzielt werden, wohingegen durch unfunktionalisierte Partikel keine Bakterien von der Matrix abgetrennt wurden.

Zusammenfassend konnte gezeigt werden, dass die im Rahmen dieses Projektes entwickelte Methode zur spezifischen Anreicherung von Bakterien aus Suspensionen und zur Separation von Bakterien aus komplexen Matrizen erfolgreich war.

Abbreviations

cDNA	Complementary Desoxyribonucleic acid
CFU	Colony forming unit
CVIA	Tetrapeptide consisting of cysteine, valine, isoleucine, and alanine
DMS C1	Dynabeads® MyOne™ Streptavidin C1
DMS T1	Dynabeads® MyOne™ Streptavidin T1
DS M270	Dynabeads® M270 Streptavidin
DS M280	Dynabeads® M280 Streptavidin
EDTA	Ethylenediaminetetraacetic acid
EHEC	Enterohemorrhagic <i>Escherichia coli</i>
HACCP	Hazard Analysis and Critical Control Points
HEWL	Hen Egg White Lysozyme
HGMF	High gradient magnetic fishing
IMS	Immunomagnetic separation
LysE35A	Lysozyme with glutamic acid exchange by alanine
LysE35Q	Lysozyme with glutamic acid exchange by glutamine
Lyswt	Wild-type lysozyme (recombinant expression)

Abbreviations

MCS	Multiple Cloning Site
PVDF	Polyvinylidene fluoride
qPCR	Quantitative Polymerase Chain Reaction
RT-PCR	Real Time Polymerase Chain Reaction
VBNC	Viable but non-cultivable

Contents

1	Introduction	1
1.1	Motivation and objectives.....	1
1.2	Emerging pathogens in distribution systems as source for contamination of drinking water and food	2
1.3	Detection and quantification of bacteria	4
1.3.1	Culture-dependent detection: bacteria plate count	4
1.3.2	Culture-independent techniques.....	6
1.3.2.1	Quantitative polymerase chain reaction (qPCR) in pathogen detection.....	7
1.3.2.2	Other rapid detection techniques.....	11
1.3.2.3	Denaturing gradient gel electrophoresis (DGGE).....	11
1.4	Bacterial Separation from Complex Sample Matrices.....	13
1.4.1	Methods of bacterial separation and concentration	13
1.4.2	Immunomagnetic Separation of Bacteria from Complex Matrices.....	14
1.5	Protein family of lysozymes and the lytic properties	17
1.6	<i>Pichia pastoris</i> : An expression organism for proteins with eukaryotic origin	18
1.7	Protein purification after recombinant expression	20
1.8	Aim of the study	25
2	Material and Methods.....	29
2.1	Materials.....	29
2.2	Strains.....	31
2.3	Plasmids	32
2.4	Methods.....	32
2.4.1	Creation of heat shock competent E. coli DH5 α cells.....	32
2.4.2	Transformation of DH5 α cells with plasmids.....	32
2.4.3	PCR-site directed mutagenesis and molecular cloning	33
2.4.4	Isolation of plasmids from DH5 α cells.....	35
2.4.5	DNA isolation from agarose gels.....	35
2.4.6	DNA sequencing.....	35
2.4.7	Transformation of P. pastoris cells	35
2.4.8	Protein expression in GS115 cells and purification with MagPrepSO ₃	36
2.4.9	Determination of adsorption isotherm for protein purification	37
2.4.10	Protein analysis	38

Contents

2.4.11	Determination of protein amount	39
2.4.12	Lysozyme activity assay	40
2.4.13	Immobilization of lysozyme on magnetic beads	40
2.4.14	Fluorescence microscopy based capture detection	41
2.4.15	Efficiency determination of magnetic beads based bacteria capture	41
2.4.16	Quantitative PCR.....	42
3	Results	45
3.1	Overview of the results chapter	45
3.2	Site directed mutagenesis and cloning	48
3.2.1	Site directed mutation into lysozyme cDNA	49
3.2.2	Cloning of wild-type and mutated lysozyme cDNAs into expression vector pPic9	51
3.2.3	Summary of chapter 3.2	54
3.3	Transformation of <i>Pichia pastoris</i> with lysozyme cDNA and protein expression	55
3.3.1	Transformation of <i>P. pastoris</i> GS115 strain	55
3.3.2	Expression analysis of recombinant lysozyme	57
3.3.3	Summary of chapter 3.3	60
3.4	Protein purification	61
3.4.1	Adjustment of cell free expression broth to higher pH values	61
3.4.2	Purification of recombinant lysozyme with MagPrepSO ₃ from expression broths	62
3.4.3	Adsorption isotherm of nano-scaled MagPrepSO ₃ for recombinant lysozyme	65
3.4.4	Lysozyme purification from <i>P. pastoris</i> cell extracts with MagPrepSO ₃	67
3.4.5	Summary of chapter 3.4	69
3.5	Enzymatic activities of mutated and wild-type lysozymes	70
3.5.1	Enzymatic activity determination with Gram positive reference bacteria <i>M. luteus</i>	70
3.5.2	Enzymatic activity determination with Gram negative reference bacteria <i>P. putida</i>	72
3.5.3	Summary of chapter 3.5	73
3.6	Immobilization of mutated and wild-type lysozymes to magnetic beads	74
3.6.1	Lysozyme immobilization to Protein G Mag Sepharose beads	74
3.6.2	Lysozyme immobilization to Dynabeads® and on M-PVA SAV2	75
3.6.3	Summary of chapter 3.6	76
3.7	Detection of lysozyme-dependent bacteria capture by fluorescence microscopy	77
3.8	Bacteria capture from tap water by using lysozyme functionalized M-PVA SAV2 beads	80
3.9	Evaluation of the specific capture yield of lysozyme functionalized magnetic particles	82
3.9.1	Evaluation of molecular biology based and cultivation based quantification	83
3.9.2	Determination of capture threshold of functionalized magnetic beads for <i>E. faecalis</i>	86

Contents

3.9.3	Enrichment of <i>E. faecalis</i> with magnetic beads from liquids.....	87
3.9.3.1	M-PVA SAV2 beads.....	88
3.9.3.2	DS M270 and DS M280.....	88
3.9.3.3	DMS C1 and DMS T1.....	89
3.9.3.4	Comparison of capture efficiencies from suspensions.....	90
3.9.4	<i>E. faecalis</i> capture from lettuce.....	91
3.9.4.1	M-PVA SAV2 beads.....	92
3.9.4.2	DS M270 and DS M280.....	93
3.9.4.3	DMS C1 and DMS T1.....	95
3.9.4.4	Comparison of capture yields of bacteria from lettuce.....	97
3.9.4.5	Influence of spacer length on capture of <i>E. faecalis</i> from lettuce.....	98
3.9.5	Influence of the immobilization of HEWL onto its bacteriolytic activity.....	101
3.9.6	Summary of chapter 3.9.....	102
4	Discussion.....	105
4.1	Mutation of lysozyme and its recombinant expression in <i>P. pastoris</i>	107
4.2	Purification of recombinant lysozyme derivatives from expression broth.....	108
4.3	Determination of lysozyme activity with Gram positive and negative bacteria.....	111
4.4	Immobilization of recombinant lysozyme to magnetic beads.....	111
4.5	Proof of principle by means of fluorescence microscopy.....	112
4.6	Application of lysozyme functionalized magnetic beads for bacteria detection in tap water and detection by means of DGGE.....	112
4.7	Determination of bacteria capture yields of lysozyme functionalized magnetic beads.....	113
4.7.1	Comparison of cultivation based quantification and quantitative PCR results.....	113
4.7.2	Determination of functionalized beads threshold for the capture of bacteria.....	115
4.7.3	Enrichment of bacteria from suspensions.....	116
4.7.3.1	Comparison of the yield for capture of bacteria of different kinds of beads.....	117
4.7.3.2	Comparison of the lysozyme functionalizations.....	118
4.7.4	Separation of bacteria from lettuce.....	120
4.7.4.1	Comparison of the yield for capture of bacteria of different kinds of beads.....	122
4.7.4.2	Comparison of the lysozyme functionalizations.....	123
5	Conclusion and Outlook.....	125
6	References.....	129
7	Appendix.....	141
8	Curriculum Vitae.....	153

1 Introduction

1.1 Motivation and objectives

Hygiene surveillance of food production processes and drinking water conditioning is a major concern in public health. Diverse types of bacterial contaminations and inadequate operation endanger the access to fresh and safe drinking water. Today, high standards are set for drinking water and food safety to avoid contamination with unwanted microorganisms. Pathogens are rarely found in European countries in drinking water and their appearance points to insufficient treatment or secondary faecal contamination of distribution systems [1]. *Campylobacter spp.* have been associated with several outbreaks from drinking water [2, 3]. They were responsible for most outbreaks associated with private water supplies in England and Wales [4]. *Campylobacter spp.* are able to exist as viable but non-cultivable states (VBNC)[5] and considered to be the major food-borne human pathogen [6, 7]. Therefore, contamination control of drinking water and of food is an important task. The standard cultivation based detection methods fail in broad range contamination detection due to non-cultivable cell physiology [22]. Consequently, cultivation independent detection methods, like molecular biology nucleic acid based techniques, came more into focus in recent years.

But the low bacteria level in drinking water, interfering compounds of food matrices with detection methods, and the high sample volumes compared to low amplification volumes necessitate enrichment or specific separation of bacteria from solid matrices like food.

A lot of physical methods exist for concentrating bacteria in liquids like filtration or centrifugation. These methods, however, are size based and therefore, difficult to apply to separation of bacteria from solid matrices like food or human tissue. The bacterial cells can remain bound to solid particles and hence, are not well-separated from the matrix. A more promising separation of bacteria from complex matrices or enrichment of bacteria in liquids is provided by immunoaffinity based methods. Such a method is the immunomagnetic separation (IMS), which uses magnetic particles that were functionalized with antibodies for surface antigens of bacterial cells. An external magnetic field enables the specific separation of bacteria bound to the

magnetic beads from the solid matrices, whereas other components of the sample matrix are not separated. This method has the disadvantage of being species specific and hence, is not applicable to a broad range of bacteria detection in samples.

The aim of this study was the development of a lysozyme and magnetic bead based separation method for the specific enrichment of a broad range of bacteria from bulk water or specific separation of intact bacteria, including VBNC bacteria, from food matrices based on lysozyme-peptidoglycan interactions. Therefore, point mutations were introduced into the active cleft of c-type lysozyme for the elimination of the bacteriolytic activity but retaining the binding ability of these proteins for bacterial cell walls. The proteins were expressed in *Pichia pastoris* and were then immobilized on μ -scale superparamagnetic beads, which enabled the lysozyme based capture of the bacteria from solutions and from food matrices. The magnetic bead-bacteria complexes were then easily enriched in liquids or separated from solid, complex food matrix by the use of a magnetic field. The captured bacteria were then subject to DNA based detection and quantification.

1.2 Emerging pathogens in distribution systems as source for contamination of drinking water and food

Pathogens can be transferred from the surface water to drinking water and downstream facilities. The proliferation and persistence of pathogens is also dependent on the natural bacterial population existing at the technical system.

The opportunistic pathogen *Pseudomonas aeruginosa* is found frequently in water exposed to fecal pollution. It is excreted in the feces of 2% - 3% of all healthy adults. The occurrence of *P. aeruginosa* in drinking water distribution systems indicates deterioration of microbial quality due to high availability of nutrients, slow flow, or increased temperatures in cold-water system. Several outbreaks caused by these organisms were documented [8, 9].

High quality standards are set for drinking water in industrialized countries and it is dictated that no pathogens should be detected. In developed countries, the fear of classic waterborne infections like cholera or typhoid fever is no longer matter of relevancy. But the appearance of pathogens in drinking water distribution systems is

a sign of insufficient water treatment or secondary faecal contamination. However, in many parts of the world, waterborne outbreaks are still a major problem. Additionally, breakdown of public water supplies during natural disasters can result in the return of diseases. In recent years, new pathogens were discovered as a problem in drinking water distribution systems. Besides enteric viruses and parasites, faecal bacteria like *Campylobacter jejuni*, pathogenic *Escherichia coli*, and *Yersinia enterocolitica* can arise. Some pathogens were known for a long time but only recently identified due to the lack of detection methods. This is especially true for *Legionella* spp., or *Cryptosporidium* sp.. Another important factor for detection of new pathogens like environmental *Mycobacteria* is the increase in number of immunocompromised persons like AIDS patients, patients receiving cancer chemotherapy or older persons. These people are subject to infections caused by organisms that do not possess a health risk for healthy adults like *Cryptosporidium parvum* that causes self-limiting diarrhea in healthy adults, whereas infections of people with immunodeficiency or infants are more severe, even fatal. Since 1982 a subset of verotoxin producing *E. coli*, enterohemorrhagic *Escherichia coli* (EHEC), was recognized as a food-borne human pathogen. The number of cases is increasing since 1982 and EHEC is considered as a serious health problem in developed countries. Recently, in 2011 an EHEC outbreak was reported in Germany that caused 885 cases of hemolytic uremic syndrome with 35 deaths and 2.987 cases of gastroenteritis with 18 deaths, most probably caused by faecal contamination of cion [10]. Most EHEC strains lack the ability of lactose fermentation and may not be detected by routine methods. Methodological problems limit the knowledge of EHEC distribution in natural water environments but they have occasionally been detected in surface and wastewater. EHEC has not been isolated from drinking water but physiological characteristics led to the assumption that they survive in water [1]. Another PCR-detected human pathogen in wastewater and drinking water is *Helicobacter pylori*, the causative of gastritis [11, 12]. More and more pathogens get discovered in drinking water distribution systems. For most of them, little is known about their behaviour in water and the influence of other microorganisms and biofilms on their survival.

The bacteria present in the water distribution systems can contaminate food through food production lines, where the high density of nutrients acts supportive to the proliferation of bacteria. If not detected in drinking water conditioning or food industry, pathogenic and opportunistic bacteria can have harmful effects on public health.

Therefore, it is essential to establish highly reliable contamination detection methods encompassing also the newly emerging pathogens in drinking water and food.

1.3 Detection and quantification of bacteria

1.3.1 Culture-dependent detection: bacteria plate count

Cultivation-based detection and enumeration of bacteria in food and environmental samples is used by microbiologists for over 100 years. Especially, bacterial reference strains in laboratory systems respond well to these procedures, but bacteria in environmental samples are exposed to different forms of stress, which can impair their growth response [13]. The standardized, culture based methods are still in use by many labs and regulation agencies, because they do not demand expensive infrastructure and are cheap in consumables and overall well accepted. But besides the restricted growth of stressed microorganisms, other drawbacks are that they demand large medium volumes of liquids and are time-consuming. Conventional cultivation based colony count methods serve still as reference for more rapid alternative methods (e.g. molecular biological detection methods) used for bacteria detection and quantification. For cultivation based colony forming unit (CFU) determination, dilutions of samples get spread onto the surface of solid agar-media (spread-plate method) or get mixed with liquefied agar medium (pour plate method). For enumeration, the plates have to be incubated for a fixed period at defined temperatures in an aerobic, micro-aerobic or anaerobic atmosphere. Each individual microorganism multiplies to a visible colony. The detection limit of classical cultural methods is 4 CFU/ml for liquid foods or 40 CFU/g for solid foods [14].

Some bacteria fail to grow on routine media but are still metabolically active and are designated as viable but non-cultivable (VBNC). This physiological state has been described for many hygienically relevant bacteria, which can regain cultivability in the human intestine. Therefore, the number and diversity of microbes in water is underestimated by standard cultivation based assays [15, 16, 17].

The VBNC state differs from the starvation survival state. Proteome study on *Enterococcus faecalis*, which is a member of the human and animal intestine and serves as an indicator for fecal contamination in monitoring water microbiology [18],

demonstrated that protein profiles of VBNC cells differ from exponentially growing cells or starved cells. This is an indicator that the VBNC state is a distinct physiological phase and probably the preferred survival strategy of non-sporulating organisms if exposed to stress situations. Whereas VBCN bacteria are non-cultivable but still alive, activation of the starvation response does not inhibit cultivation of bacteria [19]. Besides difference in protein expression pattern, specific alterations of *E. faecalis* and *Escherichia coli* KN126 envelope were reported for their VBNC state, like a substantial increase in cross-linked muropeptides of higher order than dimers lead to a harder cell wall compared to dividing cells, stationary cells or UV-killed cells [20, 21]. A large number of human pathogens including *Campylobacter* spp., *E. coli* (also EHEC strains), *Francisella tularensis*, *Helicobacter pylori*, *Legionella pneumophila*, *Listeria monocytogenes*, *Mycobacterium tuberculosis*, *Pseudomonas aeruginosa*, several *Salmonella* and *Shigella* spp., *Vibrio cholera*, *V. parahaemolyticus*, and *V. vulnificus* are known to exhibit the VBNC physiological state [22]. To capture all intact bacteria, including the non-cultivable ones, other bacteria detection strategies, like molecular biology methods, came into focus.

Besides non-cultivable state of bacteria, further challenges of plate count method for bacteria detection are the lack of a single medium that will recover and enumerate all bacteria present in an analysed sample, and different growth conditions for different bacteria. The genera enumerated by plate counting vary, depending on medium of choice, incubation time, incubation temperature, origin of sample, season of the year, and age of the water sample [23].

This is also true for contamination analysis of food and dairy. High concentration of carbohydrate, protein, and ionic strength makes food closer to the human physiology than water and provides a better environment for microbial multiplication. Food contains many thousand times more bacteria than drinking water, which is devoid of nutrients and ionic strength. Therefore, food possesses a far greater risk than drinking water. [24]. Food-borne diseases affect more than 81 million people in the United States of America each year, and their estimated therapy costs are 8-10 billion US\$. Rapid detection methods should allow detection of food-borne pathogens without waiting several days for conventional microbiologic isolation and detection. The different physical composition of foods and the variable matrices in general can interfere with consistent extraction and isolation of bacteria [25]. Besides food

composition, normal flora, that generally does not pose any health risks, can interfere with selective isolation and specific identification of pathogenic bacteria [26], which is especially critical with pathogens having low infective doses like enterohemorrhagic *E. coli*, which has a median infective dose (ID₅₀) of only 10 cells [24, 27]. Therefore, sensitive and rapid detection methods for pathogen contamination in food and drinking water are essential for public health.

1.3.2 Culture-independent techniques

The standard techniques for pathogenic risk control in drinking water and food industry are cultivation based. These methods bring along many disadvantages like long cultivation times, especially for water borne pathogen detection and the false negative results caused by VBNC cells. Culture dependent techniques are the 'gold standard' of microbiological assessment in food and water industry. But due to the above mentioned drawbacks, alternative methods, which are more rapid and able to detect growth restricted or uncultivable bacteria, came into focus. The qualitative and quantitative detection methods used in this work are mainly quantitative polymerase chain reaction (qPCR), fluorescence microscopy, and denaturing gradient gel electrophoresis (DGGE) in combination with DNA sequencing. Varela Villareal et al. (2010) successfully applied the cultivation independent techniques qualitative PCR and PCR-DGGE to water surveillance of food industry. The low bacteria amounts in water required a previous 10⁴ fold concentration by filtration. This filtration step had the disadvantage of accumulating PCR inhibitors. Therefore, addition of bovine serum albumin to the samples and a treatment with polyvinylpyrrolidone was performed for eliminating PCR inhibition [28]. Alternatively, new separation methods for bacteria are needed, which are developed in this study.

1.3.2.1 Quantitative polymerase chain reaction (qPCR) in pathogen detection

A molecular biology method for accelerated pathogen detection in environmental samples is the polymerase chain reaction (PCR) with a specific set of primers. The most important advantages are speed (4-6 h), sensitivity, selectivity, specificity, and possibility of automation. The goal in using PCR as a standard technique in diagnostic laboratories is to adopt an officially approved 'gold standard' PCR protocol. The method should fulfil the criteria of analytical and diagnostic accuracy, good detection limit (international standards dictate detection limit of 1 cell in 25 g of food for standard methods), robustness towards a range of physical and chemical parameters. This include also thermocycler performance, minimal carry-over contamination risk, flexibility with respect to various sample matrices, a point that needs to integrate pre-PCR processing in an automated manner in future [29]. Many components (for example proteinases) of homogenized food like chicken, salad or cheese and components used in DNA extraction like detergents, lysozyme, sodium hydroxide, alcohols, or ethylene glycol tetraacetic acid inhibit PCR. But on the other hand PCR is tolerant to high amounts of oil, salt, carbohydrate and amino acids. Inhibitory effects could be linked with DNA precipitation, DNA or proteinase denaturation, binding of essential Mg^{2+} ions or adding an excess of these ions [30]. The ability of DNA analysis in food to detect also dead cells are considerate to be a disadvantage, because they are not considered to be a source for hazard. But dead bacteria are an indication for a possibility of contamination during food preparation and hence a better method for contamination analysis [31].

The PCR technique, first described by Kary Mullis in the mid-1980s, is used to make numerous copies of a DNA segment. The region of amplification is determined by the chosen primers, short oligonucleotides with sequences matching to the both ends of the amplified region. Amplification is realized by a number of cycles. Each cycle starts with the heat denaturation of the double-stranded DNA template. Then the mixture is cooled down, allowing the primers to anneal to the single-stranded DNA fragments. Then the thermostable DNA polymerase can elongate the short primer sequences and synthesize the complementary strand to the template, resulting in a new double-stranded DNA fragment. In every subsequent cycle, the primers bind to the old and new strands leading to an exponential increase of DNA amount at each cycle. This method takes only 30-90 minutes. The amplified DNA is then visualized

by stained agarose gels, which provide a size dependent separation of fragments. An exact identification of the amplicons can be achieved by sequencing.

Second generation PCR technologies that use fluorescent dyes like SYBR[®] Green and DNA probes were introduced in the 1990s. In contrast to classical PCR end point quantitation, Real-Time PCR enables detection and quantification of nucleotide signal during PCR and does not require any further post-PCR processing [22]. The amount of emitted fluorescence signal is proportional to the amount of PCR product. To calculate the initial copy number at the beginning of the reaction, the determination of exponential phase of PCR is a prerequisite. The cheapest principle is the usage of intercalating dyes to double stranded DNA, but this method detects specific and unspecific PCR products. A more specific detection is achieved, if fluorescence-labeled probes are used that anneal specifically to the DNA segment of the gene of interest [32]. Principles of PCR based DNA quantification:

- SYBR[®] Green 1 technique: The dye binds to the minor groove of double stranded DNA in a sequence unspecific manner and thereby its fluorescence (at 520 nm) is greatly enhanced at the end of each extension phase.
- Hydrolysis probes (TaqMan probes) technique: The hydrolysis probe, which should be positioned within the target sequence, is conjugated with reporter fluorochrome (e.g. FAM) and a quencher fluorochrome (e.g. TAMRA). As long as the probe is intact, the fluorochromes are in closed vicinity and the signal emitted from the reporter is quenched by the quencher fluorochrome. Amplification leads to the hydrolysis of the probe due to the 5'→3' exonuclease activity of the *Taq* polymerase and this separation of reporter and quencher leads to the enhancement of the fluorescence signal. Each cycle leads to exponential accumulation of free reporter and to the enhancement of the fluorescence signal (figure 1.1)
- Hybridization probes: this technique uses the fluorescence resonance energy transfer (FRET) for quantification. Two sequence specific juxtaposed probes, one labelled with an donor fluorochrome (eg FAM) at the 3' end and the other labelled with acceptor fluorochrome (eg LC Red640) at its 5' end, should hybridize during amplification what brings the both fluorochromes into close proximity. The emitted light of the donor excites the acceptor fluorochrome.

The signal can be detected at the annealing phase and the first extension phase of the PCR cycle.

The PCR cycle at which the specific fluorescence exceeds the background fluorescence signal (threshold) for the first time is used for the calculation of the cycle threshold (C_T). The C_T value is directly proportional to the amount of target sequence. Theoretically, the difference in C_T of a non-diluted and a 10-fold diluted sample should be 3.3. The slope of a standard curve using $^{10}\log$ dilutions should be -3.3. By plotting the C_T values of unknown samples on the standard curve, the initial amount of DNA can be calculated. The normalized fluorescence (R_n) of the probe is calculated relative to the fluorescence of the internal reference fluorochrome. The increase in R_n during PCR is expressed as ΔR_n [33]. Examples for an amplification plot and a standard curve for *E. faecalis* DNA are shown in figures 1.2 and 1.3.

This method was used in this study for quantification of captured bacteria by lysozyme functionalized beads.

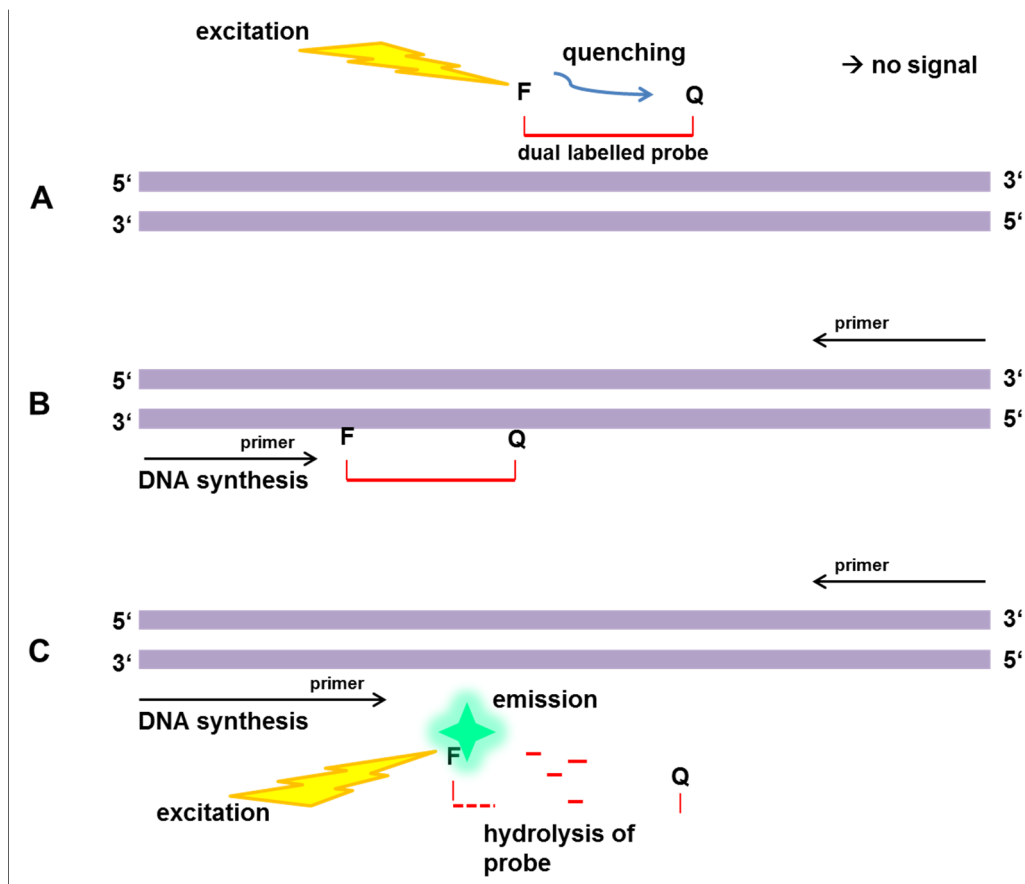


Figure 1.1: Principle of hydrolysis probe technique for quantitative PCR. A: The fluorochrome (F) and the quencher (Q) on dual labelled probe are in closed proximity. The light emission of F after excitation is quenched by quencher molecule, no signal is detected. B: The exonuclease activity of Taq

polymerase leads to the hydrolysis of the probe. C: The fluorochrome and the quencher are now distant from each other and the excitation of F results in a detectable emission signal. F: fluorochrome
 Q: quencher

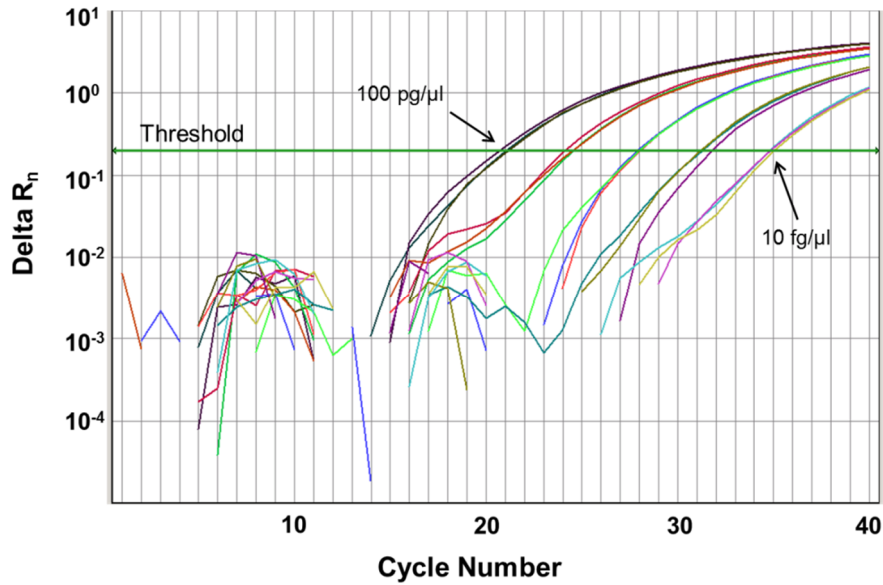


Figure 1.2: RT-PCR amplification plot of *E. faecalis* DNA. The delta R_n is recorded as a function of cycle number.

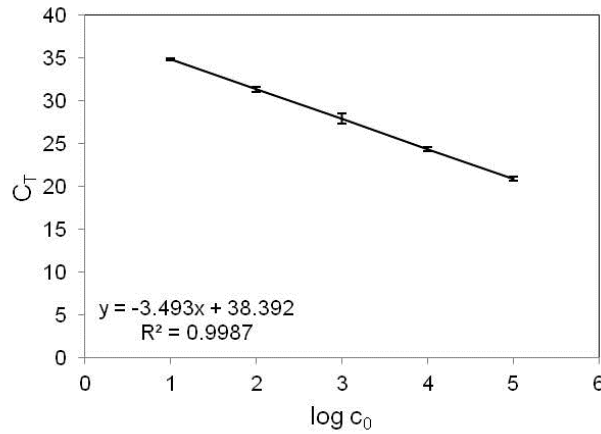


Figure 1.3: The standard curve derived from amplification plot of *E. faecalis* DNA. The C_T values are the cycle numbers, when the threshold signal is first exceeded. The DNA amounts of unknown samples are quantified by plotting their signal values to the standard curve.

1.3.2.2 Other rapid detection techniques for bacteria

1. Impedance microbiology: With the aid of bactometers (e.g. Vitek bactometer from bioMerieux, Nürtingen, Germany) the impedance deviations of nutrient media (for instance food) caused by bacterial growth are measured. 10^6 - 10^7 cells/ml are required to cause detectable changes in impedance. Measurements are completed in 24 hours [34, 35].
2. Measurement of bioluminescence: in presence of ATP, luciferin is oxidized to oxyluciferin, a reaction that releases photons. When ATP is the limiting agent, the emitted light is proportional to the amount of ATP present in the sample and hence can be converted to the number of bacterial cells per milliliter. 10^3 - 10^4 cells/ml are required for detection (e.g. Enliten test of Promega Madison, WI) [34].
3. DNA hybridization assays: Microarrays are used for monitoring gene expression, mutation analysis and microorganism characterization in environmental samples. Detection sensitivity of 10^2 - 10^3 CFU/ml and 100% specificity of pure cultures of pathogenic *Vibrio* spp. could be reached without pre-enrichment, whereas sample enrichment of 5 h followed by multiplex PCR and microarray resulted in a detection limit of 1 CFU/g oyster [36].

1.3.2.3 Denaturing gradient gel electrophoresis (DGGE)

This molecular, qualitative, culture independent approach for analysing bacterial population in a sample is based on the separation of previously amplified DNA sequences with universal primers. Muyzer et al. described the method for determining the genetic diversity of microbial population by electrophoretical separation of PCR-amplified 16S rRNA fragments in a polyacrylamide gel containing a linearly increasing gradient of denaturing agent [37]. DGGE enables the separation of fragments with the same length but different sequences. These fragments are subjected to an increasing concentration of denaturant, e.g. formamide or urea, and depending on their sequence, the fragments melt on different distinct regions called melting domains. The melting temperature (T_m) of these domains is sequence

specific. Once the melting domain for the fragment is reached, it becomes branched and this reduces the mobility. So the fragments with different base pair compositions will show different responses to the denaturing gel and run to different distances despite having the same size. The separated bands on the gel can be visualized by staining with e.g. SYBR® Green. Identification of the species to whom the bands correspond can be achieved by purification and sequencing of the distinct bands. Ribosomal DNA is a good target for population analysis via DGGE. It is conserved but has also regions that are variable and species specific. The primers for rDNA amplification should therefore anneal to conserved sequences but also span variable regions [38].

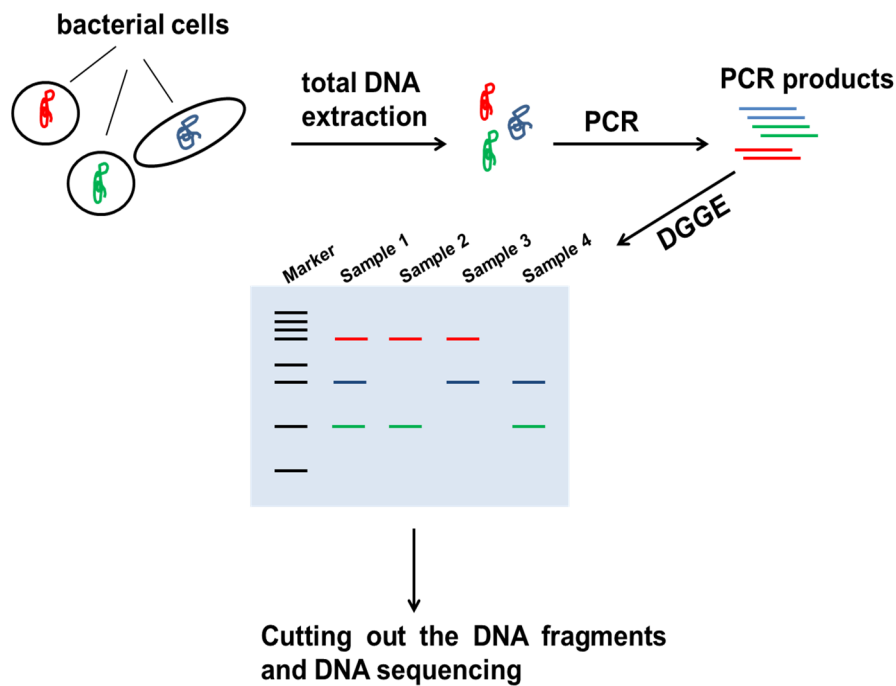


Figure 1.4: Principle of DGGE

1.4 Bacterial Separation from Complex Sample Matrices

Most rapid detection systems like DNA hybridization, agglutination, and enzyme immunoassay aim to shorten the detection time of the plating steps. Enzymatic nucleic acid amplification methods like PCR are capable of enriching single specific DNA or RNA sequence in a few hours and have a theoretical detection limit of a single bacterial cell. But the high sample volumes (>25 ml or 25 g food) compared to small amplification volumes (10-50 μ l), residual inhibitory food components and low levels of contamination are limiting factors for the widespread use of e.g. PCR in food microbiology. The expansion of rapid bacteria detection technologies in water surveillance and food safety considerations require the separation, concentration and purification of bacterial cells from the matrix prior to detection. Therefore, specific enrichment steps are necessary. The specific separation of bacteria from complex matrices would remove the matrix-associated reaction inhibitors and provide adequate sample size reductions, which would be representative for food sample sizes, preferably without disrupting bacterial cell viability [25, 39, 40].

1.4.1 Methods of bacterial separation and concentration

The methods for bacterial separation can be categorized as chemical, physical, or biological. These methods are used singly or in combination and aim the reduction of the sample sizes, removal of inhibitory components, and high recovery of viable bacteria.

Some routes for separation of bacteria from solid matrices are: adsorption of bacteria to ion exchange resins, differential centrifugation, which is based on differences in sedimentation rate of particles differing in size and density, density gradient centrifugation, and filtration methods [39].

1.4.2 Immunomagnetic Separation of Bacteria from Complex Matrices

The physical or chemical methods do not provide a prokaryote specific separation of the bacteria from the complex matrices to which they are bound to. Most of the methods mentioned above provide an initial separation of solid matrix particles that differ in size or density from each other but bacterial cells can still remain bound to matrix particles or to filters, which could decrease the bacteria recovery due to steric hindrance of e.g. the enzyme system used for detection or present inhibitory compounds that inhibit the detection method.

Biological approaches based on affinity to bacterial cells, provide a more selective separation of bacteria from solid matrices or their enrichment in liquids.

A promising method for specific bacteria enrichment and for separation from food matrices is the application of immunomagnetic beads (IMB), which were also applied to viruses and parasites [41, 42, 43].

The idea of immunomagnetic separation (IMS) came up after synthesis of perfectly spherical monosized particles in a size range from 0.5 to 100 microns in 1979 that became superparamagnetic by depositing colloidal magnetite throughout the beads [39]. Superparamagnetic beads have the advantage of being efficiently collected in a magnetic field, but they are easily suspended and show no agglomeration in the absence of a magnetic field. The particles can be coated with polymeric compounds, which provide the possibility of introducing functional groups like isocyanate-, epoxy-, and vinyl- groups, which for their part can be applied for the coupling of spacer arms with amino-, hydroxyl-, or carboxylic-end groups [44]. The attachment of antibodies to these particles enables the direct capture and isolation of cells from complex suspensions without the need for previous centrifugation. Originally developed for blood cell capture [45, 46], this method has also been applied to pathogen detection from food samples.

Some of the bacteria isolated from food or enriched from environmental water samples by IMS are: *Listeria monocytogenes* [47, 48], *Clostridium perfringens* [49, 50], *Y. enterocolitica* [51], Mycobacteria [52], *E. coli* O157:H7 [53, 54], *Leptospira* [55], and Salmonella [56].

By using the IMS-PCR method, the detection time for *Mycobacterium bovis* was shortened to two days with a minimum detection value of 1000 CFU in infected fresh bovine tissue compared to 4-8 weeks by standard detection methods [57]. Zhao et al. accomplished the simultaneous detection of *Salmonella typhimurium*, *S. flexneri*, and *E. coli* O157:H7 in artificially contaminated apple juice and milk by separation of the bacteria with a mixture of superparamagnetic nanoparticles functionalized with antibodies against each organism [58].

Besides antibody coated magnetic particles, phage-based biosorbents were also described for the capture of *S. enteritidis* from nutrient medium [59] or *Listeria monocytogenes* enrichment from suspensions and separation from food by using magnetic beads functionalized with cell wall binding domains of endolysin [60].

Bacteria captured by magnetic beads are still viable and can be detected by diverse bacteria detection methods like cultivation based methods [60], PCR [41, 42, 50, 51] or enzyme-linked immunosorbent assay (ELISA) [49].

The disadvantage of the above IMS based bacteria capture is the species specificity of the proteins used for functionalization of the magnetic beads. For broad bacteria detection in a sample with unknown bacteria composition this method is too expensive and would not succeed in capture all kinds of bacteria.

Therefore, in this study mutated derivatives of lysozymes were used. The protein family of lysozymes bind to the peptidoglycan cell wall of bacteria and in their wild-type form cause their lysis. To prohibit bacteriolysis, the catalytic amino acid glutamate 35 was replaced by alanine and glutamine.

A scheme of the principle of immunomagnetic bacteria separation and lysozyme based magnetic separation of bacteria is shown in 1.5.

A: immunomagnetic bacteria separation (species specific) B: lysozyme based magnetic bacteria separation (not specific)

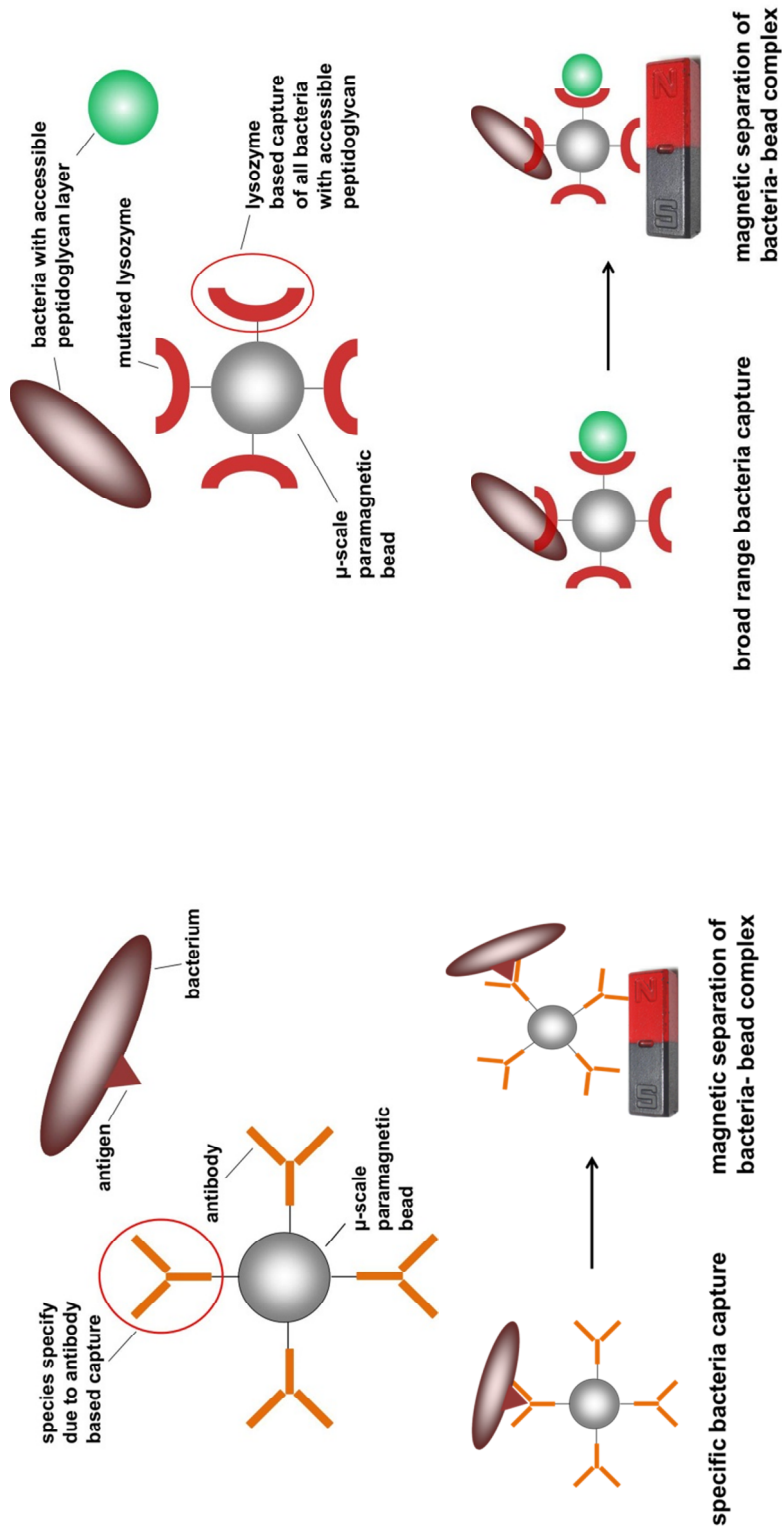


Figure 1.5: Comparison of immunomagnetic bacteria separation and lysozyme based magnetic bacteria separation.

1.5 Protein family of lysozymes and the lytic properties

Alexander Fleming first observed a “remarkable bacteriolytic element” in nasal mucus that he called lysozyme. Addition of nasal mucus to *M. lysodeiktitikus* (also called *Micrococcus luteus*) solution caused the complete disappearance of bacteria. Besides the nasal mucus, other human body secretions, human and animal tissues, some vegetable tissues, and egg white also shared this bacteriolytic property to variable degrees, and that additionally to *M. lysodeiktitikus* some other bacteria isolated from the human body are also affected by the bacteriolytic action of lysozyme [61].

All lysozymes (EC 3.2.1.17) share the ability of hydrolyzing the β -(1,4)-glycosidic bond between alternating *N*-acetylmuramic acid (NAM) and *N*-acetylglucosamin (NAG) in the bacterial peptidoglycan. In the animal kingdom three major lysozyme types have been identified: c-type (chicken or conventional-type), g-type (goose-type) or i-type (invertebrate-type) [62]. Blake et al defined six subsites for substrate binding in the active cleft of lysozyme and designated them A, B, C, D, E, and F, each of them binds to a saccharide unit. The catalytic amino acids glutamate 35 (Glu35) and aspartate 52 (Asp52) are located between the subsites D and E [63]. As in other sugar-binding proteins, tryptophan (Trp) and other aromatic amino acids are observed in the binding cleft of HEWL for example the Trp62 and Trp63 side chains in subsite C. They interact with the hydrophobic ring faces of the bound saccharides [64]. Stryanka and James [65] summarized the mechanism of lysozyme catalysis. The acidic residues Glu35 and Asp52 flank the NAM residue at side D and the NAG residue at side E. An optimal fit of the hexasaccharide to the active site requires the distortion of the D site sugar into a higher energy half chair conformation. That weakens the covalent bond of the C-1 from D site sugar and the O-4 atom of the sugar at site E. The catalytic residue Glu35 acts as a general acid catalyst and donates its proton to the O-4 of the E site sugar, which causes a bond cleavage. The D site sugar is positively charged (oxocarbenium ion) which is stabilized by the negatively charged Asp52, providing enough time for the leaving group to diffuse away.

The catalytic activity of the amino acids Glu35 and Asp52 was described by Malcolm et al.. Replacement of Glu35 by glutamine (E35Q) by site directed mutagenesis in

chicken egg white lysozyme resulted in a residual activity of only 0.1% compared to wild type lysozyme, whereas replacement of the aspartic acid 52 by its corresponding amine (D52N) showed a residual biphasic reaction kinetics against *M. luteus*. [66]. D52A mutants and the Asp52 lacking goose egg white lysozyme exhibit a catalytic activity against assisted substrates that contain a carboxylate group partially complementing the missing Asp52. This explains the observed biphasic kinetics of *M. luteus* lysis by Asp52 mutants [67, 68, 69]. For this reason, in this study the catalytic amino acid glutamic acid 35 was exchanged.

The mutated fragment was cloned into *P. pastoris* vector pPic9 for expression. The LysE35Q mutant was previously shown to have a dissociation constant of 13.3 μM , which is in the same range as wild- type lysozyme 8.6 μM [66]. This verified that at least one mutant used in this study should have an equal binding affinity to bacterial peptidoglycan.

1.6 *Pichia pastoris*: An expression organism for proteins with eukaryotic origin

Expression of eukaryotic proteins in *E. coli* has several disadvantages. First, the ATG sequence, which initiates translation in *E. coli* adds an N-terminal methionine to the proteins. The removal of this additional amino acid is catalyzed by enzymes that do not work as efficiently on recombinant eukaryotic proteins as they do on host proteins. Another drawback is that *E. coli* is unable to perform posttranslational modifications found in eukaryotic proteins and has a limited ability to facilitate extensive disulfide bond formation. The expression of eukaryotic genes in *E. coli* may cause the formation of aggregated and denatured proteins that form insoluble inclusion bodies [70, 71].

The yeast strain *Pichia pastoris* is a methylotrophic organism with several advantages over prokaryotic and eukaryotic expression systems: rapid growth rate, ease of high cell density fermentation, high levels of productivity, well characterized yeast expression vectors simply manipulated, no known human pathogenicity, ability to perform posttranslational modifications like polypeptide folding, glycosylation, methylation, acylation, able to target recombinant proteins to subcellular compartments, and secretion of recombinant protein into expression medium.

Most *P. pastoris* expression strains are derivatives of the wild-type *P. pastoris* strain NRRL-Y 11430 (Northern Regional Research Laboratories, Peoria, IL). One of these wild-type derivative strains used in this study for protein expression was GS115 (*his4*), which is defective in histidin biosynthesis [72].

P. pastoris is a suitable organism for high cell density fermentation. Compared to levels of shake flask expression, high cell densities achieved by controlled fermentation can cause a 10-fold higher protein yield [73]. Lots of different proteins from different origins were successfully expressed in *P. pastoris*, either secretional or intracellular [74].

The commercially available *P. pastoris* vector pPic9 used in this study is an *E. coli* and *P. pastoris* shuttle vector and consists of following elements: A multiple cloning site (MCS) with many endonuclease cleavage sites, methanol inducible 5' AOX1 promoter upstream of the MCS, a *Saccharomyces cerevisiae* derived α -mating factor (α -MF) secretion signal sequence upstream of the MCS for recombinant protein secretion, a transcription termination site (AOX1 derived), the selection marker HIS4 that complements the HIS4⁻ phenotype of GS115 strain, resistance gene for ampicillin (Amp^R), the replication element with pBR322 origin for plasmid propagation in *E. coli* [75]. Detailed description of the vectors and their sequences are supplied on the website of Invitrogen

<http://products.invitrogen.com/ivgn/product/K171001?ICID=search-product>.

The 5'AOX1 promoter and the 3'AOX1 transcription termination sequence flank the α -MF secretion signal, the MCS, the transcription termination sequence and the HIS4. This enables the replacement of the *AOX1* locus in genome of the GS115 strain after vector linearization. This integration into host genome is essential for sustaining the vector even in the absence of selective pressure. Furthermore, the methanol utilizing phenotype of the yeast (Mut⁺) gets replaced by slower growth of the cells on methanol medium (Mut^S) [76].

1.7 Protein purification after recombinant expression

Most of the recombinantly expressed proteins require protein purification from cell extracts or expression broth.

Isolation and crystallization of lysozyme directly from egg-white by adding sodium chloride at alkaline pH was reported in 1946 [77]. The affinity of lysozyme for chitosan brought up the idea of chromatographic lysozyme isolation in chitosan column [78].

Salting out by ammonium sulfate provides an initial protein concentration method. To produce a protein rich precipitate, concentrated salt is added to a protein solution. The protein salting-out method was discovered by Hofmeister [79]. Salts exert their effects by dehydrating proteins through competition for water molecules [80].

The most convenient tool for downstream protein purification is chromatography. The major types of separation are based on size (gel filtration or size exclusion chromatography), charge (ion exchange chromatography) and affinity (affinity chromatography) [81]. The use of chromatography for lysozyme purification from egg white was previously reported [78, 82, 83, 84, 85]. These methods are time-consuming and expensive.

Therefore alternative methods for protein purification were investigated. One method, also used in this work for protein purification, is the use of functionalized superparamagnetic beads. These beads can be derivatized with any ligand already used in chromatography. Superparamagnetic beads are easily magnetized when a field becomes applied but are free of a magnetic memory and hence do not show remanent magnetization, which allows their redispersion. Other requirements that magnetic particles have to meet are to be non-porous and spherical, possessing high specific surface areas (20-100 m²/g), and monodispersion in respect to size [86].

An advantage of magnetic bead based purification of proteins over column chromatography based separation is that the beads can also be used to concentrate the proteins, whereas column chromatography methods lead to a large volume of diluted protein solution due to elution. Commercially available beads for affinity purification are functionalized with streptavidin, antibodies, protein A, and protein G. Other affinity ligands of interest can be immobilized on particles that carry functional

groups such as carboxyl-, hydroxyl-, or amine- groups on their surfaces. In most cases the elution of isolated proteins or peptides from magnetic separation material can be submitted to standard elution protocols like pH change, change of ionic strength, use of polarity reducing agents or deforming eluents like chaotropic salts. Magnetic affinity and ion-exchange separations have been successfully employed in molecular biology, biochemistry, enzymology, and analytical chemistry and are reviewed by Safarik and Safarikova [87].

For an ion-exchanger based purification, the pI value of the target molecule is of great importance. The net charge of the molecule depends on the pH of the medium and its pI value. If the medium pH is lower than the pI, cation exchanger particles should be used for molecule binding. If the pH value is higher than the pI, anion exchanger particles should be used (Figure 1.6). The principle of magnetic beads based purification is illustrated in Figure 1.7.

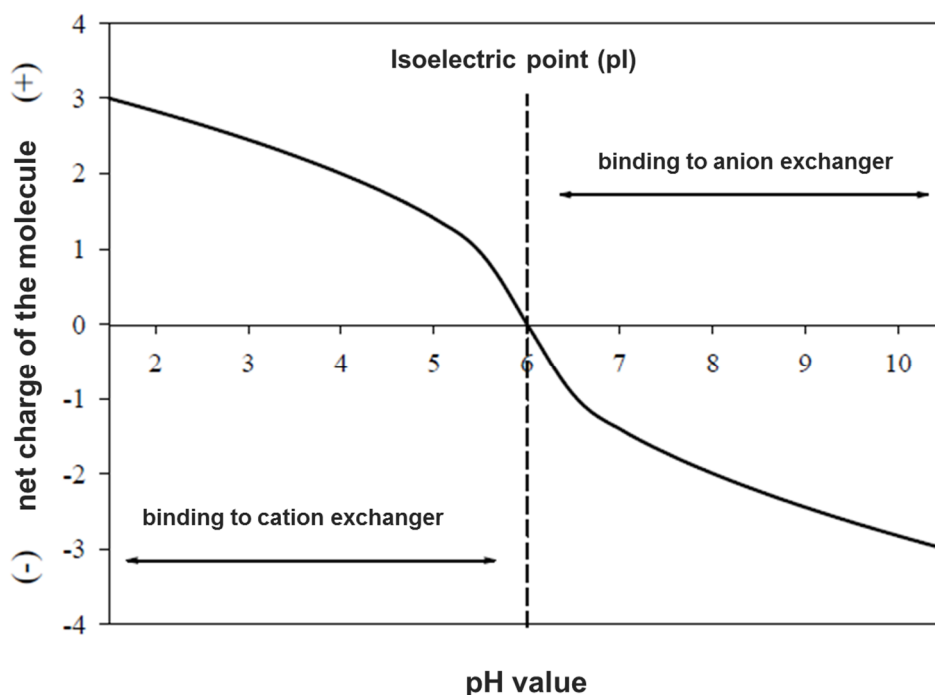
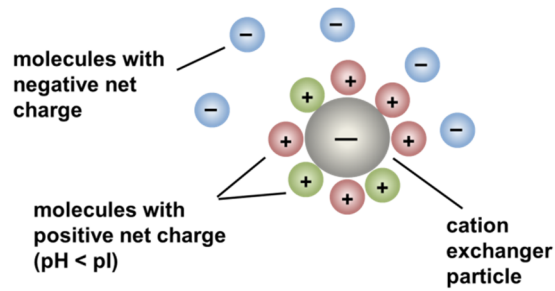
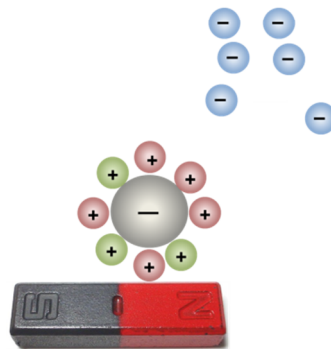


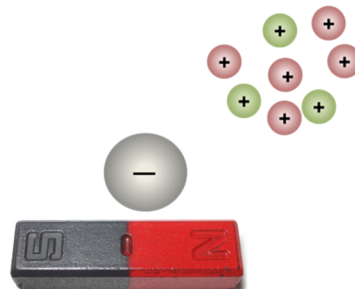
Figure 1.6: Influence of the pH on net charge of the molecule [88].



1. Specific adsorption of target molecules on ion-exchanger magnetic beads



2. Magnetic force based separation of adsorbed molecules from not adsorbed molecules



3. Elution of adsorbed target molecules from magnetic beads by elution buffer (e.g. high salt buffer)

Figure 1.7: : Principle of adsorption of positively charged molecules to cation exchanger particle. The pH value is below the pI of the target molecule(s). The negatively charged particles ($pI < pH$) do not adsorb on the magnetic bead that is functionalized with a chemical group, which has a stable negative charge over a broad pH range. After adsorption, the complex consisting of functionalized magnetic bead and adsorbed molecules is separated from the solution by using magnetic forces. Then the molecules got eluted from the beads by using high salt elution buffers.

The adsorption process of the target molecules on magnetic particles can be described by adsorption isotherms. If a sorptive is incubated with sorbents, like nano-scaled functionalized magnetic particles, for a period of time, equilibrium of binding is achieved. A portion of sorptive is bound whereas another portion remains in solution. The relation of unbound sorptive (c^*) and loading of sorbents (q^*) is described by adsorption isotherms [89].

To determine the binding behaviour of target molecules to sorbents, whether the amount of sorbent (magnetic particles) can be kept constant (\rightarrow constant L/m) and c_0 values can be changed (figure 1.8) or the c_0 value can be kept constant whereas the amount of sorbent can be changed (varying L/m values) (figure 1.9). In most cases, sorption equilibria of target proteins to the beads are described by the Temkin, Freundlich, Langmuir, or Langmuir-Freundlich model.

The Langmuir model describes the protein adsorption according to the Langmuir equation:

$$q^* = \frac{q_{max} \cdot c^*}{K_L + c^*}$$

q^* : equilibrium loading of magnetic adsorbent particles

c^* : equilibrium concentration of biomolecule remaining in solution

q_{max} : maximum binding capacity of adsorbent

K_L : dissociation constant of binary ligand-target complex

This model assumes a monolayer of adsorption with discrete places for each adsorbed protein and no interaction between adjacent proteins [89, 90, 91]. The q_{max} and K_L values can be determined by linearization of the Langmuir equation, but this method is error-prone for adsorption processes that are not in accordance with an ideal Langmuir adsorption. In this case more accurate results are achieved by non-linear regression with the software SigmaPlot® [89].

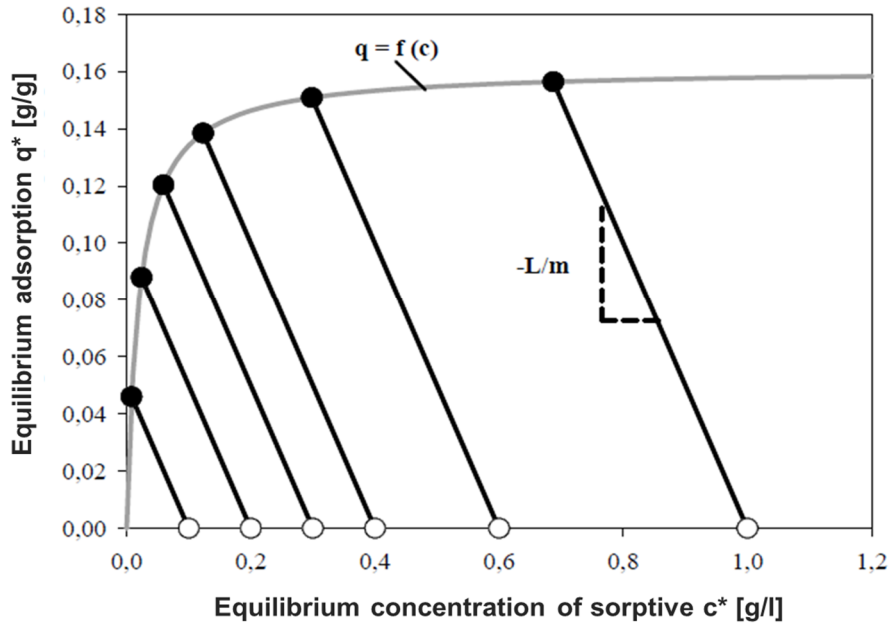


Figure 1.8: Loading lines of an adsorption approach with constant sorbent value and constant L/m but variation in initial sorptive concentrations.

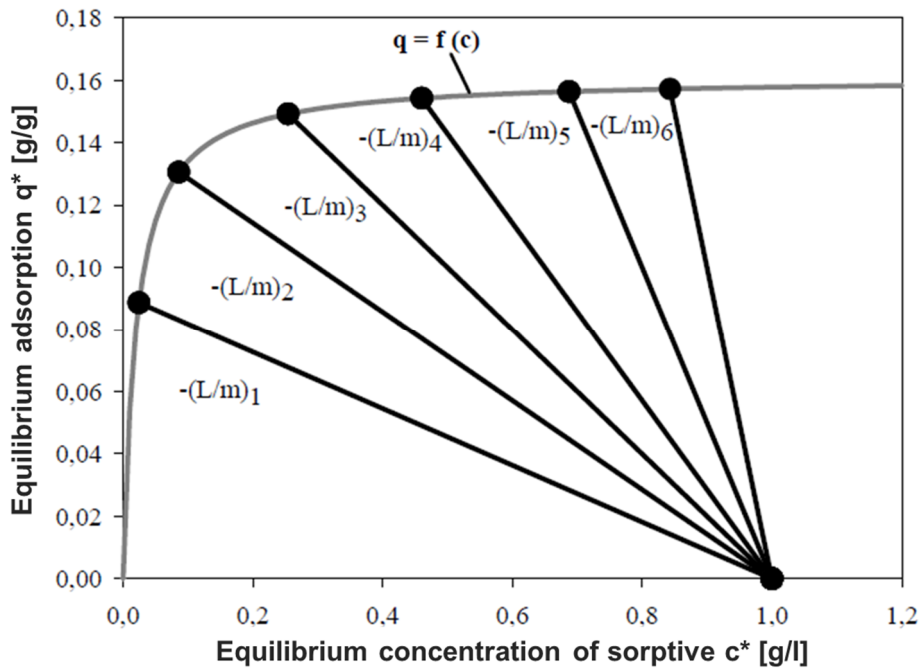


Figure 1.9: : Loading lines of an adsorption approach with differing sorbent value and different L/m values but constant initial concentrations of sorptive c_0 .

Of primary interest for adsorption-based protein purification is the binding capacity q_{\max} of particles for target proteins, ranging from 50-800 mg/g. This value depends to some degree on the size of particles. Smaller particles provide a bigger surface area and can bind more proteins [103, 104, 105]. A direct comparison of the binding parameters of particles is difficult due to the diversity of the particle types, diversity of the ligands and adsorption/desorption conditions.

Another important parameter describing the adsorption of sorptives to sorbents is the dissociation constant K_L (Langmuir constant) that describes the stability of the complex. The smaller the K_L value, the more stable is the formed complex. A low dissociation constant can be achieved with high ligand densities. Franzreb et al listed some successful applications of magnetic adsorbent based protein purification, the particles used and the K_L and q_{\max} values of the adsorption processes [86].

For small scale magnetic separation various instruments exist, ranging from simple permanent magnet racks to fully automated robotic systems [89]. For large scale protein purification the high gradient magnetic separators (HGMS) are well suited. The process, called high gradient magnetic fishing (HGMF), allows direct target molecule isolation from biologic feedstocks. Meyer et al. isolated lactoferrin from sweet whey at lab-scale and by HGMF technology. Compared to lab-scale experiments, the HGMF offered a better purity but a decreased lactoferrin yield [95].

1.8 Aim of the study

This study aims the construction and evaluation of lysozyme-magnetic beads based method for enrichment and separation of intact bacteria from liquids like tap water and complex matrices like food. As described in the previous chapters, the contamination control of aliments is essential for public health and new pathogens are emerging in technical systems. Furthermore, opportunistic bacteria that do not possess a health risk for healthy people are a problem for older persons, children and immunocompromised persons like AIDS patients.

The standard pathogen detection methods are cultivation based, but they fail when it comes to detection of bacteria in VBNC state. To circumvent this problem other methods like molecular biology methods came into focus. But the sample volume is

much higher than the detection volume of the contamination analysis method. This could result in false negative samples, especially when the contamination level is low. Additionally, bacteria are not equally distributed in suspensions like dissolved chemical contaminants. Therefore, specific bacteria enrichment and separation methods like IMS were developed. These methods seem to be very effective in pathogen detection but have the disadvantage of being species specific due to the use of antibodies for bacteria capture. IMS would fail in detecting all present bacteria in a sample with unknown bacteria composition.

In this study, the antibody functionalization in IMS was replaced by recombinant, mutated lysozyme, a protein that is able to bind to the peptidoglycan layer of all bacteria. In its wild-type form, lysozyme lyses the bacterial cell wall. Since this feature is undesired for the separation of bacteria, the catalytic activity was diminished by site directed mutagenesis. The recombinant lysozymes were expressed in *P. pastoris* strain GS115 and purified from expression broth via nano-scaled superparamagnetic cation exchanger particles. The purified proteins were checked for residual lytic activity, and after verifying that the mutant lysozymes did not exhibit any lytic activity whereas the recombinantly expressed wild-type lysozyme still did, the proteins were immobilized on commercial magnetic μ -sized beads. The success of the lysozyme based separation strategy was checked by bacteria enrichment from liquids as visualized by fluorescence microscopy and quantified by qPCR. The lysozyme functionalized magnetic beads were then applied to artificially contaminated food.

An overview of the project is illustrated in figure 1.10.

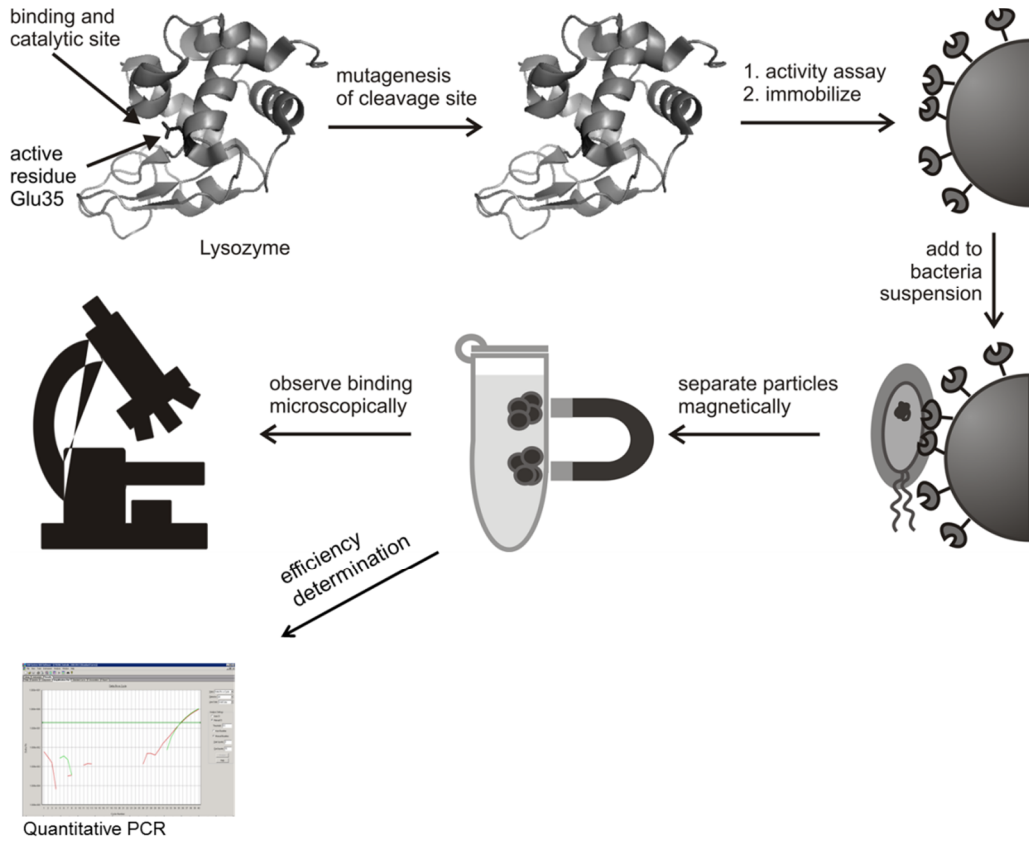


Figure 1.10: Overview of the study. The cleavage site of wild-type lysozyme was mutated by site-directed PCR. The recombinant lysozymes expressed in *P. pastoris* and purified by nano-scaled ion exchanger superparamagnetic beads from expression broth. Purified recombinant lysozymes were immobilized on μ -scale superparamagnetic beads. These complexes of lysozyme and beads were used for bacteria capture and enrichment from suspensions or separation from food matrix. The specificity of the functionalized beads compared to unfunctionalized beads were shown by fluorescence microscopy and quantified by Real-Time PCR.

2 Material and Methods

2.1 Materials

Commercial hen egg white lysozyme (HEWL) was purchased from Fluka; Buchs, Switzerland. LB-medium, ammonium sulphate, and other standard chemicals were purchased from Carl Roth GmbH (Karlsruhe, Germany), VWR (Darmstadt, Germany), or Merck KGaA (Darmstadt, Germany). *Pichia pastoris* growth medium, yeast nitrogen base for buffered minimal dextrose medium (BMD) and buffered minimal glycerol medium (BMG) were purchased from Invitrogen (Karlsruhe, Germany). The SO_3^- -functionalised MagPrep SO_3 magnetic beads used for protein purification were a kind gift of Merck (Darmstadt, Germany). Ampicillin (Sigma Aldrich, Munich, Germany) concentration for the selective growth medium was 75 mg/l.

All primers for PCR, qRT-PCR, sequencing and the carboxyfluorescein (FAM)/carboxytetramethylrhodamine (TAMRA) labelled probes were ordered from Sigma Aldrich (Munich, Germany).

dNTPs, Dream Taq polymerase, Dream Taq polymerase buffer, Pfu DNA polymerase, Pfu DNA polymerase buffer, DNA marker, protein marker (PageRuler™ Plus Prestained Protein Ladder) and all restriction enzymes and their buffers were from Fermentas GmbH (St. Leon-Rot, Germany), T4 DNA ligase and ligation buffer were purchased from New England Biolabs (Frankfurt a.M., Germany).

Reagents used for western blotting: PVDF membrane (Carl Roth), Roti®-Immunoblock protein-free blocking reagent (Carl Roth, Karlsruhe, Germany), polyclonal HEWL antibody (abcam, Cambridge, UK), HRP-coupled rabbit antibody (secondary antibody) from Santa Cruz Biotechnology (Heidelberg, Germany), Amersham™ ECL Plus Western Blotting Detection System (GE Healthcare Europe GmbH, Freiburg, Germany)

Streptavidin coated magnetic beads: MPVA SAV2, chemagen Biopolymer-Technologie AG (Baesweiler; Germany). Dynabeads® Myone™ Streptavidin C1, Dynabeads® Myone™ Streptavidin T1, Dynabeads® M270 Streptavidin, and

Dynabeads® M280 Streptavidin were purchased from Invitrogen (Karlsruhe, Germany)

Protein G coupled beads: Protein G Mag Sepharose (GE Healthcare Europe GmbH)

EZ-Link® NHS-PEG₁₂-Biotin (Spacer Arm 56 Å), EZ-Link® Sulfo NHS Biotin (13.5 Å spacer arm length), Zeba™ Desalt Spin Columns and Biotin Quantitation Kit were from Thermo Scientific Scientific (Karlsruhe, Germany)

TaqMan® Universal Master Mix (*E. faecalis* DNA detection) and TaqMan® Gene Expression Master Mix (*E. coli* DNA detection) for qRT-PCR were from Applied Biosystems (Darmstadt, Germany). Fluorescent dyes Alexa Fluor® 594 and Syto® 9 from Invitrogen.

Spectrophotometer (Agilent, Boeblingen, Germany)

Thermocycler GeneAmp® PCR System 9700 (Applied Biosystems, Darmstadt, Germany)

Horizontal gel apparatus for agarose gels (Carl Roth GmbH, Karlsruhe Germany)

Thermomixer compact (Eppendorf, Hamburg, Germany)

NanoDrop® ND 1000 (peqlab Biotechnology GmbH, Erlangen, Germany)

Lumi-Imager T1™ Roche Diagnostics (Mannheim, Germany)

pH-Meter 766 Calimatic (Knick, Berlin, Germany)

electrophoresis apparatus for vertical SDS PAGE: Mini-Protean Tetra Cell (BioRad, Munich, Germany)

SemiDry Blotter

TaqMan®: 7300 Real Time PCR System (Applied Biosystems)

Shaker: Rotishake Genie SI Scientific Industries

Axioplan2 Imaging microscope and the software AxioVision. (Carl Zeiss, Goettingen, Germany).

peqGOLD Plasmid Miniprep Kit I (PEQLAB biotechnology GmbH, Erlangen, Germany)

peqGOLD Gel Extraction Kit (PEQLAB)

BigDye® terminator v 1.1 Cycle Sequencing Kit (Applied Biosystems)

Hi-Di- Formamid

ExoSAPit

Glass capillary (47 cm x 50 µm, Applied Biosystems)

ABI PRISM® Genetic Analyser 310 (Applied Biosystems)

Sterile LiChroSolv PCR Water (Merck, Darmstadt, Germany)

DyeEx 2.0 Spin Kit (Qiagen)

Polymer POP4 (Applied Biosystems)

Lyticase (Sigma Aldrich Chemie)

2.2 Strains

For protein expression, the methylotrophic and histidine dehydrogenase- deficient *P. pastoris* strain GS115 (*his⁻ mut⁺*) and KM71 were used. For plasmid maintenance and amplification, the DH5α strain of *Escherichia coli* was utilised. All strains were purchased from Invitrogen (Karlsruhe, Germany).

As reference organisms for lysozyme activity and binding studies served the organisms *Micrococcus luteus* 20030^T (teaching strain), *Pseudomonas putida*, *Enterococcus faecalis*, and *Escherichia coli* 1103. All were purchased from DSMZ GmbH (Braunschweig, Germany).

2.3 Plasmids

Wild-type cDNA of HEWL optimised for expression in *P. pastoris* was ordered from Mr. Gene (Regensburg, Germany) in a pMK-RQ vector carrying kanamycin resistance.

The pPic9 expression vector (8.0 kb) has a *Saccharomyces cerevisiae*-derived α factor secretion signal upstream of its multiple cloning site that enables the secretion of the recombinant protein into the expression medium. The plasmid comprises an ampicillin resistance gene for selection in 75 mg/l ampicillin containing medium after DH5 α transformation and the *his4* gene encoding the histidinol hydrogenase, which confers histidin auxotrophy to the *his4* *P. pastoris* strains. The expression vector pPic9 was purchased from Invitrogen.

2.4 Methods

2.4.1 Creation of heat shock competent *E. coli* DH5 α cells

20 ml of LB medium were incubated with frozen cells and incubated overnight at 37°C. The cells were harvested by centrifugation at 4°C with 4000 rpm for 5 minutes. Then the cells were resuspended in 15 ml of 100 mM CaCl₂- solution and were incubated at 4°C for two days. After cell harvesting by centrifugation with 3500 rpm at 4°C for 5 minutes, the resulting cell pellet was resuspended in a solution consisting of 600 μ l of 100 mM CaCl₂ and 350 μ l of 60% glycerol. The competent cells were aliquoted, quick-frozen with liquid nitrogen and stored at -80°C until they were used.

2.4.2 Transformation of DH5 α cells with plasmids

Competent cells were defrosted slowly on ice. 100 μ l cell suspension was mixed with 10 μ l plasmid solution containing 1-10 μ g DNA and incubated on ice for 45 minutes. After heat shock at 42°C for 50 seconds, the cells were mixed with 1 ml LB medium and incubated on ice for 5 minutes. The cells were then incubated on 37°C for 90 minutes under constant shaking with 190 rpm. Cells were harvested by

centrifugation (1000 rpm for 1 minute) and the pellet was resolved in a desired volume and spread on agar plates containing selective media.

2.4.3 PCR-site directed mutagenesis and molecular cloning

The mutagenesis of the cDNA was carried out by *in vitro* overlap extension PCR as described by Ling and Robinson [96]. The two primers A and B introduced the restriction sites for *Xho*I (5') and *Not*I (3') restriction sites into the amplicons. Additionally, the forward primer A contained the KEX2 protease restriction site coding sequence. The point mutation was introduced by primers C and D for the mutant LysE35A and primers E and F for the mutant LysE35Q. The principle of the strategy is illustrated in figure 3.3. The sequences of the primers are shown in table 1. For cloning of the cDNA into the expression vector, first the vector and the fragments were restricted by the enzymes *Xho*I and *Not*I and then were mixed to a molar ratio of 1:3 to 1:10 and incubated with 400 units of T4 DNA ligase. The vectors with inserted lysozyme cDNAs were inserted for maintenance into the DH5 α cells by heat shock transformation immediately after ligation [97]. The cells were plated on LB-ampicillin agar plates for selection. The plasmids from selected colonies were isolated and subject to control PCR with the outside primers A and B, control digestion, and DNA sequencing with α -factor sequencing primer.

Table 1: The sequences of primers used for PCR site- directed mutagenesis of the HEWL gene.

Primer	Sequence (5'→3')	Feature
A (outside-forward)	5'GTCGAACTCGAGAAAAGAGAGGCTGAAGCTAAAGTT TTCGGTAGGTGCGAATTA 3'	Introduces KEX2 and XhoI recognition sites into the cDNA
B (outside-reverse)	5'GTCGAAAGCGGCCGCCTAAAGTCTACAACCTCTAATCCA AGC 3'	Introduces NotI recognition side into the cDNA
C (mutation)	5' GCTTCGAACTTTAATACTCAA 3'	Leads to the E35A mutation. Anneals to the sense strand of DNA
D (mutation)	5' TTGAGTATTAAAGTTCGAAGC 3'	Leads to the E35A mutation. Anneals to the antisense strand of DNA
E (mutation)	5' CAGTCGAACTTTAATACTCAA 3'	Leads to the E35Q mutation. Anneals to the sense strand of DNA
F (mutation)	5' TTGAGTATTAAAGTTCGACTG 3'	Leads to the E35Q mutation. Anneals to the antisense strand of DNA
α-factor sequencing primer	5'TACTATTGCCAGCATTGCTGC 3'	Sequencing primer to check the in frame insertion of cDNA into expression vector pPic9
5' AOX primer	5' GACTGGTTCCAATTGACAAGC 3'	Anneals to bases 855-875 on pPic9
3' AOX primer	5' GCAAATGGCATTCTGACATCC 3'	Anneals to bases 1327-1347 on pPic9

2.4.4 Isolation of plasmids from *DH5 α* cells

The plasmid isolation was performed with peqGOLD Plasmid Miniprep Kit I from overnight cultures of transformed *DH5 α* cells according to manufacturers' instructions.

2.4.5 DNA isolation from agarose gels

The DNA fragments (amplicons or linearized plasmids) were separated according to their sizes in 1%-2% agarose gels including ethidium bromide. The fragments become visible when radiated with UV-light. These bands were cutted off from gels and then purified with by peqGOLD Gel Extraction Kit according to manufacturers' instructions for subsequent cloning, introduction in yeast or sequencing.

2.4.6 DNA sequencing

A volume of 5 μ l of isolated DNA from agarose gels were digested with 2 μ l ExoSAPit for 15 minutes at 37°C and 15 minutes at 80°C (denaturation of enzyme). 7 μ l of this DNA were diluted with 21 μ l PCR-H₂O and 1 ml of this diluted sample was added to the sequencing mixture consisting of 2 μ l BigDye® Terminator Premix, 0.125 μ l 40 μ M sequencing primer, 6.875 μ l PCR-water. This mixture was then incubated for five minutes at 96°C, and then 25 cycles of 10 seconds at 96°C, five seconds at optimal annealing temperature, and one minute at 60°C followed. The mixture was purified by DyeEx Spin columns. 5 μ l of the pure sequencing sample was mixed with 9 μ l Hi-Di-formamide and loaded onto ABI PRISM® Genetic Analyzer 310. The DNA sequences were analyzed with Sequencing Analysis Software.

2.4.7 Transformation of *P. pastoris* cells

The pPic9 and pPic3.5 vectors containing lysozyme cDNA were digested with *Bgl*II for transformation of GS115. Transformation was performed by PEG 1000 method as described in the Invitrogen handbook for *Pichia pastoris* expression. For this transformation method, competent cells were mixed with linearized vector carrying the wild-type or the mutant lysozyme cDNA, and with carrier DNA (salmon

sperm DNA) and then incubated at 37°C for five minutes. Afterwards, 40% PEG 1000, including the buffer B component of the *P. pastoris* Expression Kit, was added to the mixture and incubated at 30°C for one hour. Then, the cells were washed and resuspended in 0.15 M NaCl and 0.01 M Bicine containing buffer C and plated on histidin-free minimal medium agar for selective growth.

GS115 colonies that grew well on glucose containing medium were subsequently streaked on minimal methanol plates for selection for the Mut^S phenotype indicating a successful integration.

For PCR control of gene insertion into the *aox1* locus of host genome, colonies were picked from MD agar plates and suspended in 20 µL ddH₂O. To lyse the cells for an access to the DNA, 50 units of lyticase (Sigma Aldrich Chemie) were added and the solution was incubated for 1 hour at 30°C. For a subsequent alkaline lysis, NaOH was added to a final concentration of 20 mM to the lyticase digested cells and the solution was incubated at 99°C for ten minutes.

Gene insertion into the host genome was analysed by PCR with the primer pair 5'AOX1 (forward primer) and 3'AOX1 (reverse primer) which have annealing sites on the pPic9 vector and also on the *aox1* gene of *P. pastoris*.

2.4.8 Protein expression in GS115 cells and purification with MagPrepSO₃

100 mL BMG or MG medium were inoculated with a single colony of transformed yeast GS115 cells and incubated at 30°C for three days (growth and starvation) at 190 rpm. To induce and maintain recombinant protein expression, methanol was added to a final concentration of 0.5- 2% every day up to five days. For a better oxygen supply, the flasks were shaken at 270 rpm after methanol addition. Cells were removed by centrifugation and the medium supernatant was subject to either protein precipitation by 2 M (NH₄)₂SO₄ and centrifugation at 4°C with 14000 rpm or to protein enrichment by incubation of the expression medium (after removal of cells by centrifugation) with the SO₃⁻ functionalised superparamagnetic beads (MagPrepSO₃).

The beads were washed three times with 20 mM sodium phosphate buffer pH 7 before use and incubated with the cell-free expression medium for one hour at room temperature under constant shaking at 300 rpm. The beads were separated

magnetically and washed three times with 0.02 M phosphate buffer with a pH of 7. To find the optimal salt concentration for elution the proteins were eluted in a stepwise manner by incubation with 500 μ L NaCl solution increasing in concentration from 100 mM to 2 M under constant shaking with 1000 rpm at room temperature for one hour.

2.4.9 Determination of adsorption isotherm for protein purification

Volumes of 500 μ L cell-free Lyswt and LysE35A expression media with a pH value of 8.5 were mixed with nano-scale SO_3 -functionalised MagPrep SO_3 magnetic beads increasing in amounts from 1 mg to 10 mg. After 2 hours incubation under shaking at 300 rpm at room temperature, the beads were separated using a permanent magnet. The steady-state concentrations of unbound lysozyme molecules remaining in the supernatant were determined densitometrically after western blot analysis. The wildtype lysozyme binding capacity of MagPrep SO_3 particles was determined by adding stepwisely increasing amounts of magnetic particles to commercial lysozyme dissolved in 0.1 M pH 7 phosphate buffer without any other proteins included in the solvent. Afterwards, the mixture was shaken at 300 rpm and 25°C. The particles were separated magnetically and the proteins remaining in the supernatant were determined.

For sorption process the equation 1 is valid:

$$q \cdot (L_m - L) = c \cdot (0 - 0_m) \quad (1)$$

c_0 = initial concentration of sorptive

q_0 = initial loading of the sorbent

L = volume of fluid

m = mass of sorbent (magnetic particle)

If unloaded particles ($q_0 = 0$) are used, the equation is simplified to:

$$q = \frac{L}{m} \cdot (c_0 - c) \quad (2)$$

This equation describes the loading line. It starts at the c_0 value at the abscissa and has an intercept point with the adsorption isotherm $q = f(c)$. The slope of the load line is $-L/m$. During particle loading, the concentration c of sorptive changes along the loading line until the concentration in equilibrium c^* is reached. Together with the equation of the loading line and the c^* value, the $q^*=f(c^*)$ can be determined. To describe the adsorption process several points in equilibrium have to be recorded.

The Langmuir model describes the protein adsorption according to the equation 3:

$$q^* = \frac{q_{max} \cdot c^*}{K_L + c^*} \quad (3)$$

q^* : equilibrium loading of magnetic adsorbent particles

c^* : equilibrium concentration of biomolecule remaining in solution

q_{max} : maximum binding capacity of adsorbent

K_L : dissociation constant of binary ligand-target complex

2.4.10 Protein analysis

For electrophoretic protein separation, 17% polyacrylamide-containing SDS gels were used. The gels were run at a voltage of 140 V for 90 minutes in SDS buffer. The probes were mixed with sample buffer previous to separation and then loaded onto the gels for electrophoresis.

Ingredients of 17% polyacrylamide separation gels: 5.6 ml 30% acrylamide solution, 2.5 ml 1.5 M Tris-buffer pH 8.8, 10% SDS 100 μ l, 1.7 ml H₂O, 100 μ l 10% APS, 5 μ l TEMED

Ingredients of 5% polyacrylamide stacking gels: 670 ml 30% acrylamide solution, 1 ml 0.5 M Tris buffer pH 6.8, 40 ml 10% SDS solution, 2.3 ml H₂O, 40 µl 10% APS solution, 5 µl TEMED.

5x sample buffer: 2 ml Tris/HCl pH 6.8, 2.5 ml glycerol, 2.5 ml 20% SDS solution, 75 µl 1% bromophenol blue, 1.25 ml β-mercaptoethanol, H₂O to a final volume of 10 ml.

10x SDS running buffer: 30.3 g Tris, 144.1 g glycine, 10 g SDS, water to a final concentration of 1 litre.

For specific lysozyme detection by immunoblotting, the protein gels were blotted on PVDF membrane according to manufacturer's instructions. The membrane was incubated with Roti[®]-Immunoblock protein-free blocking reagent for two hours and then incubated with 13 µg mL⁻¹ polyclonal HEWL antibody and 80 ng mL⁻¹ HRP-coupled rabbit antibody (secondary antibody). HRP-coupled secondary antibody was visualised by the Amersham[™] ECL Plus Western Blotting Detection System and documented on a Lumi-Imager Working Station.

For unspecific visualization of proteins in expression medium before and after purification, silver staining of the gels after electrophoretic separation was performed: The gels were first incubated in a solution containing 30% ethanol and 15% acetic acid. Then the gels were incubated for 30 minutes in incubation solution (0.5 % glutaraldehyde, 0.5 M sodium acetate-trihydrate, 0.2% sodium thiosulfate, 20% ethanol) after washing three times with water (5 minutes) the gels were incubated in staining solution that includes 0.1% silver nitrate and 0.02% formaldehyde. The gels were washed with ddH₂O for few seconds, and then protein band became visualized in a solution containing 0.24 M sodium carbonate and 0.02% formaldehyde. The staining was terminated with 5% acetic acid containing water.

2.4.11 Determination of protein amount

The total protein amount was determined with a Nanodrop ND1000 spectrophotometer at the A280 protein measurement mode with lysozyme as reference employing an extinction coefficient of 26.4 for a 1% lysozyme solution.

To determine the amount of lysozyme on western blot membranes, the chemiluminescence intensities of the samples were compared with that of a lysozyme standard on the same blot by the software Lumianalyst 3.0 (Roche Diagnostics, Mannheim, Germany).

2.4.12 Lysozyme activity assay

The activities of recombinant proteins were determined by the standard *Micrococcus luteus* turbidity assay at 450 nm with a spectrophotometer as described by Shugar [98]. Therefore, either 200 µl of expression medium containing lysozyme was applied or the proteins were concentrated from expression medium by 2 M (NH₄)₂SO₄ precipitation or enriched by MagPrepSO₃ ion exchanger magnetic beads and resolved in 0.1 M pH 5.5 phosphate buffer. The proteins were then incubated with *M. luteus* corresponding to an initial OD₄₅₀ value of 0.2- 0.75 absorption units and the OD₄₅₀ values were recorded at different time points for up to 24 h.

2.4.13 Immobilization of lysozyme on magnetic beads

Purified recombinant lysozyme molecules were biotinylated with the EZ-Link[®] NHS-PEG₁₂-Biotin (Spacer Arm 56 Å) or the EZ-Link[®] Sulfo NHS Biotin (13.5 Å spacer arm length) Kit according to the manufacturer's instructions. Unbound biotin molecules were removed by Zeba[™] Desalt Spin Columns. Streptavidin-functionalised M-PVA SAV2 particles, Dynabeads[®] Myone[™] Streptavidin C1, Dynabeads[®] Myone[™] Streptavidin T1, Dynabeads[®] M270 Streptavidin, or Dynabeads[®] M280 Streptavidin were labelled with Alexa Fluor[®] 594 fluorescence dye according to the manufacturer's instructions. After washing three times with PBS buffer, the labelled particles and biotinylated proteins were incubated for several hours under gentle shaking in the dark. Then, the magnetic beads were separated from the solution by magnetic forces and washed three times with PBS buffer.

2.4.14 Fluorescence microscopy based capture detection

An overnight culture of *M. luteus* and *P. putida* was incubated with Syto[®]9 for 30 minutes, centrifuged, and washed three times. The cells were dissolved in PBS buffer and then incubated with lysozyme functionalized, fluorescent dye labelled particles for two hours under gentle shaking at room temperature. After incubation, the particles were separated magnetically and washed with PBS buffer. The visualisation of captured bacteria was achieved by using the Axioplan2 Imaging microscope and the software AxioVision.

2.4.15 Efficiency determination of magnetic beads based bacteria capture

For bacteria capture efficiency determination, first the magnetic beads were coated with biotinylated recombinant lysozyme. The biotinylation of proteins was done according to the manufacturer's instructions.

For protein immobilization on magnetic beads, a 2-20 times molar excess of biotinylated lysozyme in regard to the maximum binding capacity of the beads were used. The proteins and beads were incubated for 30 minutes at room temperature under constant shaking in phosphate buffer with a pH value of 7 that contained 0.1% bovine serum albumin. The beads were collected by using a permanent magnet, the supernatant was discarded. The beads were washed 3x with phosphate buffer containing 0.05% Tween[®] 20 and resuspended in phosphate buffer to a desired concentration.

To determine if there is a correlation in the used amount of magnetic beads and capture of bacteria, 100 µg to 700 µg particles were incubated with cells for 2 h in a volume of 0.5-1 ml phosphate buffer with a pH value of 7 containing 0.1% or 0.5% BSA for prevention of unspecific bacteria adsorption to the beads. After incubation, the beads were separated from bacteria solution and washed 3x with phosphate buffer containing 0.05% Tween[®] 20 and 4x with phosphate buffer without Tween[®] 20. The cells were resuspended in sterile PCR-water a portion of the suspension was spread on agar plates for culture based CFU determination. Another portion was used as template for quantitative PCR.

The efficiency of bacteria capture from phosphate buffer was determined by incubating a defined amount of particles in bacteria solution with known bacteria amount. The quantification was done via quantitative real-time PCR or plate counting.

In the case of gram negative bacteria, the bacterial cells were treated with 10 mM EDTA before capture.

For determining the particles capture efficiency in bacteria capture from food, lettuce was chosen. Two approaches, 6 g each, were spiked with an overnight culture of *E. faekalis* or *E. coli* cells in 20 ml of tap water. After incubation overnight, the lettuce was washed 2x with 30 ml tap water and then incubated for one hour in 10 ml water containing 0.5% Tween® 20 for elution of bacteria. For determining the efficiency one approach, only the eluat was used for particle capture. The other 6 g were homogenized and then incubated with lysozyme coated particles. The bound amount of bacteria was determined by quantitative real time PCR or plate counting.

For the final determination of captured cell amount extrapolated to initial capture volume, the dilution or concentration factors were considered.

2.4.16 Quantitative PCR

E. faecalis detection: Target gene 23S rDNA [99]

Table 2: Primers and probes used for quantitave PCR based *E. faecalis* detection

Primers and probes	Sequences (5'→3')
Ecst784F	AGAAATTCCAAACGAACTTG
Enc854R	CAGTGCTCTACCTCCATCATT
Gpl813TQ	FAM-TGGTTCTCTCCGAAATAGCTTTAGGGCTA-TAMRA

E. coli 1103 detection: Target gene *uidA* encoding for Glucuronidase [100]Table 3: primers and probes used for quantitative PCR based *E. coli* detection

Primers and probes	Sequences (5'→3')
ECOuidAF	GTGTGATATCTACCCGCTTCGC
ECOuidAR	AGAACGGTTTGTGGTTAATCAGGA
ECOuidAP	FAM-TCGGCATCCGGTCAGTGGCAGT-TAMRA

For bacteria quantification by PCR, the TaqMan hydrolysis probe technique was chosen. The sequences of primers and labelled probes are listed in tables 2 and 3. PCR was accomplished by using 5 µl template in 25 µl amplification volume containing 300 nM of each primer, 200 nM of FAM/TAMRA-labelled probe, and 12.5 µl TaqMan[®] Universal Master Mix (*E. faecalis* detection) or TaqMan[®] Gene Expression Master Mix (*E. coli* detection). Duplicates or triplicates for each sample were run. The template for the negative control (no template control, NTC) was sterile, DNA free PCR-water. All samples were run at the standardized temperature profile of 2 min at 50°C, 10 min at 95°C, 45 cycles of 15 s at 95°C and 1 min at 60°C. Results were analyzed with ABI Prism 7300 SDS software [28].

3 Results

3.1 Overview of the results chapter

To generate constructs consisting of μ -scale magnetic beads with lysozyme functionalization for the capture of bacteria from liquids and complex matrices, point mutations were introduced into the wild-type hen egg white lysozyme cDNA by site-directed overlap connection PCR. This yielded fragments coding for mutated lysozymes, in which the catalytic amino acid glutamic acid 35 was exchanged by alanine (LysE35A) and by glutamine (LysE35Q). The mutated fragments were then cloned into *P. pastoris* expression vector pPic9, which has a secretion signal upstream to its MCS, allowing recombinant protein secretion into the expression broth. Besides the mutants, the wild-type cDNA was also cloned into the vector. The protein product of this wild-type cDNA, Lyswt, served as a reference protein, which provided the evaluation of the impact of secretional expression of protein and the protein purification steps on the activity of proteins.

The expression of proteins was optimized, resulting in recombinant protein yields of up to 30 mg/ml. Then the recombinant lysozymes were purified and enriched up to 12.5-fold from expression broth with nano-scaled, magnetic cation exchange particles MagPrepSO₃.

To determine residual enzymatic activity of the recombinantly expressed lysozymes, the turbidity assay was applied with *M. luteus* cells. This Gram positive bacterium is used as a reference organism in standard lysozyme activity determination assays [98]. The assay revealed a residual activity for the recombinant wild-type lysozyme, Lyswt, whereas the mutated proteins LysE35A and LysE35Q did not exhibit bacteriolytic activity. The turbidity assay was also executed with Gram negative reference bacterium *P. putida*. It was shown that adding 10 mM EDTA, which caused disruption of the outer membrane and exposure of the peptidoglycan cell wall, to the samples was enough to induce bacteriolysis by commercial, wild-type hen egg white lysozyme (HEWL) and recombinantly expressed wild-type lysozyme (Lyswt), whereas the mutated proteins, LysE35A and LysE35Q, did not cause lysis of bacteria.

The purified lysozymes were biotinylated and immobilized on streptavidin-functionalized μ -scaled magnetic beads: M-PVA SAV2, Dynabeads® Streptavidin M270 (DS M270), Dynabeads® Streptavidin M280 (DS M280), Dynabeads® MyOne™ Streptavidin C1 (DMS C1), and Dynabeads® MyOne™ Streptavidin T1 (DMS T1).

A proof of principle that immobilized lysozymes are able to bind bacteria cells and lyse them was achieved by fluorescence microscopic detection of *M. luteus* lysis by constructs consisting of the magnetic beads M-PVA SAV2 and commercial, active, wild-type hen egg white lysozyme (HEWL) functionalization. This method demonstrated that the constructs were able to lyse bacteria despite the immobilization of lysozyme on the surface of the magnetic particles.

After verification that lysozyme is suitable for functionalization, the same assay was performed with constructs consisting of M-PVA SAV2 beads functionalized with recombinant lysozymes. The lysozyme functionalization showed a higher capture of bacteria than achieved by unfunctionalized beads, indicating that unspecific adsorption of bacteria to the surface of the beads was low.

In order to demonstrate a possible technical application, the lysozyme-magnetic bead constructs were applied to capture of bacteria from tap water. A DGGE analysis showed that the enrichment of bacteria was essential to encompass the bacterial diversity of the analysed sample. But this method is qualitative and not suitable for quantitative assessment of the capture yield of the beads for lysozyme-dependent, specific capture.

To determine the efficiency of the capture of bacteria by lysozyme functionalized beads, quantification by colony based CFU and quantitative PCR (qPCR) methods were compared. This evaluation showed that the colony based method is not suitable for determination of the efficiency of the lysozyme-beads based capture method and that qPCR provide more reliable results.

For the determination of the capture recovery, all the lysozyme functionalized beads mentioned above and their unfunctionalized counterparts were applied to enrichment of *E. faecalis* cells from suspensions and subsequent quantification by qPCR. *E. faecalis* serves as an indicator of faecal contamination in monitoring water

microbiology [18] and its detection in environmental samples by hydrolysis probe technique qPCR is well established [28, 99].

The functionalized and unfunctionalized beads were then used for the separation of bacteria from artificially contaminated lettuce.

An overview of the results chapter is shown as a flow chart in Figure 3.1.

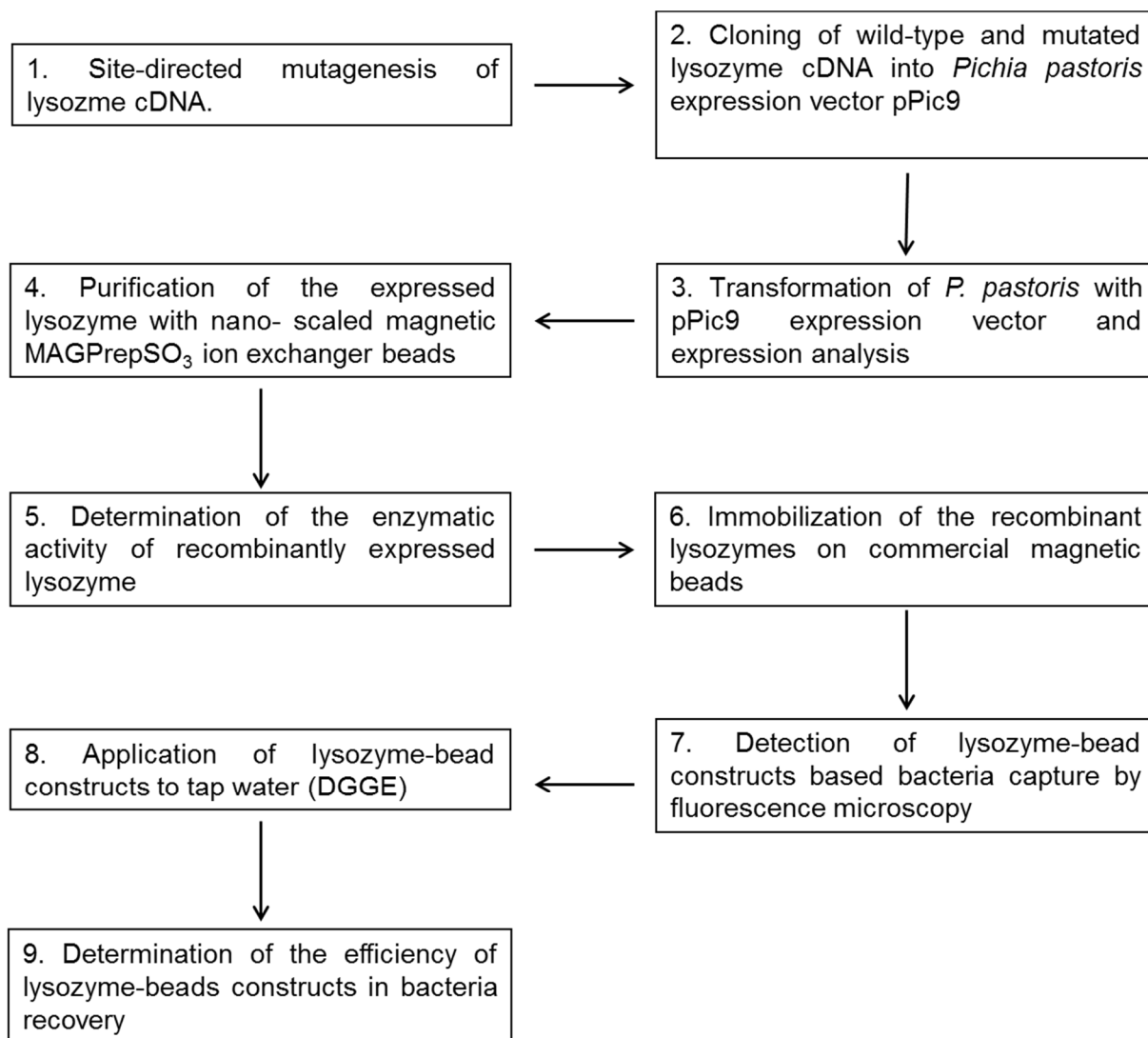


Figure 3.1: Overview of the different steps shown in the results chapter.

3.2 Site directed mutagenesis and cloning

The first step for the development of a construct for the specific bacteria capture was the expression of a protein that is able to bind a broad range of bacteria in a sample that should be analysed. Hen egg white lysozyme binds to the peptidoglycan of bacterial cell walls and was chosen as a pivotal protein. Wild-type lysozyme does not only bind to the cell wall of bacteria, it also lyses it, which is an undesired property. To diminish the bacteriolytic activity but retain the binding ability a point mutation was introduced into the catalytic centre of the lysozyme by exchanging the catalytic amino acid glutamate 35 with its corresponding amine glutamine. This protein was designated as LysE35Q. In a second approach, the same catalytic amino acid was exchanged by alanine, resulting in a protein that was designated as LysE35A. The mutations were introduced by codon exchange with site-directed overlap connection PCR. The wild-type cDNA of the hen egg white lysozyme served as template in this method. The sequence of the cDNA was optimized for expression in *Pichia pastoris* by free, on-line software of cDNA suppliers. The wild-type lysozyme DNA sequence was delivered in a commercial plasmid (Figure 3.2). First, the plasmid was checked for containing the desired cDNA by conventional PCR. For amplification of the lysozyme cDNA, the forward and reverse primer pair A and B (see Table 1 in the Material and Methods chapter) was used for PCR. The amplicon is in accordance with the expected lysozyme cDNA size of 435 bp (Figure 3.3).

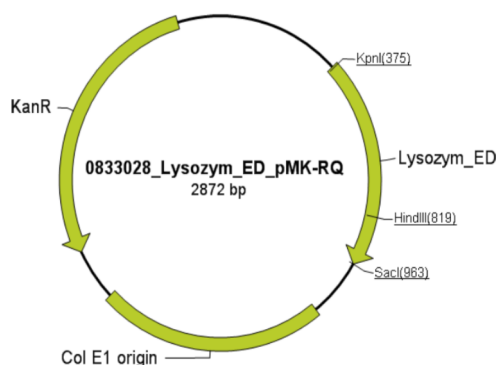


Figure 3.2: Scheme of the commercial vector 0833028_Lysozym_ED_pMK-RQ. This vector contains the wild-type HEWL cDNA that is optimized for expression in *Pichia pastoris*.

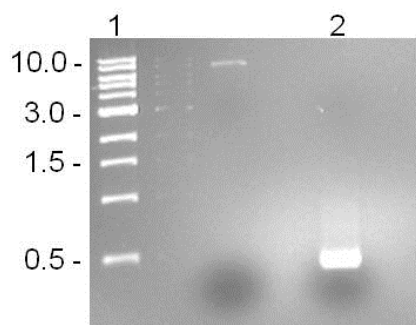


Figure 3.3: Agarose gel of the lysozyme cDNA amplification. The PCR amplification verified that lysozyme cDNA is present in the commercial plasmid 0833028_Lysozym_ED_pMK-RQ. Lane 1: DNA ladder size in kbp, lane 2: amplified lysozyme cDNA fragment.

3.2.1 Site directed mutation into lysozyme cDNA

Site directed overlap connection PCR was performed to change the catalytic amino acid glutamic acid 35 (Lyswt) to its corresponding amine glutamine (LysE35Q) or alanine (LysE35A), respectively. The mutation was induced into the lysozyme cDNA in three PCR steps. A scheme of the mutation principle is shown in Figure 3.4: the wild-type cDNA of lysozyme serves as template (1.) for two different PCR approaches (2.). One approach was performed with the primer A, which anneals to the antisense strand of the DNA and was extended by the coding site for KEX2 protease recognition sequence and the XhoI restriction enzyme recognition site (dashed line) and with the mutational primer C or E. These mutational primers anneal to the sense strand of lysozyme DNA but contain the codon for amino acid exchange (glutamic acid 35 exchange by alanine or glutamine) at their 5' end (black dashed line). The second PCR approach was performed with the primer B that contains the *NotI* restriction site at its 5' end (dashed line) and the mutation primer D or F that anneals to the antisense strand and carries the codon for the point mutation (glutamate 35 exchange by alanine or glutamine) at its 5' end (dashed black line). These two PCR approaches resulted in amplification of two fragments, F1 with 154 bp in size and F2 with 281 bp in size. These fragments contained the codon exchange at their ends (3.). These codons (black dots) are complementary to each other causing the annealing of the sense strand of one fragment with the antisense strand of the other fragment at this codon. A third PCR approach with the primers A and B caused the amplification of the mutated fragment (4.). The result of the three PCRs is a lysozyme cDNA containing a codon coding for alanine instead of

glutamate 35 (LysE35A) and glutamate instead of glutamate 35 (LysE35Q). Furthermore, the cDNA of the wild-type lysozyme was extended by the restriction site for *XhoI* and KEX2 protease recognition site encoding sequence upstream to the cDNA and by the *NotI* restriction site downstream. The size of this cDNA was 435 bp. The sequences of the used primers are listed in the chapter Materials and Methods in Table 1. The extension of the primer A by KEX2 protease recognition site and *XhoI* restriction site and the *NotI* restriction site extension of the primer B were chosen according to the multiple cloning site of the expression vector pPic9 (see Appendix).

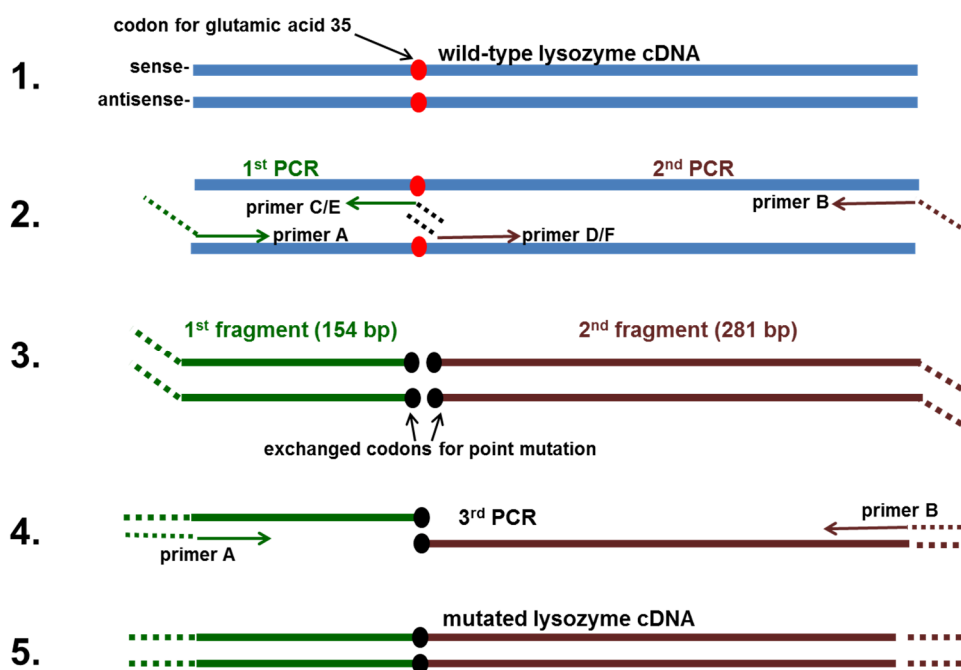


Figure 3.4: Principle of site-directed overlap connection PCR. Three PCRs were performed for generating mutated lysozyme cDNA which is extended by the recognition sites for the DNA restriction enzymes *XhoI* and *NotI* and the coding sequence for KEX2 protease recognition region.

The fragments were visualized on an agarose gel (Figure 3.5) and purified from the gel, previous to cloning. Besides mutated cDNA, wild-type lysozyme cDNA was also amplified by using the outside primer pair A and B. The expressed lysozyme (Lyswt) served as reference for protein activity after expression.

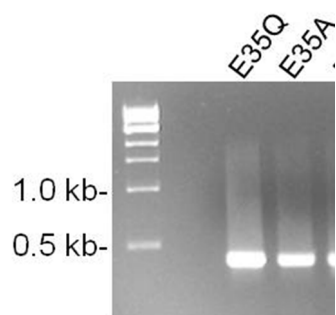


Figure 3.5: Agarose gel of mutated cDNA fragments. The amplicons were generated after the 3rd PCR of the site-directed connection overlap PCR. The full-length fragment had a size of 435 bp.

3.2.2 Cloning of wild-type and mutated lysozyme cDNAs into expression vector pPic9

For cloning of the mutated cDNAs into the expression vector pPic9, the PCR fragments were purified from agarose gels. The fragments were first restricted with 10 U of *NotI* for 90 minutes at 37°C. Then the fragments were purified and restricted with 20 U *XhoI*. These restrictions generated the sticky ends that were essential for the ligation of the cDNA inserts to the multiple cloning site (MCS) of the pPic9 vector. The vector was also restricted with the same restriction enzymes. For pPic9 digestion, 5 µg pPic9 was first incubated with 5 U *XhoI* overnight and then with 10 U *NotI* for five hours. The concentrations of these two fragments after their restriction and purification are listed in Table 4.

Table 4: Fragment concentrations after restriction with *NotI* and *XhoI* and purification from agarose gels

fragment	pPic9	LysE35Q (glutamate 35 exchanged by glutamine)	LysE35A (glutamate 35 exchanged by alanine)
c (fmol/µl)	4	87.7	123

For ligation, the linearized vector and the fragments were incubated in a molar ratio of 1:4 to 1:12 for several hours. For plasmid amplification the ligated constructs were introduced into DH5α cells. The pPic9 vector encodes for ampicillin resistance, therefore the transformed DH5α cells were spread on nutrient agar containing ampicillin. The growth of the cells on selective agar medium indicated the successful transformation of the DH5α cells with pPic9 expression vector. This transformation resulted in the growth of colonies transformed with LysE35Q cDNA (exchange of

glutamate 35 codon by glutamine codon), inserted into the MCS of pPic9 (pPic9-LysE35Q), Lyswt cDNA (wild-type lysozyme cDNA), inserted into the MCS of pPic9 (pPic9-Lyswt), and LysE35A cDNA (exchange of glutamate 35 codon by alanine codon) inserted into the MCS pPic9 (pPic9-LysE35A). In order to get a first hint for the presence of the cDNAs in the pPic9 expression vector, the plasmids of the grown colonies were isolated and served as a template for a PCR with the outside primers (A and B) and the mutation primers (C, E, D, F). The amplification of fragments with sizes corresponding to 154 bp (1st fragment F1) and 281 bp (2nd fragment F2) confirmed the presence of the cDNAs.

Besides control PCR, the plasmids isolated from the grown colonies were subject to control digestion with the restriction enzymes *Bgl*I, *Xho*I-*Not*I (double-digestion), and *Sca*I. For the pPic9 expression vector with wild-type lysozyme cDNA (pPic9-Lyswt) insert, the digestion with *Bgl*I should result in four fragments with the sizes 4456 bp, 1420 bp, 1262 bp, and 1255 bp in size. The last two fragments have a very similar size and therefore, it would not be possible to detect them as two different bands on agarose gel after electrophoresis. The double digestion with *Xho*I-*Not*I should result in fragments corresponding to 435 bp (lyswt cDNA) and to nearly 8 kb (residual fragment) whereas *Sca*I has only one restriction site in pPic9-Lyswt and should result in only one fragment with 8.4 kb. In Figure 3.6 the agarose gel with the electrophoretically separated digested plasmids that were isolated from two colonies grown on selective agar medium are shown. Only the digested plasmids from colony one (c1) showed the expected pattern for pPic9-Lyswt and were then subject to DNA sequencing. The other colony did not exhibit a correct Lyswt insertion in isolated plasmid. The same experiments were performed with grown colonies that were transformed with pPic9-LysE35A and pPic9-LysE35Q (data not shown) and the plasmids that exhibited the expected patterns were checked by DNA sequencing.

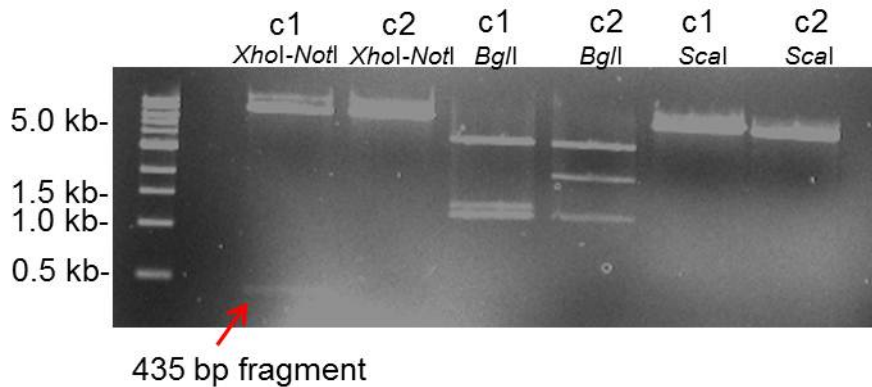


Figure 3.6: Agarose gel of digested plasmids isolated from grown DH5 α cells after transformation. The plasmids were isolated from colony 1 (c1) and colony 2 (c2) that grew on selective medium after transformation with pPic9-Lyswt. The plasmids were restricted with *XhoI-NotI* and the expected 435 bp fragment seem to be present in plasmids from c1. The expected fragments of *BglI* restriction 1255/1262 bp, 1420 bp, and 4458 bp could also be detected in plasmids isolated from c1. The restrictions with c2 did not show the expected fragments and thus the plasmids did not contain Lyswt cDNA.

The control PCRs and the control digestions of the isolated plasmids from DH5 α cells that grew on selective agar delivered a first hint for insertion of the cDNAs for Lyswt, LysE35A, and LysE35Q into the MCS of the vector pPic9. For a verification of in-frame insertion of the cDNAs into the MCS, and to verify that the correct mutation sequence was introduced into LysE35A and LysE35Q cDNAs, DNA sequencing was performed. Therefore, the isolated expression vectors pPic9-Lyswt, pPic9-LysE35A, and LysE35Q were subject to amplification PCR with the primer pair 3'AOX1 and 5'AOX (for sequences see Table 1). This primer pair anneals to the vector pPic9 and flanks the MCS. The flanked part includes also the α -factor primer site, where the primer used for sequencing anneals. The electrophoretic separation of the PCR samples on agarose gels showed two bands (Figure 3.7). One fragment had the size of 927 bp, which corresponds to lysozyme cDNA insertion into pPic9. The second fragment had the size of 497 bp. This fragment was amplified from pPic9 vectors without the lysozyme cDNA ligated into their MCS. The appearance of both fragments from one plasmid preparation showed the contamination of the clone cultures with cells that were transformed with insert-free pPic9. These colonies were streaked out until pure colonies containing pPic9 with inserted lysozyme cDNAs were achieved.

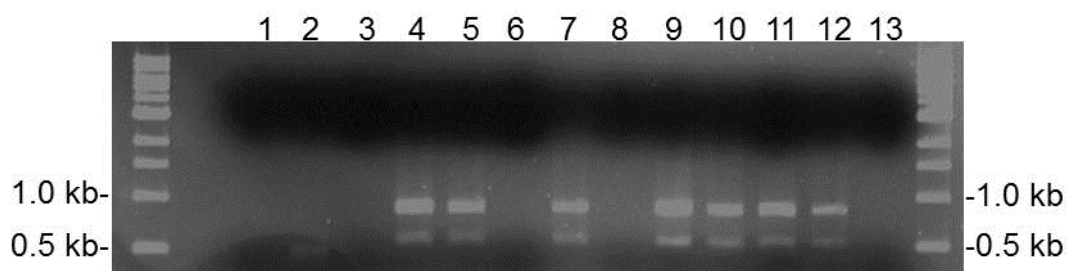


Figure 3.7: Agarose gel of electrophoretic separation of PCR fragments achieved by amplification with the primer pair 5'AOX1 and 3'AOX1. As template served plasmids isolated from cells previously proven to contain the lysozyme cDNA (wild-type and mutated) by control digestion and control PCR. Lane 1: no template control Lane 2: pPic9 Lane 3: pPic9-Lyswt c1 Lane 4: pPic9-LysE35Q c1 Lane 5: pPic9-LysE35Q c2 Lane 6: pPic9-LysE35Q c3 Lane 7: pPic9-LysE35Q c4 Lane 8: pPic9-LysE35Q c5 Lane 9: pPic9-LysE35Q c6 Lane 10: pPic9-LysE35Q c7 Lane 11: pPic9-Lyswt c1 lane 12: pPic9-LysE35A c1 lane 13: pPic9-LysE35A c2.

The sequencing primer anneals to site 1152 to 1172 on the pPic9 expression vector, which is upstream to the MCS and the sequencing results show if the ligation of cDNA was in frame. According to the DNA sequencing data, the ligation approach resulted in one in-frame ligation for pPic9-Lyswt, one for pPic9-LysE35A, and one for pPic9-LysE35Q. These vectors were used for the transformation of the GS115 strains of the yeast *Pichia pastoris*.

3.2.3 Summary of chapter 3.2

To introduce point mutations into lysozyme site-directed overlap connection PCR was performed. Therefore, a commercial plasmid containing the wild-type lysozyme cDNA (exons only) sequence optimized for *P. pastoris* expression was used as template. Besides outside primers A and B, mutational primers that introduced the codon substitution for replacement of the catalytic amino acid glutamate 35 by alanine (LysE35A) or glutamine (LysE35Q) were used. As a reference, wild-type lysozyme (Lyswt) cDNA was also amplified. The cDNAs were cloned into expression vector pPic9 and introduced into *E. coli* DH5 α for vector maintenance. After growth of cells on selective agar, the plasmids were isolated and checked by PCR and restriction enzyme digestion for lysozyme cDNA insertion. To check in-frame ligation, the isolated plasmids were subject to amplification PCR with primer pair 5'AOX1 and

3'AOX1. These PCRs led to amplification of two fragments revealing that the transformed cells were contaminated with untransformed cells. The cells were streaked out until pure colonies were achieved and plasmids of those colonies were subject to DNA sequencing. Only pPic9 vectors with in-frame ligated cDNAs were used for *P. pastoris* GS115 transformation.

3.3 Transformation of *Pichia pastoris* with lysozyme cDNA and protein expression

3.3.1 Transformation of *P. pastoris* GS115 strain

The pPic9 vectors with in-frame ligated lysozyme cDNAs Lyswt, LysE35Q, and LysE35A were digested with restriction enzyme *Bgl*II for the recombinant insertion of the linearized pPic9-Lysozyme expression vector into the genome of the *P. pastoris* strain GS115. The linearized pPic9-Lys fragments insert to the *AOX1* locus of the host genome. This locus encodes alcohol oxidase, a protein that is involved into a biochemical pathway that utilizes methanol as carbon- and energy source. The insertion of the expression vector into the locus inhibits the growth of transformed cells on methanol containing medium (Mut^S phenotype). The transformed GS115 cells were first streaked on histidin-free, glucose containing minimal medium agar for selective growth. After four days of incubation, the grown colonies were transferred to methanol containing minimal medium agar. As expected, the colonies that were grown on histidin-free selective medium did not show any growth due to their Mut^S phenotype. These cells were lysed and the lysates served as template for control PCRs with the outside primers A and B. A band on an agarose gel that corresponded to the 435 bp fragment of lysozyme cDNA verified the occurrence of that fragment in host genome of GS115 cells transformed with pPic9-Lyswt (Figure 3.8). The same PCR protocol was performed with GS115pPic9-lysE35A and GS115pPic9-LysE35Q.

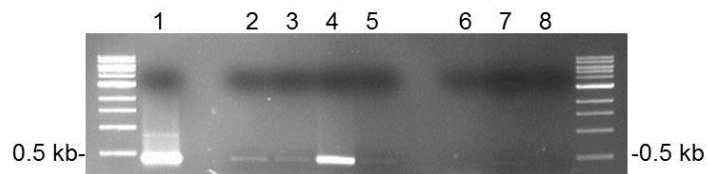


Figure 3.8: Agarose gel of PCR performed for pPic9-Lyswt insertion into GS115 cells as an example. As primers for amplification primers A and B were used. One colony (lane 4) gave a clear band that corresponds to the 435 bp Lyswt cDNA. The bands of colonies 1, 2, and 4 are very weak (lanes 2, 3, and 5). Lane 1: positive control pPic9-Lyswt Lanes 2-5: colonies that grew on selective agar medium after transformation Lane 6: non-transformed GS115 cells Lane 7: pPic9 without Lyswt Lane 8: no template control

After verifying that the lysozyme cDNA was integrated into the GS115 genome by the primers A and B, a further PCR was performed with the primer pair 5'AOX1 and 3'AOX1. These PCRs were performed to check the purity of grown colonies on selective agar medium. With untransformed cells, this PCR resulted in a 2.2 kbp fragment due to the annealing of the primers to the *AOX1* locus of host genome. In the case of pPic9-Lys cDNA integration into the *AOX1* locus, the gene is replaced by the *Bgl*II digested expression vector. This replacement causes the amplification of a fragment with the size of 927 bp. Most of the colonies tested by PCR showed both fragments (Figures 3.9 and 3.10), indicating that the colonies were not generated by pure transformed cells, except colony 3 of GS115 cells transformed with pPic9-Lyswt (Figure 3.9 lane 4). The other colonies were a mixed population of transformed and untransformed cells. These mixed colonies did not express the recombinant proteins, because the transformed cells did not grow well in methanol containing medium whereas the untransformed ones grew very fast due to their methanol utilization phenotype (Mut^+). Therefore, the cells were again streaked out until pure colonies consisting of only transformed cells were achieved (data not shown). These pure colonies of the transformed GS115pPic9-Lyswt, GS115pPic9-LysE35A, and GS115pPic9-LysE35Q strains were subject to expression analysis.

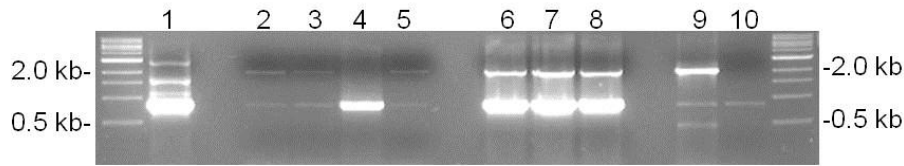


Figure 3.9: Agarose gel of purity control of GS115pPic9-Lyswt and GS115pPic9-LysE35A. The cell lysates served as templates for PCR with primers 5'AOX1 and 3'AOX1. Lanes 2-5: GS115pPic9-Lyswt (mixed culture of transformed and untransformed cells) Lanes 6-8: GS115pPic9-LysE35A (mixed culture of transformed and untransformed cells) Lane 4: GS115pPic9-Lyswt c3 (pure transformed cells) Lane 1: pPic9Lyswt Lane 9: GS115 (untransformed) Lane 10: no template control

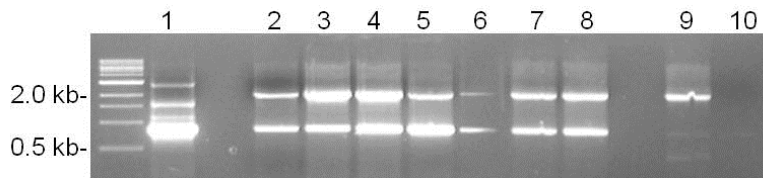


Figure 3.10: Agarose gel of purity control of GS115pPic9-LysE35Q. The cell lysates served as templates for PCR with primers 5'AOX1 and 3'AOX1. Lane 1: pPic9Lyswt Lanes 2-8: GS115pPic9-LysE35Q (fragments 2.2 kb and 927 bp present indicating presence of transformed and untransformed cells) Lane 9: GS115 (untransformed) Lane 10: no template control

3.3.2 Expression analysis of recombinant lysozyme

Histidin-free, glycerol medium was inoculated with pure colonies of GS115pPic9-Lyswt, GS115pPic9-LysE35A, and GS115pPic9-LysE35Q. The cells were grown in glycerol medium for three days. Afterwards, expression was induced by daily adding of methanol for 5 days. Each day, samples were taken from the expression broth for the determination of total (see Table 6) and recombinant protein concentrations. A Western blot expression analysis was performed after removing the cells by centrifugation and subsequent protein precipitation with 3 M ammonium sulphate. The analysis showed that the highest protein concentration was achieved on day 5 of expression. In Figure 3.11 the western blot analysis of two transformed GS115 strains with pPic9-LysE35A cells (GS115pPic9-LysE35A-1 and GS115pPic9-LysE35A-2) are shown. GS115pPic9-LysE35A-2 had better expression efficiency

than GS115pPic9-LysE35A-1. Therefore, these cells were used for further protein expression. The expression analysis was also performed with GS115pPic9-Lyswt and GSpPic9-LysE35Q cells.

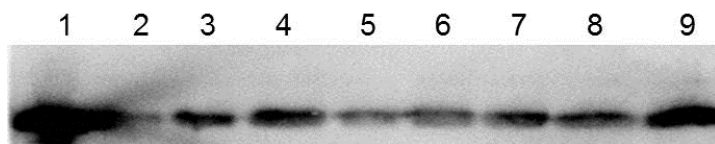


Figure 3.11: Western blot expression analysis exemplary for GS115pPic9-LysE35A cells. Lane 1: commercial hen egg white lysozyme (HEWL), 150 ng. Lanes 2-4: GS115pPic9-LysE35A -1 at day 3 to day 5 of methanol induced expression. Lanes 5-9: GS115pPic9-LysE35A-2 at day 1 to day 5 of expression. The proteins were precipitated with 3 M ammonium sulphate previous to precipitation.

Table 5: Total protein concentrations of expression medium.

strain	GS115pPic9	GS115pPic9-Lyswt	GS115pPic9-LysE35A	GS115pPic9-LysE35Q
total protein (mg ml ⁻¹)	0.4	0.26	0.22	0.2

The specific, recombinant lysozyme amounts were determined by densitometry on Western blots. The values of ammonium sulphate precipitated lysozymes were between 0.16 and 0.6 $\mu\text{g ml}^{-1}$. Compared to the values of total protein recombinant lysozyme values were very low and weak or not detectable on silver stained SDS-PAGE (Figure 3.12).

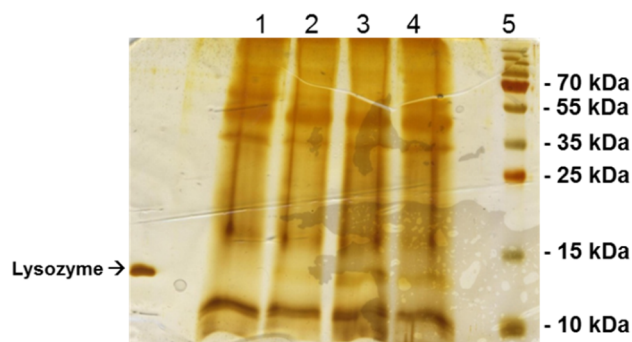


Figure 3.12: Silver stained SDS gel of total protein precipitates from cell-free expression broths. Lane 1: precipitate of GS115-pPic9 Lane 2: precipitate of GS115-pPic9Lyswt Lane 3: precipitate of GS115-pPic9LysE35A Lane 4: precipitate of GS115-pPic9Lyswt

To improve the protein yield expression conditions were changed. First of all, expression temperature was lowered from 30° to 25°C. This change had no significant impact on the protein yield. Other changes were 1) the increasing of methanol concentration to 2% from 0.5%, 2) the addition of potassium phosphate buffer and 1% casamino acids to the expression broth, which increased the pH value from 2.6 to 5.3. Figure 3.13 shows the effect of adding casamino acids and buffer to the expression medium. Without these additives, no protein was detectable by immunoblotting (Figure 3.13 lanes 2, 4, 6). But, in presence of the additives, protein yields increased and became visible on the Western blot (Figure 3.13 lanes 3, 5, and 7).

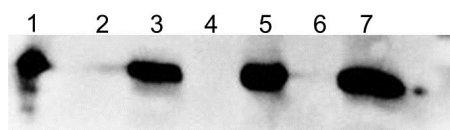


Figure 3.13: Western blot analysis of protein expression for different media compositions. Positive control: commercial HEWL 40 ng (lane 1). Expression in medium without buffer and casamino acids: wild-type (lane 2), LysE35A (lane 4), LysE35Q (lane 6). Lysozyme expression in medium containing casamino acids and buffer (lane 3), LysE35A (lane 5), LysE35Q (lane 7)

A Western blot analysis of the precipitates and the expression supernatants showed that ammonium sulphate precipitation caused high protein losses (Figure 3.14). The expression medium previous to precipitation contained more lysozyme than the precipitates of 2 M or 3 M ammonium sulphate. Therefore, the ammonium sulphate precipitation step was omitted. The optimization of expression parameters and

omitting the ammonium sulphate precipitation resulted in lysozyme yields from 2 to 30 mg l⁻¹.

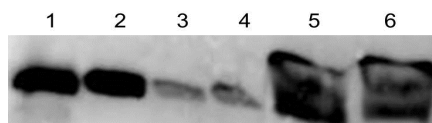


Figure 3.14: Western blot analysis of different lysozyme fractions before and after ammonium sulphate precipitation. Lane 1: commercial HEWL (10 ng), lane 2: recombinant wild-type lysozyme (Lyswt), lanes 3 and 4: Lyswt after precipitation with 2 M and 3 M ammonium sulfate, lanes 5 and 6: residual Lyswt protein in the supernatant after precipitation.

3.3.3 Summary of chapter 3.3

As the Mut^S phenotype on methanol medium is a hint for successful integration of the expression vector into *AOX1* locus of host genome, the GS115 cells that grew on histidin-free glucose medium after transformation with pPic9, pPic9-Lyswt, pPic9-LysE35A, and pPic9-LysE35Q, the cells were streaked out on methanol medium. Other verification for the insertion of the expression vector carrying the cDNA of lysozyme was derived from PCRs with outside primer pairs A and B and 5' *AOX1* and 3' *AOX1*. The later primer pair also showed that the grown colonies were contaminated with untransformed cells. The primers annealed to sequences on expression vector, leading to fragments with 927 bp in size (vector and lysozyme cDNA), and also to the host *AOX1* locus, leading to a fragment with 2.2 kb in size. Those contaminated colonies did not succeed in recombinant lysozyme expression. Therefore, they were streaked out until pure colonies were achieved. These colonies were used for the expression of the target proteins. The highest lysozyme concentrations were achieved in medium containing 0.1 M potassium phosphate buffer, 1% casamino acids at 5th day of induction with 2% methanol. The recombinant lysozyme amount was between 2 and 30 mg l⁻¹. Ammonium sulphate precipitation of proteins caused the precipitation of lysozyme amount that ranged between 0.16 and 0.6 µg ml⁻¹. Residual lysozymes remained in supernatant. Therefore, the precipitation by ammonium sulphate was omitted in further purification steps.

3.4 Protein purification

3.4.1 Adjustment of cell free expression broth to higher pH values

The optimization of expression parameters and omitting the ammonium sulphate precipitation resulted in lysozyme yields of up to 30 mg l^{-1} but the trials to purify lysozyme by means of column chromatography failed. Alternatively, nano-scaled ion exchanger magnetic particles, MagPrepSO₃, functionalized with sulphonate groups were used. After recombinant protein expression, the *P. pastoris* cells were removed by centrifugation. The hen egg white lysozyme has a high isoelectric point (pI) value of 11. Therefore, the pH of the expression medium, which was at pH values around 5 after expression, was adjusted to a value of 8.5. This caused the precipitation of a bulk amount of proteins probably with pI values lower than 8.5. The precipitates were removed. A silver stained SDS gel of the supernatants showed that a pH increase led to the precipitation of most of the other undesired proteins from expression medium (Figure 3.15).

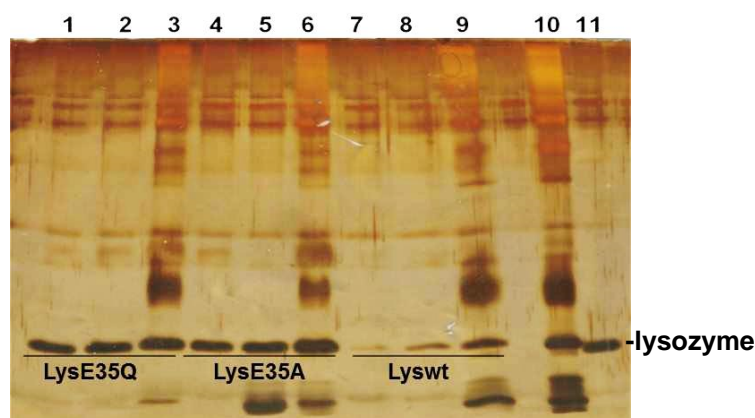


Figure 3.15: Silver stained SDS gel of cell free expression medium at different pH values. Lanes 9, 6, and 3: at pH values of 5. Lanes 2, 5, and 8: after pH adjustment to 7. Lane 10: protein length standard.

The pH shift also caused the co-precipitation of low amounts of lysozyme. To determine the co-precipitation-based lysozyme loss, a Western blot detection of lysozyme in supernatants before and after pH adjustment, and of the 20-fold concentrated pellets was performed (Figure 3.16). The lysozyme signals on the blot were quantified densitometrically with software “Lumianalyst”. The calibration curve was determined using commercial hen egg white lysozyme. The protein amounts are listed in Table 6. The lysozyme concentrations in pellets were extrapolated to

unconcentrated samples. The recombinant lysozyme losses due to co-precipitation fluctuated between 5% and 15%.

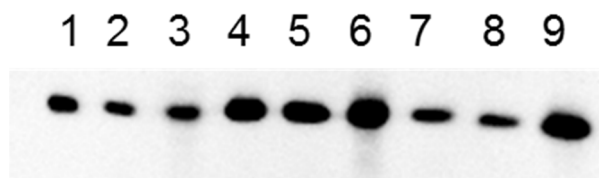


Figure 3.16: Western blot of expression media supernatants before and after pH shift to 8.5 and the precipitates. The quantification was performed densitometrically. Lanes 1-3: Lyswt pH 5, pH 8.5, and pellet (20x concentrated). Lanes 4-6: LysE35A pH 5, pH 8.5 and pellet (20x concentrated). Lanes 7-9: LysE35Q pH 5, pH 8, pellet (20x concentrated)

Table 6: Densitometrically determined lysozyme concentrations of expression medium before and after pH shift and pellets

protein	wt pH 5	wt pH 8.5	wt pellet	E35A pH 5	E35A pH 8.5	E35A pellet	E35Q pH 5	E35Q pH 8.5	E35Q pellet
concentration (ng μl^{-1})	5.8	3.7	0.28	20	18.66	1.015	5.2	4.1	0.8

3.4.2 Purification of recombinant lysozyme with MagPrepSO₃ from expression broths

To purify the recombinantly expressed lysozymes from the expression broth, superparamagnetic MagPrepSO₃ cation exchange beads were applied. These beads have a size of 100 nm and are functionalized with sulphonate groups, which are negatively charged over a broad pH range. Therefore, positively charged molecules in a suspension can be bound due to ionic interactions and subsequently separated from the suspension by magnetic forces. The beads do not have a “magnetic memory” and can be resuspended after removing the external magnetic field.

For purification of the proteins the pH of cell free expression broth was adjusted to 8.5 and MagPrepSO₃ beads were added to the broth. After incubation for 30 to 60

minutes the beads were separated by a permanent magnet and the adsorbed proteins were eluted by using a NaCl containing elution buffer. To determine the optimal salt amount for elution, an elution series was performed with phosphate buffer containing NaCl amounts ranging from 100 mM to 2 M. The elution buffer had a pH of 7. To remove the unspecifically bound proteins, the particles were first washed with 20 mM phosphate buffer, which also resulted in loss of lysozymes (Figure 3.17 lane 3). Then the particles were first incubated in elution buffer containing 100 mM NaCl, then the same particles were incubated in elution buffer with stepwise increasing salt concentrations until no more lysozyme desorption was detected (Figure 3.17 lane 12). The figure shows that 1.5 M NaCl was enough to elute all the lysozyme specifically (Figure 3.17 lane 11). A further increase of salt concentration to 2 M NaCl did not lead to a further desorption of more lysozyme (Figure 3.17 lane 12) from the beads but incubation in 1% SDS containing buffer at 95°C for one hour resulted in desorption of a bulk amount of lysozymes that could not be eluted with high salt buffer (Figure 3.17 lane 13).

A pH increase of the elution buffer to 9 by using bicine buffer did not significantly influence the desorption efficiency. A silver stained gel (Figure 3.18) of expression medium containing the recombinant protein Lyswt before and after incubation with 1 mg cation exchanger magnetic particles (Figure 3.18 lanes 2 and 3) showed that the amount of particles used was not enough to bind all the target proteins. The wash step of the beads with 20 mM phosphate buffer pH 7 eluted a protein with a molecular weight of approximately 25 kDa. The eluates (Figure 3.18 lanes 5-7) show a very specific purification of lysozyme.

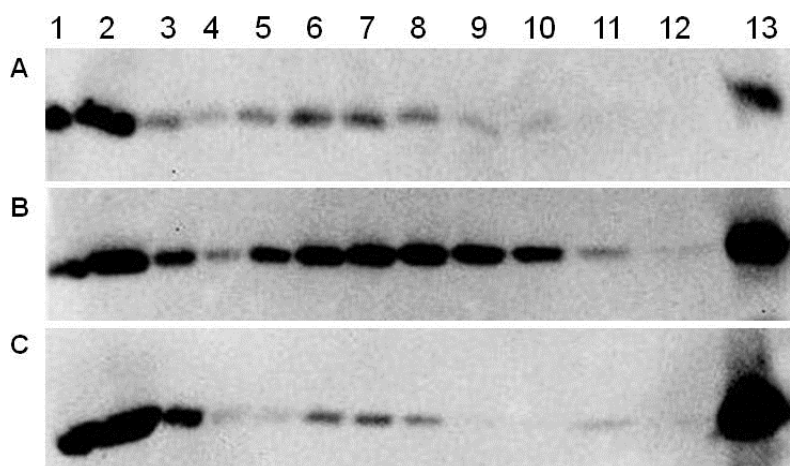


Figure 3.17: Western blot of the elution series after MagPrepSO₃ incubation in expression broth. A: Lyswt purification, B: LysE35A purification, C: LysE35Q purification. Lane1: commercial HEWL 10 ng. Lane 2: cell-free expression medium lane 3: supernatant of magnetic beads washed with 20 mM Na₃PO₄. Lanes 4-8: elutions 100 mM-500 mM NaCl. Lane 9: 750 mM NaCl. Lane 10: 1 M NaCl. Lane 11: 1.5 M NaCl. Lane 12: 2 M NaCl. Lane 13: tightly bound proteins removed after incubation in PBS buffer containing 0.1% SDS at 95 °C for 1 hour.

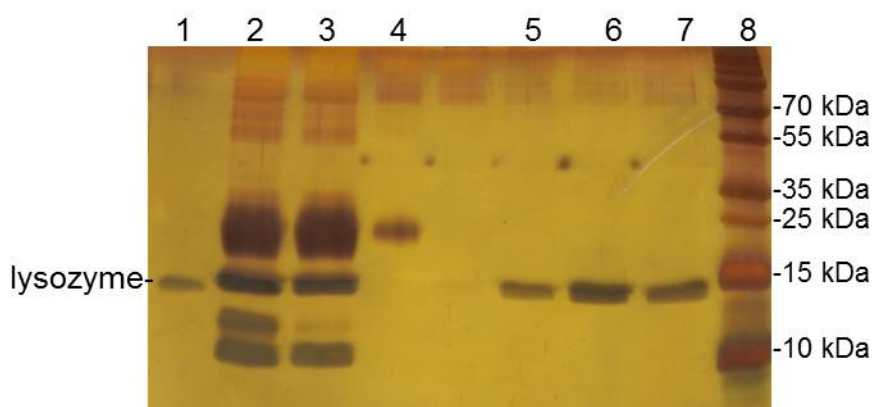


Figure 3.18: Silver stained gel of Lyswt expression broth and purified Lyswt. Lane 2: before incubation with cation-exchanger particles. Lane 3: After incubation with 1 mg magnetic beads. Lane 4: wash fraction with an approximately 25 kDa protein but no lysozyme in detectable amounts. Lanes 5-7: Eluates of buffer with 1.5 M NaCl that caused a very specific purification of the target recombinant lysozyme. Lane 1: lysozyme standard Lane 8: protein ladder

The bead based purification method, the target lysozymes were enriched 12.5- fold.

3.4.3 Adsorption isotherm of nano-scaled MagPrepSO₃ for recombinant lysozyme

To determine the binding capacity of the MagPrepSO₃ particles for wild-type and mutant lysozyme LysE35A, an adsorption isotherm at 25°C was determined. For determination of the q_{\max} and K_L values, the protein concentration was kept constant, whereas the magnetic bead concentration was gradually increased. The isotherm was first recorded for the adsorption of the pure, commercial lysozyme in 0.1 M phosphate buffer at a pH value of 7. The bead concentrations ranged from 700 $\mu\text{g ml}^{-1}$ to 6.25 mg ml^{-1} . The q_{\max} and K_L values were determined as 64.4 mg g^{-1} and 10.2 mg l^{-1} (7×10^{-1} μM) by least square regression for the Langmuir equation using SigmaPlot 10.0 analysis software (Figure 3.19). For the determination of the adsorption of Lyswt from cell-free expression medium that was adjusted to a pH value of 8.5, magnetic particles at amounts ranging from 1 mg to 7 mg were used in 500 μl expression medium. The least square regression resulted in an apparent maximal bead loading capacity of $q_{\max, \text{app}}$ of 254 $\mu\text{g g}^{-1}$ and an apparent $K_{L, \text{app}}$ value of 10.3 $\mu\text{g l}^{-1}$ (7×10^{-1} nM) (Figure 3.20). So, the loading capacity of Lyswt adsorption onto nano-scale ion exchange magnetic beads from expression broth under described conditions was only 0.4% of single-component wild-type lysozyme (HEWL) adsorption from neutral 0.1 M phosphate buffer. Besides Lyswt adsorption, the adsorption of the mutated protein LysE35A was determined at 25°C by adding increasing amounts of MagPrepSO₃ ranging from 1 mg to 10 mg to 500 μl cell-free, alkaline expression broth (c_{particle} : 2-20 g l^{-1}). The resulted $q_{\max, \text{app}}$ value was 751 $\mu\text{g g}^{-1}$, which was only 1.2% of the HEWL loading capacity of MagPrepSO₃ particles (Figure 3.21). The $K_{L, \text{app}}$ value obtained for LysE35A adsorption was 79 $\mu\text{g l}^{-1}$ (5.6 nM) In general, the binding capacity of the beads for recombinant lysozymes from alkaline expression broth was lower compared to the single component adsorption of commercial hen egg white from neutral phosphate buffer.

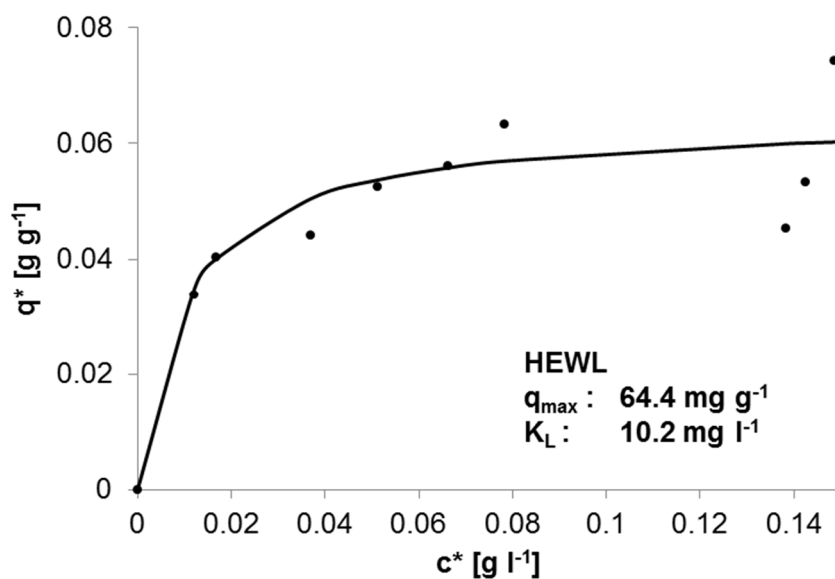


Figure 3.19: Adsorption isotherm of commercial lysozyme. The single component adsorption on MagPrepSO₃ beads in 0.1 M phosphate buffer with neutral pH value was determined at 25°C. The q_{\max} was determined as 64.4 mg g⁻¹ and the K_L as 10.2 mg l⁻¹ by non-linear regression.

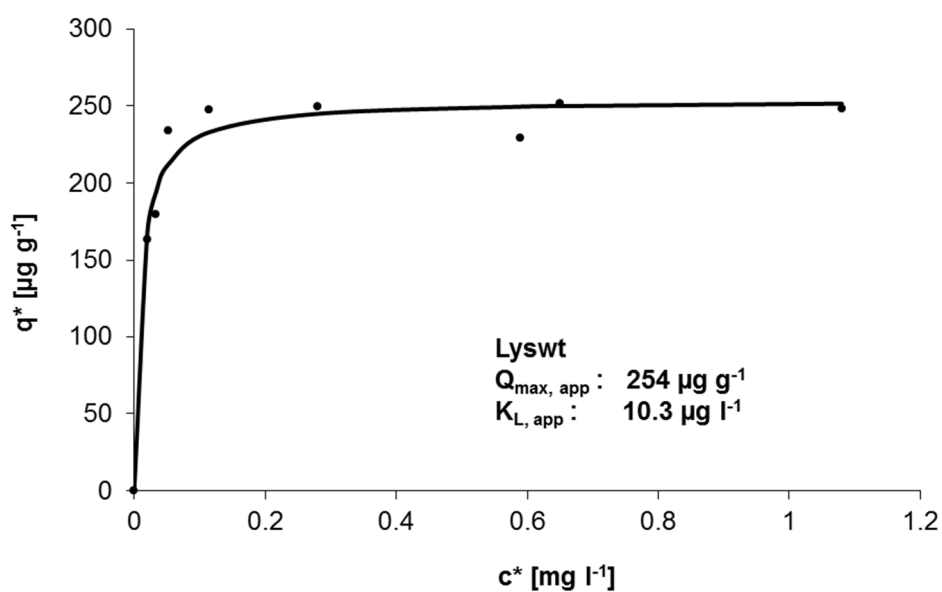


Figure 3.20: Adsorption isotherm of recombinant Lyswt. The multi component adsorption from cell-free expression supernatant at pH 8.5 on MagPrepSO₃ beads was determined at 25°C. The $q_{\max, \text{app}}$ was determined as 254 µg g⁻¹ and the $K_{L, \text{app}}$ as 10.3 µg l⁻¹ by non-linear regression.

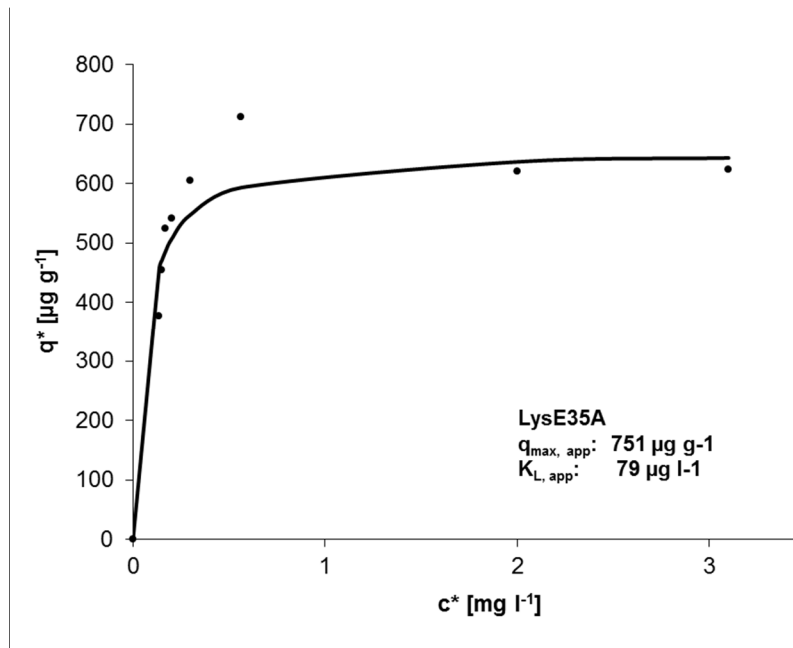


Figure 3.21: Adsorption isotherm of recombinant LysE35A. The multi component adsorption from cell-free expression supernatant at pH 8.5 on MagPrepSO₃ beads was determined at 25°C.. The q_{\max} was determined as 751 $\mu\text{g g}^{-1}$ and the K_L as 79 $\mu\text{g l}^{-1}$ by non-linear regression.

3.4.4 Lysozyme purification from *P. pastoris* cell extracts with MagPrepSO₃

The expression vector pPic9 for *P. pastoris* used for cloning in this project caused the secretion of the recombinant protein into the expression medium. Nevertheless, a small amount of target proteins remained in the cells. Therefore, the purification of the expressed target proteins were also performed from cell extracts. The Western blot analysis of extracts of cells corresponding to an OD₆₀₀ of 20 is shown in Figure 3.22. Besides the distinct band at 15 kDa that corresponds to the molecular weight of lysozyme, signals at higher molecular weights also appeared on the blot in commercial lysozyme standard (Figure 3.22 lane 1) and the transformed cells that induced for lysozyme expression, probably caused by oligomerization of lysozyme. Figure 3.23 shows the cell-free expression medium of GS115pPic9-Lyswt (Figure 3.23 lane 2), GS115pPic9-LysE35A (Figure 3.23 lane 3), GS115pPic9-E35Q (Figure 3.23 lanes 4 and 5) after pH adjustment to pH 8.5 and the extracts of these cells after lysis (Figure 3.23 lanes 6-8). For purification of the recombinant lysozymes, the cell extracts were resuspended in 1 ml phosphate buffer pH7 and incubated with 1.75 mg magnetic, nano-scaled cation exchange MagPrepSO₃ for purification of the recombinant lysozymes and washed with buffer (Figure 3.24 lanes 8, 9, and 10 for

Lyswt, LysE35A, and LysE35Q). Afterwards, the proteins were eluted from the particles with a high salt buffer at pH 7, with bicine buffer pH 9, and with bicine buffer pH 9 containing 2 M NaCl (Figure 3.24 lanes A, B, and C). Denaturation in SDS containing buffer by heat incubation at 95°C showed that several different proteins could not be eluted by pH shift or high salt amount and remained bound to the beads (Figure 3.24 D). In summary, lysozyme could not be purified from cell extracts by applying the MagPrepSO₃ beads.

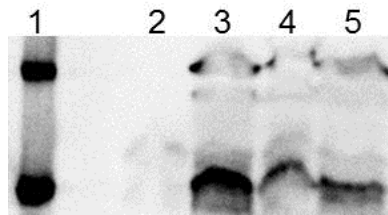


Figure 3.22 Figure 3.22: Western blot analysis of lysed GS115 cells corresponding to 20 OD₆₀₀. Lane 1: 100 ng commercial lysozyme, lane 2: extract of GS115pPic9, lane 3: extract of GS115pPic9-Lyswt, lane 4: GS115pPic9-LysE35A, lane 5: GS115pPic9-LysE35Q

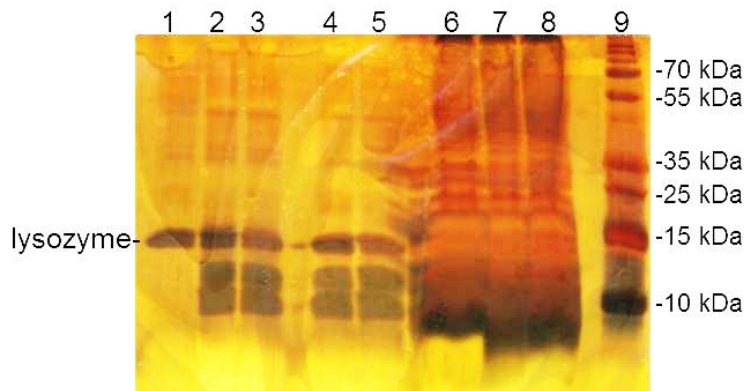


Figure 3.23: Silver stained SDS page of expression broths and cell extracts. Lane 1: 20 ng lysozyme standard, lane 2: Lyswt broth, lane 3: LysE35A broth, lanes 4 and 5: LysE35Q broth, lane 6: GS115pPic9-Lyswt extract, lane 7: GS115pPic9-LysE35A extract, lane 8: GS115pPic9-LysE35Q, lane 9: protein ladder

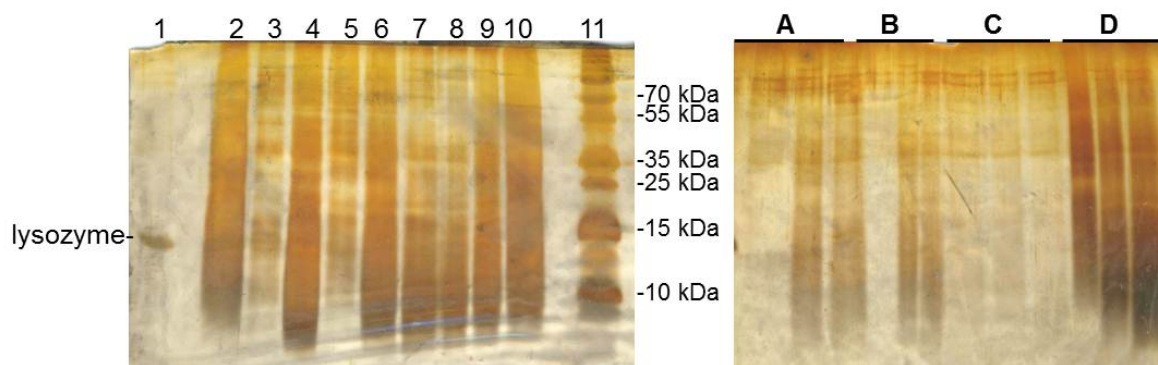


Figure 3.24: Silver stained gels of cell extracts and purification attempts of lysozymes with MagPrepSO₃ particles. Lanes 2-4 extracts of GS115pPic9-Lyswt/LysE35A/LysE35Q before and after incubation with beads (lanes 5-7). Lanes 8-10: supernatants of wash buffer for Lyswt, LysE35A, and LysE35Q. Lane 11: protein ladder. The second gel shows the eluates of beads incubated in cell extracts that expressed Lyswt, LysE35A, and LysE35Q, respectively. A: elution with 2 M NaCl pH7, B: elution with bicine at pH 9, C: elution with bicine pH 9 containing 2 M NaCl and D: incubation in SDS containing buffer at 95°C.

3.4.5 Summary of chapter 3.4

The *P. pastoris* expression broths for recombinant lysozymes Lyswt, LysE35A, and LysE35Q contained a lot of proteins besides the target protein lysozymes. This required the purification of the target protein from the expression broth. Due to the low concentration of lysozymes (2-30 mg l⁻¹) standard column-chromatography based purification attempts failed and the purification via sulphonate functionalized, nano-scaled magnetic MagPrepSO₃ particles served as an alternative method for the purification. Due to the sulphonate functionalization, the particles have a negative charge over a broad pH range and the lysozyme has a relatively high pI value of 11 meaning that the adjustment of the expression broth pH value to 8.5 retained a positive net charge on the target lysozymes. Upon adjusting the expression broth to an alkaline value, most of the other proteins precipitated and the lysozyme loss due to precipitation was only 5-15%. These precipitates were removed by centrifugation resulting in a pre-purification of the lysozyme, which remained soluble in the supernatant. After incubation of the alkaline expression broth with magnetic particles, the particles were subject to elution series increasing NaCl concentrations. This showed that elution buffer with a concentration of 1.5 M NaCl eluted the lysozymes in a very pure form. An increase in NaCl concentration above 1.5 M or pH shift did not

cause the further desorption of lysozyme. Heat incubation of the beads in buffer containing SDS showed that a bulk amount of lysozymes remained bound to the particles, which is a detriment of the particles. Adsorption isotherms showed that the binding capacity of the particles is very low for recombinant protein adsorption from alkaline expression broth (Lyswt $q_{\max, \text{app}} = 254 \mu\text{g g}^{-1}$ and LysE35A $q_{\max, \text{app}} = 751 \mu\text{g g}^{-1}$) compared to single component adsorption of commercial lysozyme from neutral buffer ($q_{\max} = 64.4 \text{ mg g}^{-1}$). The low capacity was compensated by repeated use of the particles and the same elution buffer to up to 15 times resulting in an enrichment of lysozymes to up to 12.5- fold.

Purification of target lysozyme from cell extracts by MagPrepSO₃ particles failed.

3.5 Enzymatic activities of mutated and wild-type lysozymes

The reason for mutating the wild-type hen egg white lysozyme to LysE35A and LysE35Q was to diminish the bacteria lysis property (muramidase activity) of the wild-type lysozyme. To check if the mutated proteins have lost their muramidase activity, a turbidimetric activity assay with reference bacteria, *Micrococcus luteus* and *Pseudomonas putida*, was performed. The Gram positive *M. luteus* is used as the standard reference bacterium in lysozyme activity determination assays [98]. To determine the conditions for Gram negative bacteria binding by lysozyme *P. putida* was chosen as the model organism in this work. In the turbidimetric assay, the bacterial cells were mixed with the lysozyme variants and the time-dependent absorption at 450 nm was recorded. A decrease in absorption referred to bacteria lysis due to an active enzyme.

3.5.1 Enzymatic activity determination with Gram positive reference bacteria *M. luteus*

The determination of the lysozyme activity via turbidimetry assay was performed at 30°C with 1 μg of recombinant lysozymes that were purified and enriched with magnetic MagPrepSO₃ beads. Commercial, fully active lysozyme served as positive control, whereas cell free expression broth of GS115pPic9 cells, which are yeast cells that were transformed by lysozyme cDNA free pPic9, served as negative

control. Figure 3.25 shows that after 24 hours of incubation the Lyswt protein caused an absorption decrease to 35% of the initial value. These significant decrease of absorption showed that the protein purification with MagPrepSO₃ particles and the elution with high salt buffer as well as desalting did not denature the recombinant lysozymes. Additionally, it was shown that the mutated lysozymes LysE35A and LysE35Q did not exhibit bacteriolytic activity. The negative control did not show absorption decrease. These results showed that the exchange of the catalytic amino acid glutamate 35 by alanine (LysE35A) and by glutamine (LysE35Q) diminished the catalytic activity of the lysozyme. The chosen point mutations were suitable for deleting the lytic activity of the lysozymes. As the recombinantly expressed wild-type lysozyme (Lyswt) was still catalytically active, also the purification strategy was suitable for purification of lysozyme from the expression broth. The assay was performed at different temperatures and also with ammonium sulphate precipitated lysozymes. All results showed a significant OD decrease by Lyswt and the positive control, whereas the mutated proteins LysE35A and LysE35Q did not cause an OD decrease and thus, are not bacteriolytic.

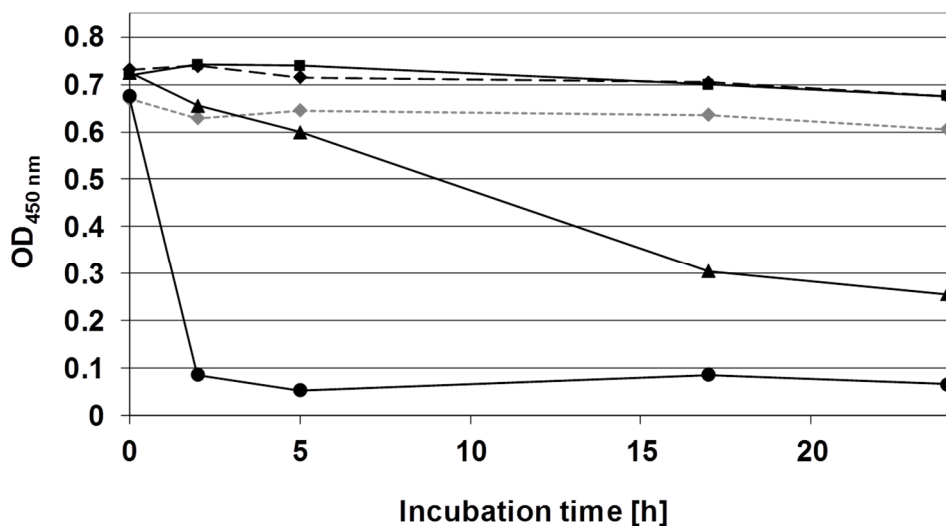


Figure 3.25: Determination of recombinant lysozyme activities with *M. luteus* cells. The lysozymes were purified with magnetic MAGPrepSO₃ beads. Fully active commercial hen egg white lysozyme (HEWL) served as positive control and expression broth of GS115pPic9 without lysozyme cDNA as negative control (no lysozyme). The temperature was 30°C.

--◇-- no lysozyme ● HEWL ▲ Lyswt -◇- -LysE35Q ■ LysE35A

3.5.2 Enzymatic activity determination with Gram negative reference bacteria *P. putida*

The above showed results were performed with Gram positive *M. luteus* bacteria. To test the lytic activity of lysozyme on Gram negative bacteria, the assay was accomplished with *P. putida*. To disrupt the outer membrane of the Gram negative bacterium, which hinders the binding of lysozyme to the peptidoglycan cell-wall, EDTA was added to the samples. The assay was performed at EDTA concentrations of 10 mM (shown in Figure 3.26), 25 mM, 50 mM, and 100 mM (shown in Figure 3.27). The *P. putida* cells were incubated with active wild-type commercial lysozyme (HEWL), HEWL and EDTA, EDTA without lysozyme (EDTA), Lyswt and EDTA, LysE35A and EDTA, and LysE35Q and EDTA. The assays were repeated two times. The standard deviations of the assay results with 100 mM EDTA were less than 5% and not shown as error bars. The presence of 100 mM EDTA alone caused a lysozyme-independent absorption decrease to up to 55%. Therefore, 10 mM EDTA was determined to be suitable for binding of bacteria and specific lysis by lysozyme. This amount also led to an OD decrease in the absence of lysozyme but the decrease was lower than with 100 mM EDTA, whereas in presence of HEWL or recombinant wild-type lysozyme (Lyswt) the absorption decrease was significantly higher. An absorption decrease was also recorded in samples including 10 mM EDTA and LysE35A or LysE35Q, which is rather caused by the EDTA and not by the mutated lysozymes. Therefore, all further Gram negative bacteria capturing experiments were performed with 10 mM EDTA.

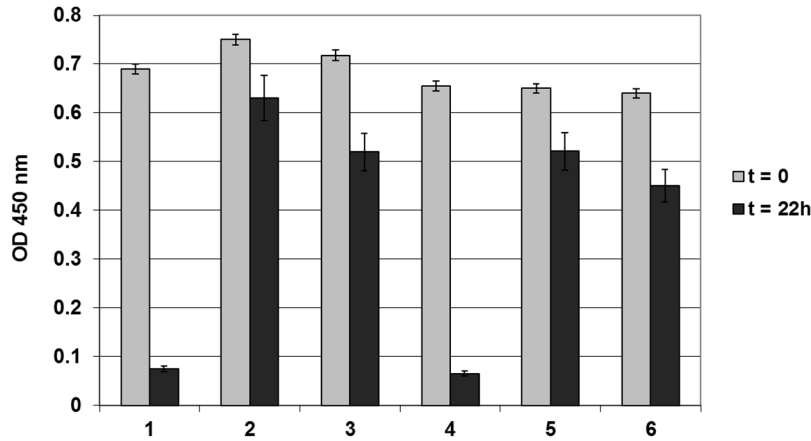


Figure 3.26: Enzymatic activity determination of recombinant lysozymes with *P. putida* cells and 10 mM EDTA. 1: 10 mM EDTA + 5 µg HEWL, 2: 5 µg HEWL, 3: 10 mM EDTA, 4: Lyswt + 10 mM EDTA, 5: LysE35A + 10 mM EDTA, 6: LysE35Q + 10 mM EDTA

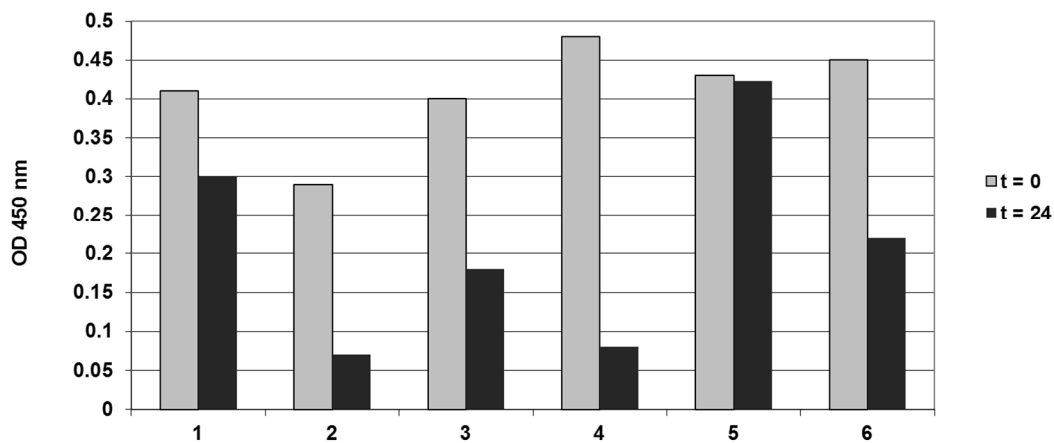


Figure 3.27: Enzymatic activity determination of recombinant lysozymes with *P. putida* cells and 100 mM EDTA. 1: 5 µg HEWL 2: 5 µg HEWL + 100 mM EDTA 3: 100 mM EDTA 4: Lyswt + 100 mM EDTA 5: LysE35A + 100 mM EDTA 6: LysE35Q + 100 mM EDTA

3.5.3 Summary of chapter 3.5

The determination of lytic activity of recombinantly expressed wild-type and mutated lysozymes (Lyswt, LysE35A, and LysE35Q) by turbidimetric assay with Gram positive reference bacterium *M. luteus* and the Gram negative bacterium *P. putida* showed that the point mutations introduced into lysozyme successfully diminished the catalytic bacteria lysis property of the mutants whereas the recombinant Lyswt

exhibited a significant OD decrease, which indicated that the recombinantly expressed wild-type lysozyme was still active. This showed that the secretional expression of the lysozymes in *P. pastoris* GS115 strains and the purification of the recombinant lysozymes from alkaline expression broth with MagPrepSO₃ particles did not denature the lysozymes. Furthermore, the suitable EDTA concentration for lysozyme binding on Gram negative bacteria due to outer membrane disruption was determined to be 10 mM.

3.6 Immobilization of mutated and wild-type lysozymes to magnetic beads

The recombinantly expressed and purified lysozymes were immobilized on commercial magnetic beads that served as the solid phase for further bacteria capture experiments. For this purpose, the purified recombinant lysozymes Lyswt, LysE35A, and LysE35Q were biotinylated by the use of the “EZ-Link® Sulfo-NHS-Biotin” kit (Thermo Scientific) in which the biotin is provided with an spacer arm with the length of 13.5 Å. The free biotins of the samples were removed by Zeba™ Desalt Spin Columns (Thermo Scientific). Biotinylated lysozymes were immobilized on the magnetic beads, which can be easily removed from samples containing other solid contaminations by magnetic forces. Due to their superparamagnetic character, the beads do not have a “magnetic memory” and were easily resuspended after permanent magnet removal. The magnetic beads used in the project were commercially available magnetic beads functionalized with protein G (Protein G Mag Sepharose) or streptavidin (MPVA SAV2, Dynabeads® M270 Streptavidin (DS M270), Dynabeads® M280 Streptavidin (DS M280), Dynabeads® MyOne™ Streptavidin T1 (DMS T1), Dynabeads® MyOne™ Streptavidin C1 (DMS C1)). All immobilizations were performed according to the manufacturer’s instructions (GE Healthcare, Chemagen, Invitrogen).

3.6.1 Lysozyme immobilization to Protein G Mag Sepharose beads

The immobilization of the lysozymes onto protein G functionalized 100 µm particles was mediated by HEWL antibodies that were bound by protein G. The beads were incubated with the antibody and washed to remove unbound proteins and subsequently incubated with the purified recombinant lysozymes Lyswt, LysE35A,

and LysE35Q. The success of immobilization of the lysozymes was checked by Western blot analysis of the proteins after their elution with 2.5% acetic acid (Figure 3.28). This elution condition is known to cause desorption of the antibodies from protein G. Therefore, the samples blotted onto membrane also contained anti-lysozyme IgG. Besides the lysozyme band corresponding to the MW of 14.6 kDa, more bands are seen on the blot with higher molecular weights (Figure 3.28 lanes 4-7). These could correspond to oligomeres of lysozyme, IgG bound lysozymes, and also to free IgG eluted from the beads. These additional bands hindered the quantification of previously bound lysozymes. A negative control sample that consists of an eluate of Protein G Mag Sepharose beads without lysozyme immobilization was loaded on lane 7 (Figure 3.28).

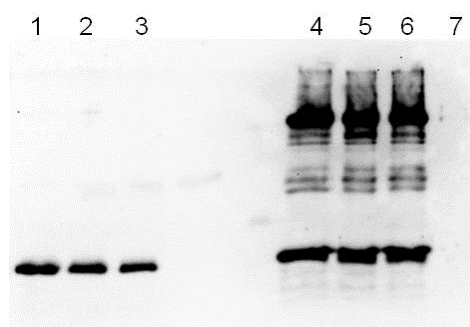


Figure 3.28: Western blot for immobilization analysis of lysozymes to Protein G Mag Sepharose particles. Lanes 1-3: lysozyme standard 10, 7, and 5 ng. Lanes 4-6: acetic acid eluates from Protein G Mag Sepharose beads after lysozyme immobilization. Lane 7: negative control.

3.6.2 Lysozyme immobilization to Dynabeads® and on M-PVA SAV2

The lysozyme immobilization to Dynabeads® and to M-PVA SAV2 beads was based on streptavidin-biotin interactions. Therefore, the purified recombinant lysozymes were biotinylated at their primary amines by commercial kit (EZ-Link® Sulfo-NHS-Biotin/ Thermo Scientific). The biotins used had a spacer arm with a length of 13.5 Å. The biotinylated lysozymes were incubated with MPVA SAV2, DS M270 (designated as M270), DS M280 (designated as M280), DMS T1 (designated as T1), and DMS C1 (designated as C1) for immobilization. The beads were washed to remove the unspecifically adsorbed proteins and then the whole lysozyme-bead constructs were blotted onto a PVDF membrane. During the steps of immunoblotting, the beads were

partially washed away. This prohibited the quantification of bound lysozymes, thus was only a qualitative determination of the success of the lysozyme immobilization on the beads. The blots are shown in Figures 3.29 and 3.30.

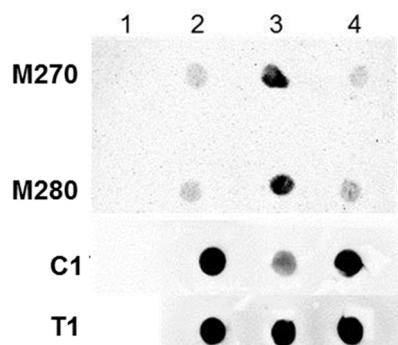


Figure 3.29: Western blot for immobilization analysis of lysozymes to Dynabeads®. M270: Dynabeads® Streptavidin M270, M280: Dynabeads® Streptavidin M280, C1: Dynabeads® Myone™ C1, T1: Dynabeads® Myone™ T1. Lane 1: negative control; unfunctionalized beads, lane 2: beads functionalized with Lyswt, lane 3: beads functionalized with LysE35A, lane 4: beads functionalized with LysE35Q

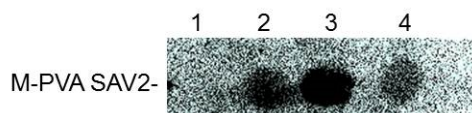


Figure 3.30: Western blot for immobilization analysis of lysozymes to M-PVA SAV2. Lane 1: negative control; unfunctionalized beads, lane 2: beads functionalized with Lyswt, lane 3: beads functionalized with LysE35A, lane 4: beads functionalized with LysE35Q.

3.6.3 Summary of chapter 3.6

For Protein G Mag Sepharose, immobilization was achieved by Protein G-antibody-lysozyme interaction. For M-PVA SAV2 and Dynabeads® Streptavidin, immobilization was achieved by streptavidin-biotin interaction. The Western blots showed that immobilization was successful with all the types of beads that were used and consequently all the beads were used for further bacteria capture experiments.

3.7 Detection of lysozyme-dependent bacteria capture by fluorescence microscopy

A rapid proof of principle for specific, lysozyme-dependent capture of bacteria with lysozyme functionalized beads was performed by fluorescence microscopy. For this assay, the streptavidin-functionalized magnetic M-PVA SAV2 beads were labelled with Alexa Fluor® 594 previous to protein immobilization. This caused a red or orange-yellow fluorescence of the beads. First, HEWL, which exhibited bacteriolytic activity, was biotinylated and then immobilized to the streptavidin functionalizes M-PVA SAV2 beads. These constructs were immobilized to the surface of μ - channels of biotinylated, Poly-L- lysine covered microscopy slides. Afterwards, Syto9 labelled, green fluorescing *M. luteus* cells were loaded to the channels and then the channels were washed few times with buffer. In channels with immobilized lysozyme functionalized beads the bacteria were attached to the constructs. Furthermore, after an incubation period of two hours, an elongation of the *M. luteus* cells observed. This indicated the lysis of the spherical bacteria by the active lysozyme on the beads (Figure 3.31). Fluorescence microscopy showed that immobilization of the wild-type lysozyme to the beads surface did not diminish the bacteriolytic activity. Hence, the use of magnetic beads as an easy separable solid phase for lysozyme based bacteria capture was applicable to bacteria enrichment and separation with immobilized recombinant lysozymes.

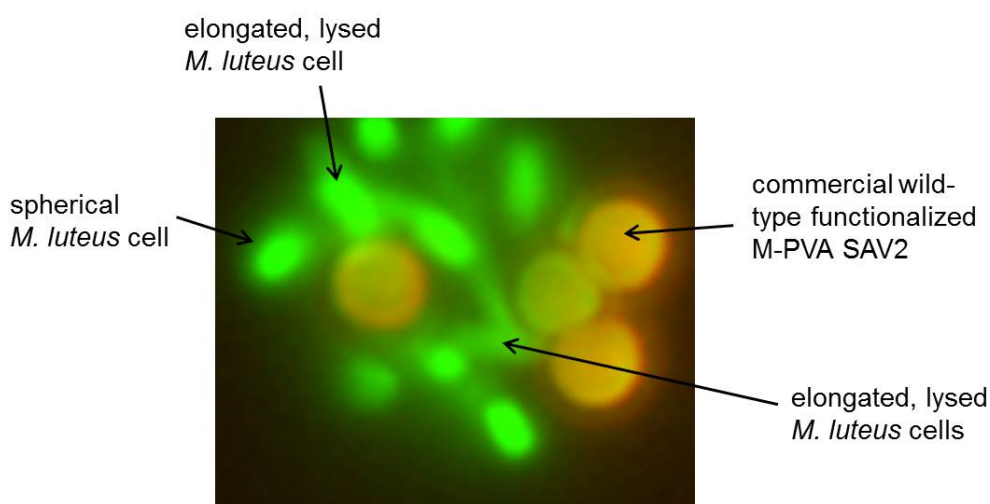


Figure 3.31: Fluorescence microscopy images of *M. luteus* cells lysed by commercial lysozyme functionalized magnetic beads.

The microscopy assay demonstrated that immobilization of lysozyme on μ -scaled magnetic particles via streptavidin- biotin interaction does not influence the bacteria binding capability of lysozyme. Hence, the recombinant wild-type lysozyme (Lyswt) and the mutated lysozymes (LysE35A and LysE35Q) were immobilized on fluorescence labelled M-PVA SAV2 particles and these constructs were used for capture of Syto9® labelled bacteria from suspensions. After incubation with bacteria, the beads were separated with a magnetic rack, washed with buffer to remove the unspecifically attached bacteria and then resuspended for fluorescence-microscopy detection. To determine if there was also unspecific adsorption of bacteria to the surface of the beads, non-functionalized M-PVA SAV2 beads were also tested. The functionalized and unfunctionalized beads were tested on *M. luteus* cells (Figure 3.32) and also on the Gram negative *P. putida* cells (Figure 3.33). The figures show that the particles performed well in specific bacteria capture as the unfunctionalized beads did not separate a significant amount of bacteria. The Alexa Fluor® 594 labelled beads appeared red or orange, the microorganisms had a green fluorescence due to the Syto9® label. The fluorescence microscopy based assay delivered the first hint for the success of the method in enrichment of Gram positive and Gram negative bacteria from solution. This was a qualitative method and did not allow the quantification of the recovery of bacteria by the beads. Therefore, further experiments for proving the applicability of the beads to bacteria capture were performed.

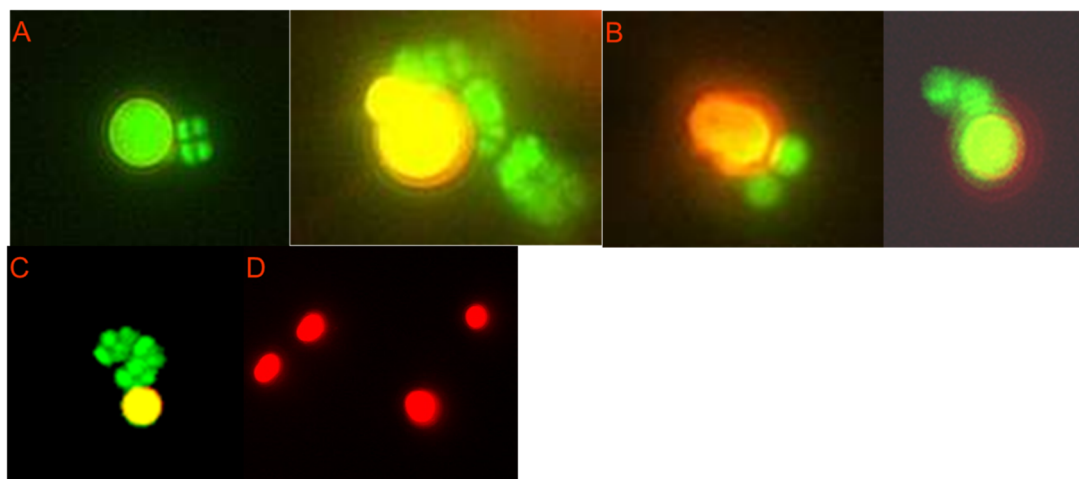


Figure 3.32: Fluorescence microscopy images of *M. luteus* cells captured by recombinant lysozyme functionalized magnetic beads. The cells were incubated with DNA intercalating fluorescent dye Syto9® and appear therefore green. The magnetic beads were labelled with Alexa Fluor® 594 and appear orange-yellow or red. The beads were incubated with a *M. luteus* (green) suspension and were separated by a permanent magnet from solution and washed with buffer. The immobilization of the recombinant proteins LysE35A (A), LysE35Q (B), and Lyswt (C) was achieved by biotin-streptavidin interactions.

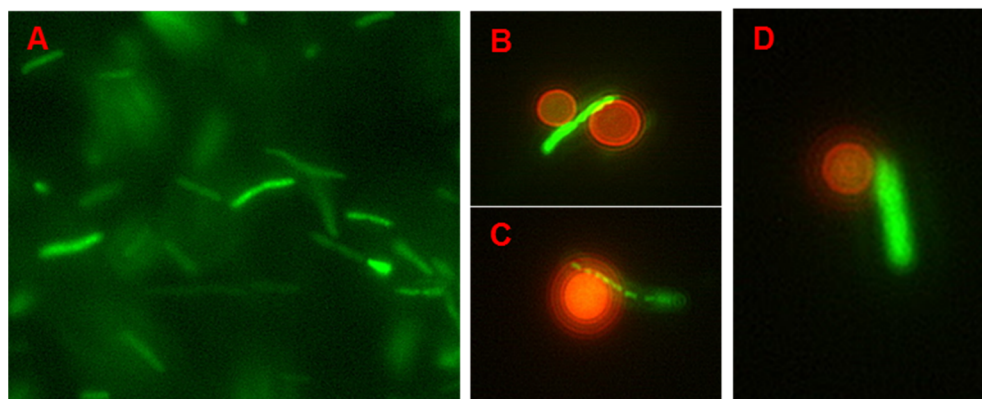


Figure 3.33: Fluorescence microscopy images of *P. putida* cells captured by recombinant lysozyme functionalized magnetic beads after incubating the Syto9® stained bacteria with 10 mM EDTA. The stained *P. putida* cells are shown in A. The immobilization of the recombinant proteins Lyswt (B), LysE35A (C), and LysE35Q (D) was achieved by streptavidin-biotin interactions.

3.8 Bacteria capture from tap water by using lysozyme functionalized M-PVA SAV2 beads

After verification of the lysozyme functionalized magnetic beads based specific bacteria capture by fluorescence microscopy, the constructed particles were applied to capture of bacteria from tap water. An amount of 300 μg of lysozyme functionalized M-PVA SAV2 beads were incubated for two hours with 400 μl of 10^4 -fold concentrated tap water. The particles were washed two times with 0.1 M phosphate buffer at pH 5.5, and subsequently were resuspended in 50 μl buffer. Then the cells were lysed by freeze-thaw cycles. 5 μl of the samples were used as templates for amplification PCR using the universal primer pair GC 27F/GC517R. The PCR results are shown in Figure 3.34. As positive control *Pseudomonas aeruginosa* DNA was used (Figure 3.34 lane 1)

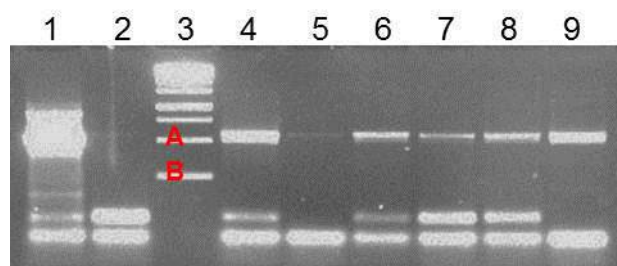


Figure 3.34: Agarose gel of PCR results of 10^4 fold concentrated tap water after bacteria capture with lysozyme coated M-PVA SAV2. The primer-pair used was GC 27F/GC517R. Lane 1: DNA of *P. aeruginosa*, lane 2: steril water, lane 3: DNA marker, lane 4: 10^4 - fold concentrated tap water, lane 5: unconcentrated tap water, lane 6: tap water incubated with unfunctionalized M-PVA SAV2 particles, lane 7: concentrated water incubated with M-PVA SAV2-Lyswt, lane 8: concentrated water incubated with M-PVA SAV2-LysE35A, lane 9: concentrated water incubated with M-PVA SAV2-LysE35Q. A: 1.0 kb band B: 0.5 kb band.

After amplification of the DNA of by PCR, 50 μl of the templates were used for denaturing gradient gel electrophoresis (DGGE) with an urea concentration ranging from 40% to 70%. The results are shown in Figure 3.35. The comparison of the bacteria pattern of the concentrated water sample by centrifugation (Figure 3.35 lane 2) and the patterns of samples that were subject to magnetic bead based bacteria capture (Figure 3.35 lanes 4-7) with unconcentrated tap water sample (Figure 3.35

lane 3) show that a concentration step was necessary to reflect the high bacteria diversity present in tap water. Therefore, contamination analysis of tap water without previous bacteria enrichment does not encompass the whole range of bacteria present in the water and hence, can result in false negative outcomes. Analysis of the samples that were subject to bead based capture (Figure 3.35 lanes 4-7) show that the beads largely succeeded in catching the bacteria that were enriched by centrifugation. The beads have the same pattern but with lower band intensities. In contrast to the fluorescence microscopy based assay, the bacteria pattern of the sample enriched with unfunctionalized beads, exhibited the same pattern as the functionalized beads. This indicated an unspecific, lysozyme-independent adsorption of bacteria onto the surface of the beads. The quantification of the unspecific capture of bacteria, however, is not possible by this method considering the PCR amplification previous to DGGE and its qualitative nature.

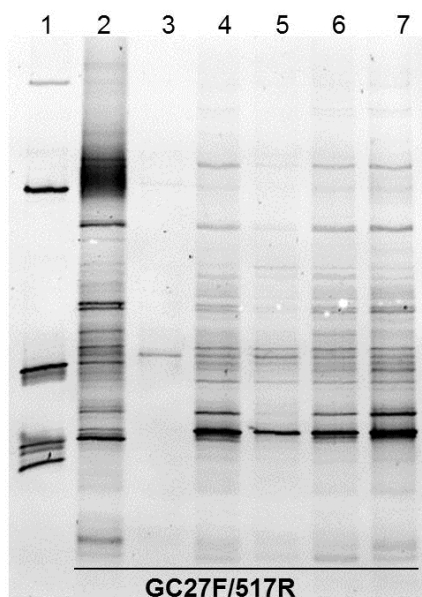


Figure 3.35: DGGE gel with 40%-70% urea.

Lane 1: DNA marker, lane 2: 10^4 - fold concentrated tap water previous to magnetic beads based bacteria capture, lane 3: unconcentrated tap water, lane 4: bacteria captured with unfunctionalized beads (unspecific capture), lane 5: bacteria captured with M-PVA SAV2-Lyswt, lane 6: bacteria captured with M-PVA SAV2-LysE35A, lane 7: bacteria captured with M-PVA SAV2-LysE35Q.

3.9 Evaluation of the specific capture yield of lysozyme functionalized magnetic particles

The based capture detection of the capture of bacteria by the means of fluorescence microscopy and DGGE were only qualitative methods for evaluating the success of the specific enrichment of bacteria with the lysozyme functionalized magnetic beads. For the quantification of the capture yield and additionally evaluating the amount of unspecific capture with unfunctionalized beads, quantitative PCR (qPCR) detection with the hydrolysis probe technique or colony counting on nutrient agar were performed after bacteria enrichment from solutions. Unspecific bacteria adsorption onto the bead surface was abated by adding 0.1% BSA to the samples. After incubation of the magnetic beads with bacteria, they were separated by permanent magnets, washed with buffer and then resuspended in a desired volume, enabling the concentration of the captured bacteria. If the amount of captured bacteria was analysed by qPCR, the sample was subject to freeze-thaw lysis to set the DNA free for nucleic acid based quantification. Previous to lysis, $450 \mu\text{g ml}^{-1}$ polyadenine were added to the solution, in order to inhibit DNA adsorption to the beads surface during freeze-thaw lysis, which limits DNA detection due to steric reasons. For DNA detection duplicates or triplicates of the bead-free supernatants were used. Figure 3.36 shows the amplification plot of the qPCR based DNA detection of *E. faecalis* DNA with known amounts. A 10-fold dilution series with known DNA amounts was used to generate a standard curve and the DNA amounts of the unknown samples were determined by plotting them to the standard curve (Figures 3.36 and 3.37). The lowest detectable DNA amount was $10 \text{ fg } \mu\text{l}^{-1}$. This corresponds to 3 *E. faecalis* cells. The number of the captured cells were calculated based on the DNA amounts detected. The genome weight of *E. faecalis* was determined to be 3.1 fg DNA per cell [114]. Final bacteria amounts in PCR templates and recovery efficiencies of the beads were calculated under consideration of dilution or concentration factors.

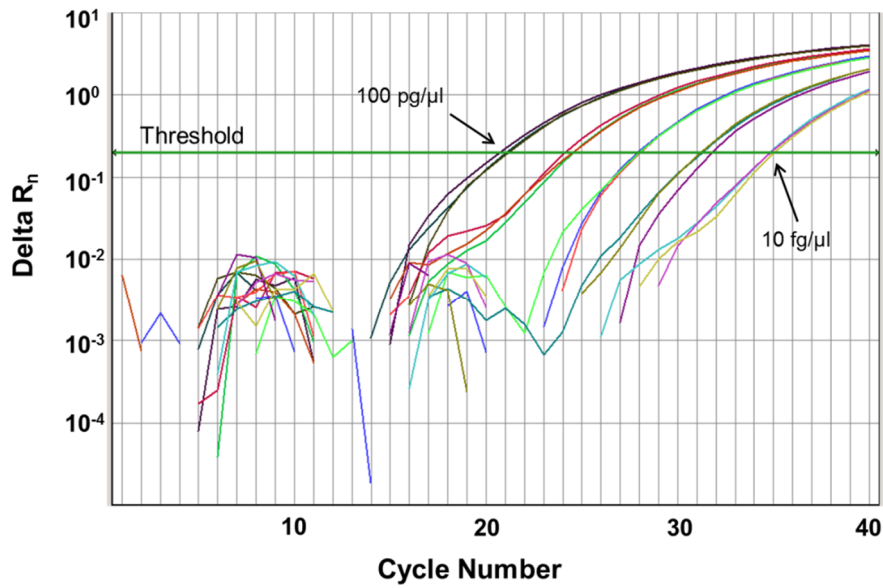


Figure 3.36: Amplification plot of 10-fold dilutions of *E. faecalis* DNA.

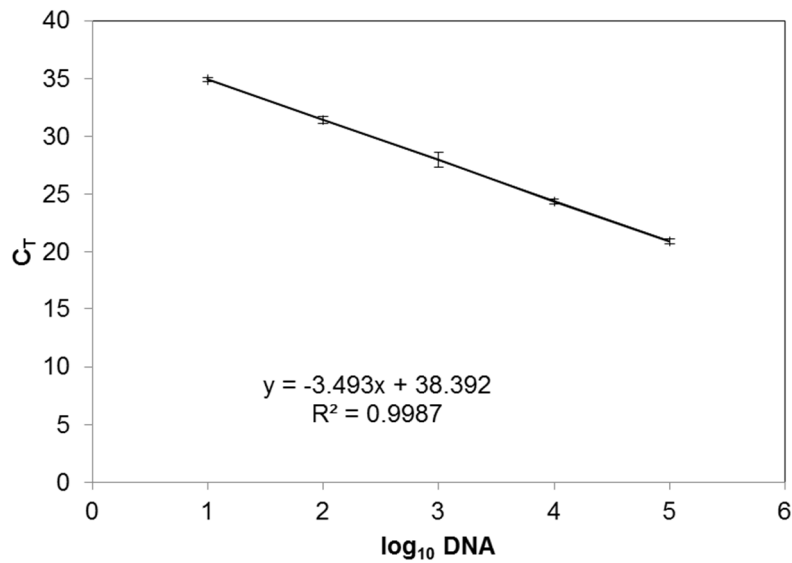


Figure 3.37: Standard curve for PCR based DNA quantification for *E. faecalis*. The C_T values were the threshold fluorescence is exceeded first is shown as a function of DNA amount.

3.9.1 Evaluation of molecular biology based and cultivation based quantification

Two methods for the quantification of the captured bacteria cells were evaluated: cultivation based detection on nutrient agar plates and qPCR. Duplicates of Lyswt

functionalized DS M270 particles in concentrations ranging from $100 \mu\text{g ml}^{-1}$ to $700 \mu\text{g ml}^{-1}$ were used for the capture of *E. faecalis* in a 1 ml suspension. The initial bacteria value was determined to be $4000 \text{ cells ml}^{-1}$ by qPCR whereas CFU determination via plate counting resulted in 1000 CFU ml^{-1} for the same bacteria suspension. After incubation of the beads with bacteria, they were separated by a permanent magnet, washed three times with buffer and then resuspended in 1 ml. A portion of $5 \mu\text{l}$ magnetic bead-free supernatant was used as template for qPCR after freeze-thaw lysis. The DNA concentrations determined in $5 \mu\text{l}$ template were extrapolated to 1 ml initial capture volume. This PCR based quantification of bacteria showed a correlation between the applied particle concentration and calculated number of captured bacteria cells, ranging from 30% to 64% for the first series of experiments. For the second series, a recovery ranging from 19% to 60% was determined. A correlation between the used particle concentration and recovery of bacteria was proven, with the highest recovery provided with a particle concentration of $700 \mu\text{g ml}^{-1}$ (Figure 3.38 and Table 7). The duplicates were in good accordance with each other.

For determination of the CFU values by colony counting, $100 \mu\text{l}$ of the resuspended beads were directly plated on nutrient agar. The bacteria were not eluted from the beads previous to plating. This method did not reveal any correlation between captured cells and particles and additionally the duplicates varied from each other, although the same initial amounts of bacteria and particles were used (Figure 3.39 and in Table 7). The determination of bacteria recovery by cultivation seemed to be unsuitable for quantification of bacteria capture by magnetic beads.

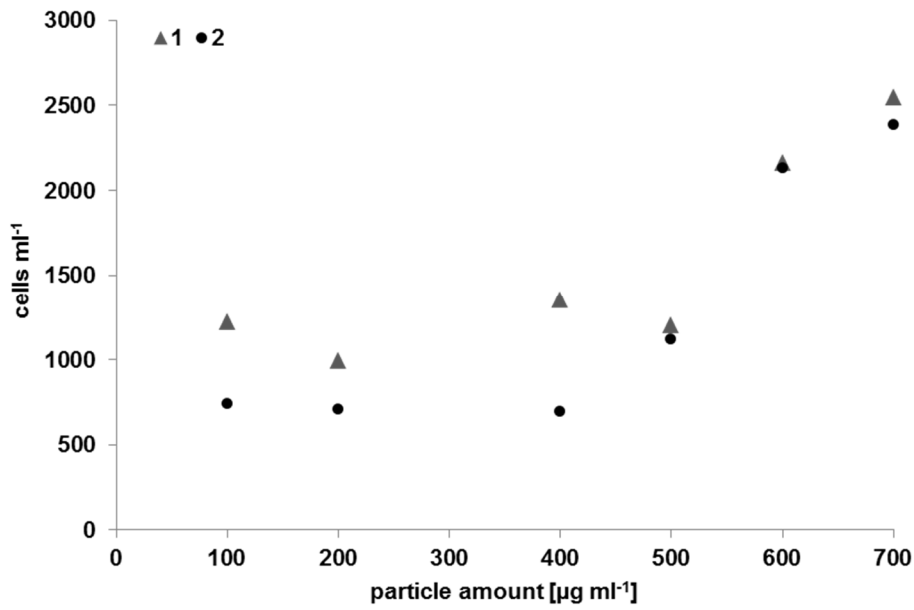


Figure 3.38: The cell capture as a function of particle amount. Determined based on DNA detection by qPCR

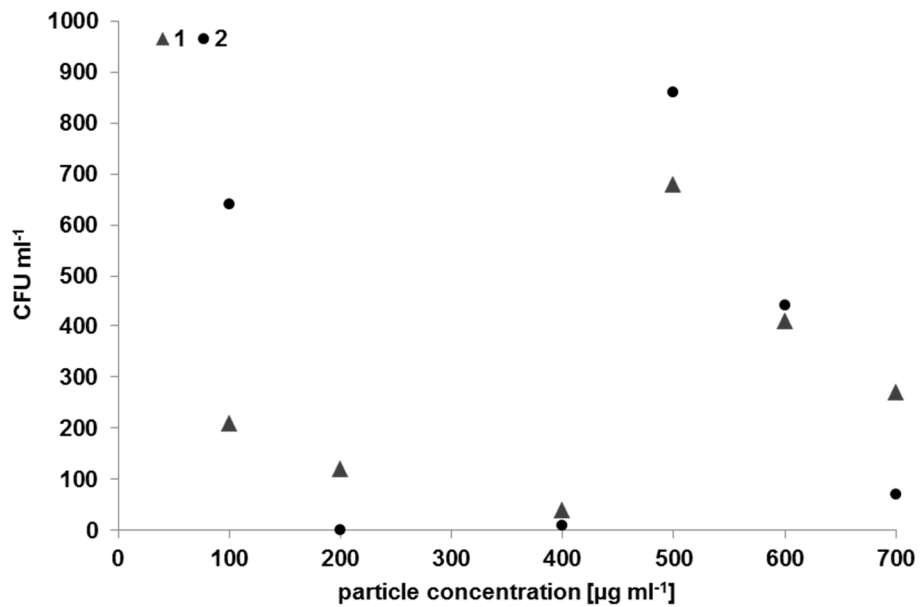


Figure 3.39: The captured CFU amount as a function of particle amount. Determined based on colony counting.

Table 7: The recovery of Lyswt functionalized DS M270 determined by qPCR and colony counting on nutrient agar.

Particle amount [$\mu\text{g ml}^{-1}$]	100	200	400	500	600	700
PCR recovery-1 (of 4000 cells ml^{-1})	30%	25%	34%	30%	54%	64%
PCR recovery-2 (of 4000 cells ml^{-1})	19%	18%	17 %	28%	53%	60%
Plate count recovery-1 (of 1000 CFU ml^{-1})	21%	12%	4%	68%	41%	27%
Plate count recovery-2 (of 1000 CFU ml^{-1})	64%	0%	1%	86%	44%	7%

3.9.2 Determination of capture threshold of functionalized magnetic beads for *E. faecalis*

To determine the threshold of the bacteria detection of DS M270 and DS M280 that were either functionalized with the recombinant wild-type lysozyme Lyswt or the two mutated proteins LysE35A and LysE35Q, 250 $\mu\text{g ml}^{-1}$ ($1.5\text{-}1.75 \times 10^7$ beads) of the particles were incubated in 1 ml of 10-fold dilutions of *E. faecalis* suspension ranging from 10 to 10^4 cells ml^{-1} .

In two out of six variations of the beads 270-LysE35Q and 280-LysE35A captured 70% and 60% out of 10 cells ml^{-1} . All of the beads used were successful in detection of *E. faecalis* cells from the bacteria suspensions with initial cell concentrations of 10^2 cells ml^{-1} . The maximal cell number of captured bacteria with 250 μg beads was 1070 (270-LysE35Q) from an initial bacteria value 10^4 cells ml^{-1} . This corresponds to 10.7% of the initial amount of bacteria (Table 8).

Table 8: Recovery of *E. faecalis* with functionalized Dynabeads® M270 and M280 Streptavidin.

Beads Bacteria ml ⁻¹	DS M270			DS M280		
	Lyswt	LysE35A	LysE35Q	Lyswt	LysE35A	LysE35Q
10	0%	0%	70%	0%	60%	0%
10 ²	16%	16%	10%	6%	13%	6%
10 ³	4.8%	13.2%	9.9%	10.5%	2.7%	8.7%
10 ⁴	2.04%	5.4%	10.7%	0.97%	3.11%	0.95%

3.9.3 Enrichment of *E. faecalis* with magnetic beads from liquids

To determine the efficiencies of the functionalized magnetic beads, bacteria capture assays were performed in phosphate buffer. To additionally determine the unspecific bacteria adsorption on magnetic surfaces, an equal amount of unfunctionalized beads was used. The beads used for these assays were M-PVA SAV2, Dynabeads® M-270 Streptavidin (DS M270), Dynabeads® M-280 Streptavidin (DS M280), Dynabeads® MyOne™ Streptavidin C1 (DMS C1) and Dynabeads® MyOne™ Streptavidin T1 (DMS T1).

3.9.3.1 M-PVA SAV2 beads

600 $\mu\text{g ml}^{-1}$ of M-PVA SAV2 beads were used for *E. faecalis* capture in a total volume of 1 ml. After the capture, the beads were washed three times with buffer containing 0.1% Tween20™ and then with detergent-free buffer. The total concentration of bacteria in the sample was determined as 3×10^4 cells ml^{-1} by qPCR. For M-PVA SAV2, the highest capture efficiency of 27% was achieved by recombinant the functionalization with wild-type lysozyme (Lyswt). The beads functionalized with mutated lysozyme (LysE35A 13% and LysE35Q 5%) yielded even in a lower bacteria capture than unfunctionalized beads (13%) (Figure 3.40).

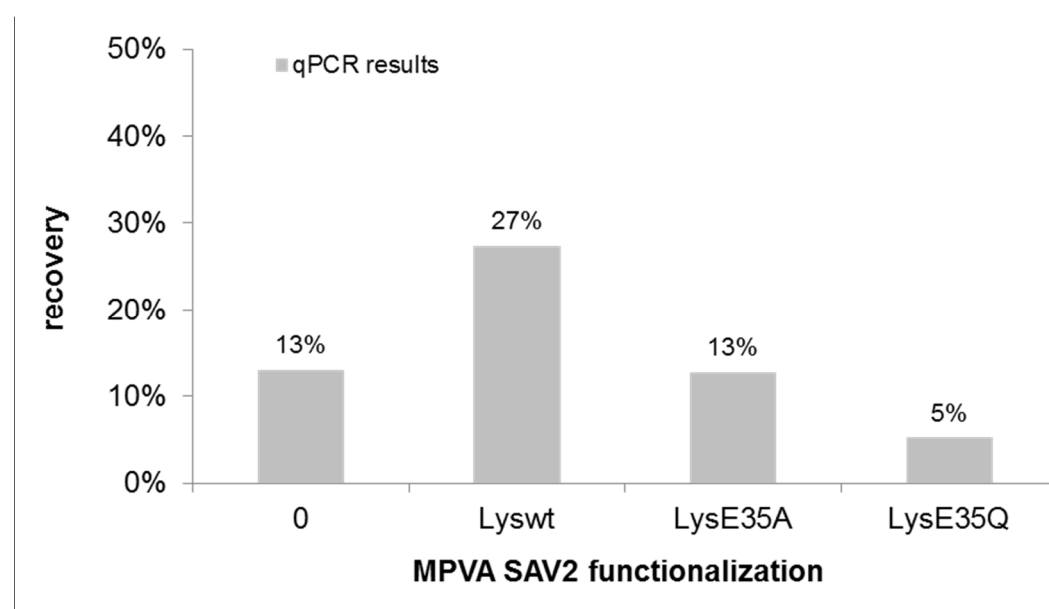


Figure 3.40: Recovery of bacteria with 600 μg of lysozyme functionalized and unfunctionalized M-PVA SAV2 beads. The initial amount of bacteria was 3×10^4 cells ml^{-1} .

3.9.3.2 DS M270 and DS M280

The recovery rates of the beads DS M270 (designated as 270) and DS M280 (designated as 280) are shown in Figure 3.41. The initial cell concentration was 4.6×10^4 cells ml^{-1} and the concentration of the beads was $150 \mu\text{g ml}^{-1}$. For both kinds of beads DS M270 and DS M280, the functionalization with LysE35Q achieved the highest recovery. This was a recovery of 86.4% for DS M270 and 9.5% for DS M280. The unfunctionalized beads 270-0 and 280-0 had unspecific capture yields of 2.8% and 0% from initial amount of bacteria. The beads 270-EA, 280-wt, and 280-EA had

recoveries lower than 2% whereas the 270-wt and 280-EQ beads had a recovery of nearly 10%.

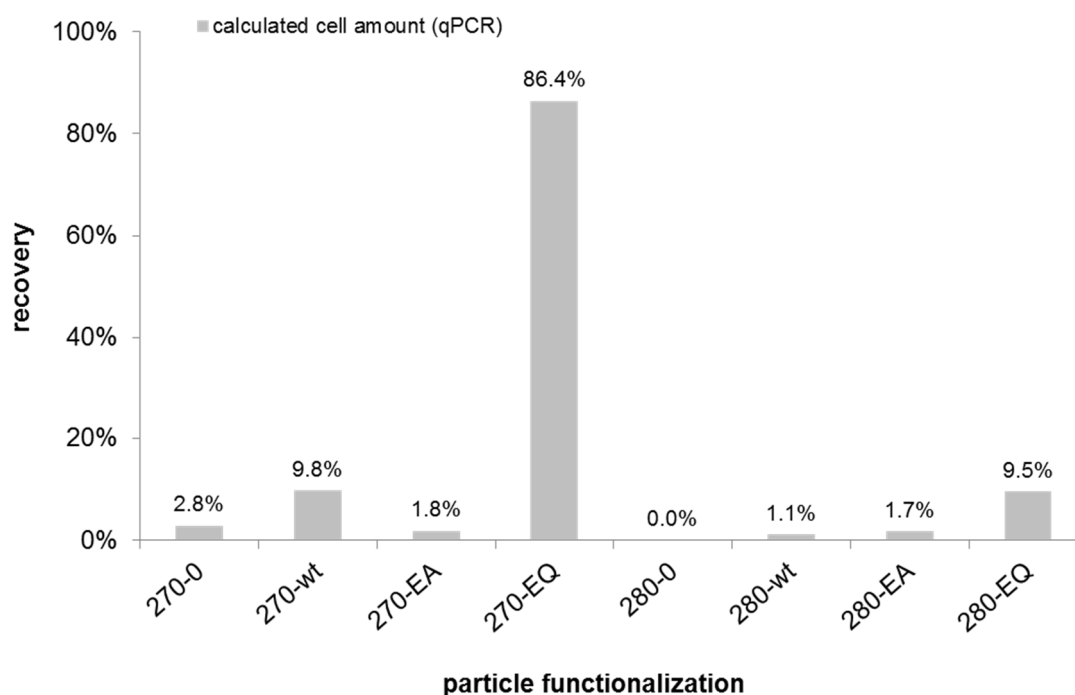


Figure 3.41: The qPCR based cell capture recovery of lysozyme functionalized and unfunctionalized Dynabeads M-270/M-280 Streptavidin for *E. faecalis*. Initial cell amount was 4.6×10^4 cells ml^{-1} .

3.9.3.3 DMS C1 and DMS T1

The recovery rates of the beads DMS C1 (designated as C1) and DMS T1 (designated as T1) are shown in Figure 3.42. The initial cell concentration was 7×10^6 cells ml^{-1} and the concentration of the beads was $150 \mu\text{g ml}^{-1}$. The LysE35Q functionalized beads (C1-EQ and T1-EQ) led to the highest recovery of 2.6% and 4.4%, respectively. This low recovery values are related to the relatively high initial cell concentrations (see Chapter 3.9.3.4). The unspecific capture with unfunctionalized beads (C1-0 and T1-0) were only 0.04% and hence, less than 1% of lysozyme-dependent capture of bacteria achieved with DMS C1 and 1.5% of the lysozyme-dependent capture achieved with DMS T1.

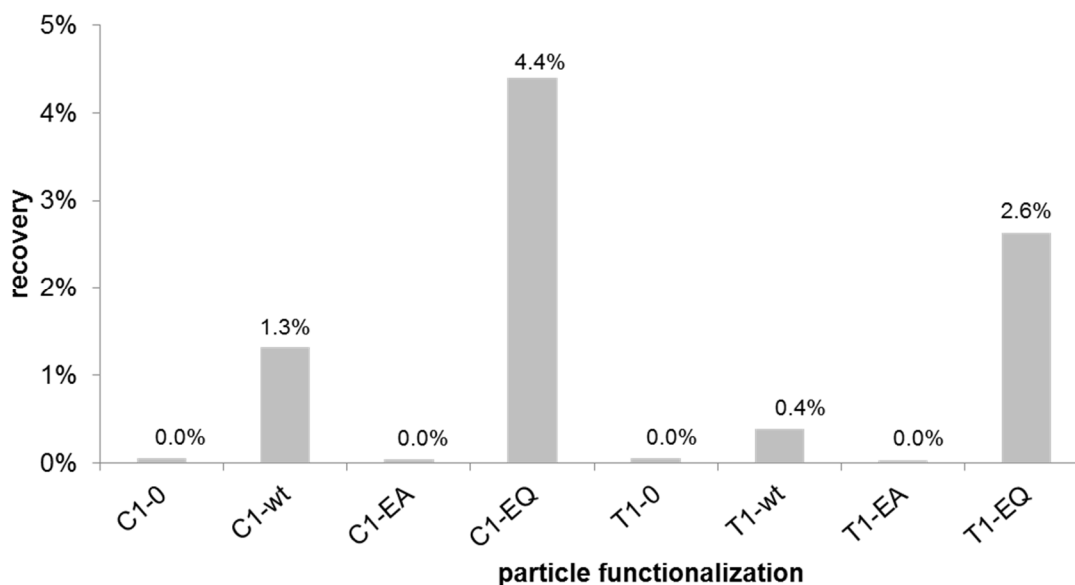


Figure 3.42: The *E. faecalis* recovery with functionalized and unfunctionalized MyOne™ Streptavidin C1 and MyOne™ Streptavidin T1 beads determined with qPCR. The initial cell amount was 7×10^6 cells ml^{-1} .

3.9.3.4 Comparison of capture efficiencies from suspensions

The concentration of the applied beads during the capture experiments varied among the different kinds of beads. Therefore, the calculated recoveries of capture of bacteria were standardized to 1 μg beads and listed in table 9. The amounts of captured cells were extrapolated to the initial capture volume of 1 ml. From this table, the evaluation of the performance of the beads was set out. The highest number of cells was captured with LysE35Q functionalized DMS C1 beads ($2053 \text{ cells } \mu\text{g}^{-1} \text{ml}^{-1}$) and DMS T1 beads ($1213 \text{ cells } \mu\text{g}^{-1} \text{ml}^{-1}$), whereas the unfunctionalized DMS beads did not capture a detectable amount of bacteria. This indicates that this functionalization is very efficient for bacteria capture and the beads do unspecifically adsorb bacteria to their surface.

The initial cell concentrations were 3×10^4 cells ml^{-1} in capture experiments with M-PVA SAV2, 4.6×10^4 cells ml^{-1} in capture experiments with DS M278 and DS M280, and 7×10^6 cells ml^{-1} in capture experiments with DSM C1 and DSM T1.

Table 9: Relative number of captured bacteria cells calculated for 1 μg magnetic particles with different functionalizations

	M-PVA SAV2	DS M270	DS M280	DMS C1	DMS T1
unfunctionalized (cells $\mu\text{g}^{-1} \text{ml}^{-1}$)	6.5	8.6	0	0	0
Lyswt (cells $\mu\text{g}^{-1} \text{ml}^{-1}$)	13.5	30	3.4	606	187
LysE35A (cells $\mu\text{g}^{-1} \text{ml}^{-1}$)	6.5	5.5	2.6	0	0
LysE35Q (cells $\mu\text{g}^{-1} \text{ml}^{-1}$)	2.5	265	29	2053	1213

3.9.4 *E. faecalis* capture from lettuce

After successful application of the functionalized beads to bacteria enrichment from suspensions, artificially spiked food with *E. faecalis* were subject to bacteria capture. The lysozyme functionalized magnetic beads M-PVA SAV2, Dynabeads® M-270 Streptavidin (DS M270), Dynabeads® M-280 Streptavidin (DS M280), Dynabeads® MyOne™ Streptavidin C1 (DMS C1) and Dynabeads® MyOne™ Streptavidin T1 (DMS T1) were applied for these experiments.

Iceberg lettuce leaves were artificially contaminated overnight with bacteria, homogenized and then incubated with the functionalized magnetic beads. 12 g of lettuce were incubated in tap water, which was artificially contaminated with *E. faecalis*, for 14 hours under constant shaking with 140 rpm at 25°C. The tap water was then removed and lettuce was washed two times with tap water, not contaminated with *E. faecalis*. To elute the bacteria from lettuce, the leaves were incubated for 4 hours in phosphate buffer containing 0.5% Tween20™. Then two different capture methods were applied as described in Figure 3.43. A: Tween containing buffer after removal of the lettuce was used for capture of bacteria with magnetic beads and B: the lettuce was homogenized in the Tween containing buffer and then filtrated. The filtrate was further used as template for the magnetic beads based capture of bacteria. Those samples were designated as A or B, accordingly.

The elution buffers and homogenized lettuce were diluted with water previous to the capture experiments. The water contained 0.1% BSA to inhibit unspecific bacteria

adsorption to bead surface. The quantification of the capture efficiencies was done by qPCR.

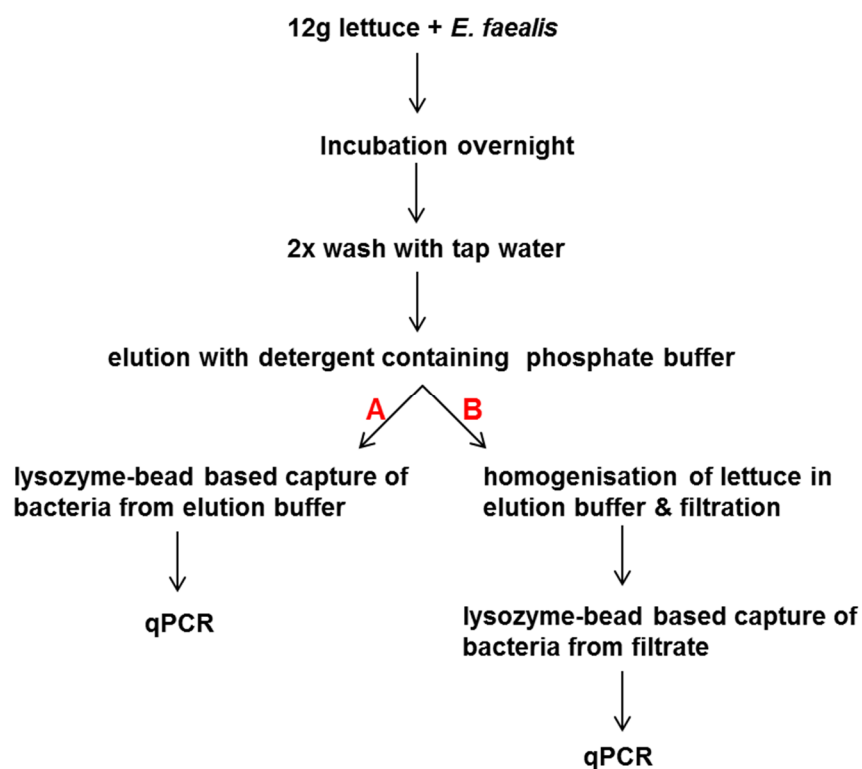


Figure 3.43: Scheme of sample preparation for lysozyme-bead based *E. faecalis* capture from food.

3.9.4.1 M-PVA SAV2 beads

The results for the *E. faecalis* capture experiments with M-PVA SAV2 beads are shown in Figure 3.44. 500 $\mu\text{g ml}^{-1}$ beads were used for approaches A and B. Initial bacteria amounts were determined to be 10^4 cells ml^{-1} (A) and 5.8×10^3 cells ml^{-1} (B). The unfunctionalized beads in each capture preparation (A SAV2-0 and B SAV2-0) did not capture a detectable amount of bacteria. Whereas Lyswt functionalized beads from approach A (A SAV2-wt) captures 40.9%, LysE35A and LysE35Q functionalized beads from approach B (B SAV2-EA and B SAV2-EQ) captured bacteria amounts of 57.4% and 57.4% of the initial bacteria value. These results showed that the capture yield of the beads was specific and based on lysozyme-peptidoglycan interaction.

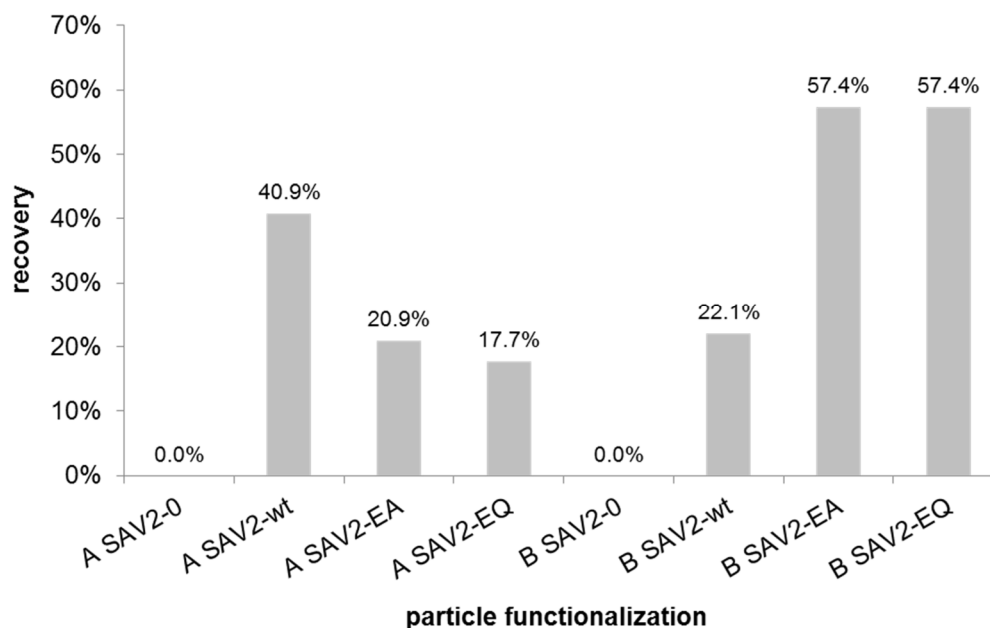
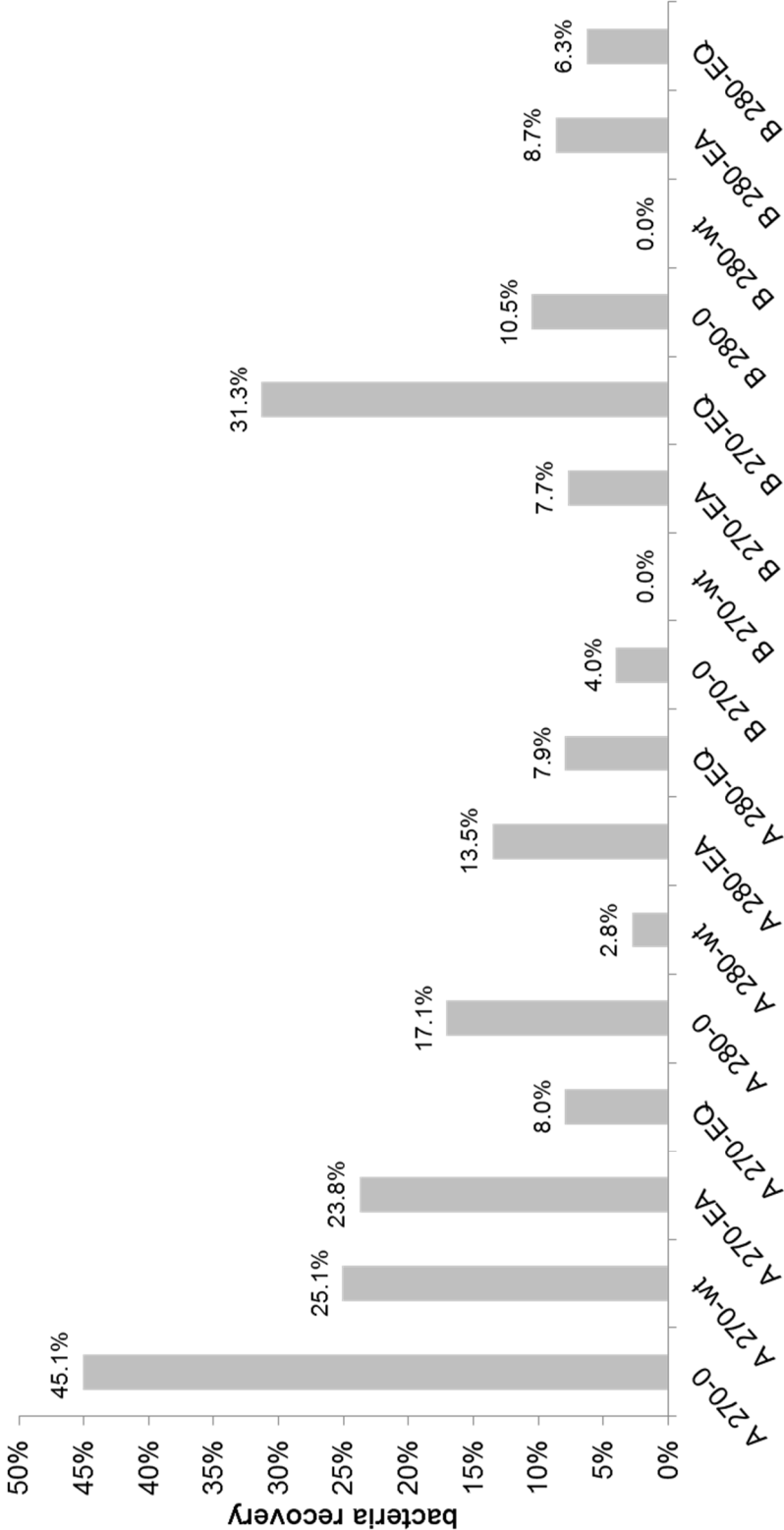


Figure 3.44: Bead based *E. faecalis* recovery with M-PVA SAV2 beads from lettuce. The initial cell amounts were 10^4 cells ml^{-1} (A) and 5.8×10^3 cells ml^{-1} (B) (qPCR).

3.9.4.2 DS M270 and DS M280

The results for capture recoveries of *E. faecalis* with DS M270 (270) and DS M280 (280) are shown in figure 3.45. For the capture, $500 \mu\text{g ml}^{-1}$ of lysozyme functionalized and unfunctionalized beads were used. The initial amount of bacteria was determined as 1.1×10^4 cells ml^{-1} (A) and 6.5×10^3 cells ml^{-1} (B) by qPCR. With these particles, the highest capture was achieved with unfunctionalized DS M270 in approach A (A 270-0) with a recovery value corresponding to 45.1%. The lowest capture efficiencies were achieved with Lyswt functionalized 280-wt beads in approach A and 270-wt and 280-wt beads in approach B. In approach B, the highest capture was achieved with LysE35Q functionalized 280 particles with a recovery of 31.3%.



particle functionalization

Figure 3.45: *E. faecalis* recovery with Dynabeads® M-270 Streptavidin and Dynabeads® M-280 Streptavidin from lettuce. The spacer length was 13.5 Å. The initial cell values of 1.1×10^4 cells ml^{-1} (A) and 6.5×10^3 cells ml^{-1} achieved after capture with beads in approaches A and B.

3.9.4.3 DMS C1 and DMS T1

The results for the *E. faecalis* capture experiments with DMS C1 (designated as C1) and DMS T1 (designated as T1) beads are shown in Figure 3.46. 500 $\mu\text{g ml}^{-1}$ beads were used for approaches A and B. The initial bacteria amounts were determined to be 10^5 cells ml^{-1} (A) and 5.5×10^4 cells ml^{-1} (B). The recoveries achieved with DMS C1 were 94.6% with LysE35Q (B C1-EQ) followed by a capture of 40.4% with Lyswt (B C1-wt) and 31.8% by LysE35A coated beads in approach B. The maximum of the recovery rate achieved with unfunctionalized beads was 14.45% in preparation B with C1 beads, whereas the unfunctionalized beads C1-0 and T1-0 in approach A and T1-0 in approach B had recoveries of 1.1%, 0.7%, and 13.1%. Therefore, it can be concluded that the DMS C1 and DMS T1 beads were suitable for specific capture of bacteria from lettuce with significantly low unspecific adsorption on unfunctionalized beads.

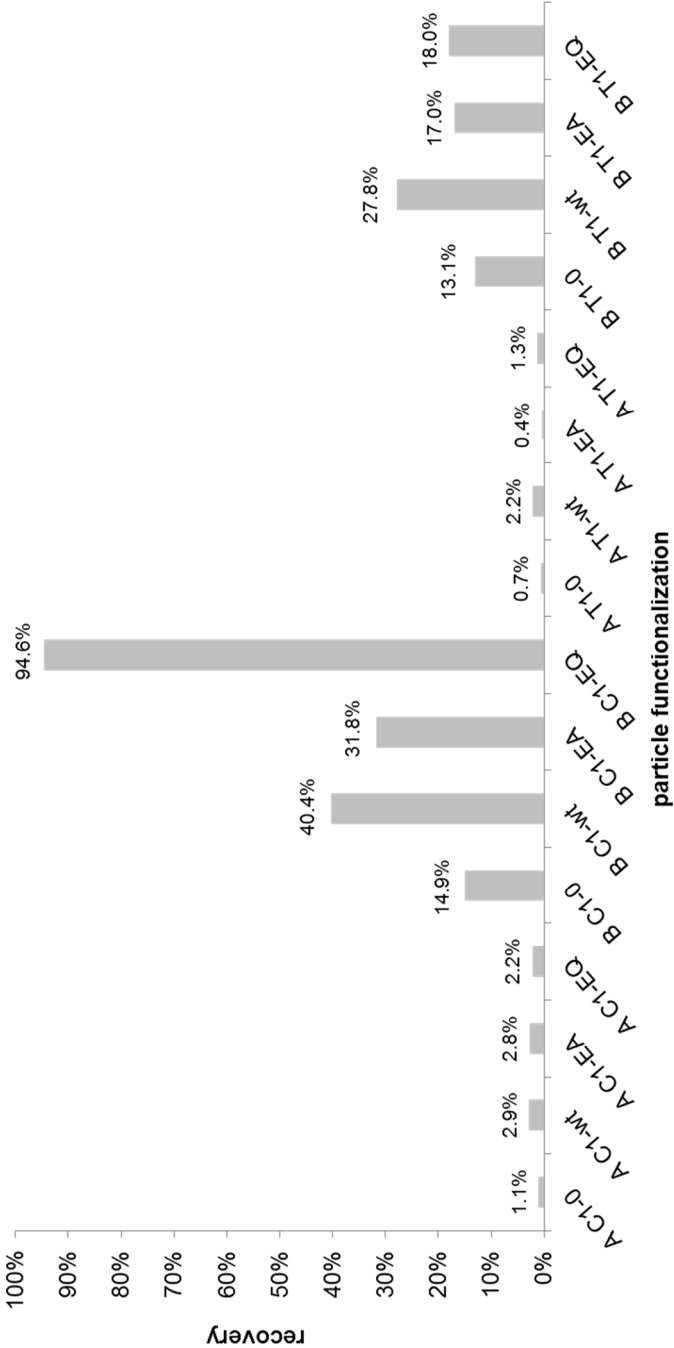


Figure 3.46: *E. faecalis* recovery with Dynabeads® MyOne™ Streptavidin C1 and Dynabeads® MyOne™ Streptavidin T1 from lettuce. The initial bacteria amounts were 1×10^5 cells ml^{-1} (A) and 5.5×10^4 cells ml^{-1} (B).

3.9.4.4 Comparison of capture yields of bacteria from lettuce

The amount of captured bacteria calculated for 1 µg of each type of bead is listed in the Tables 10 for approach A and 11 for approach B. The number of captured cells was extrapolated to the initial capture volume of 1 ml.

Approach A: For the capture experiments exhibited with the beads DS M270 and DS M280, the highest capture yields were obtained from the unfunctionalized beads, whereas in capture experiments with the beads M-PVA SAV2, DMS C1 and DMS T1 functionalization with Lyswt provided the highest yields. The initial bacteria concentrations were 10^4 cells ml⁻¹ in capture experiments with M-PVA SAV2, DS M270, and DS M280 capture experiments and 10^5 cells ml⁻¹ in capture experiments with DSM C1 and DSM T1.

Approach B: For capture experiments with the beads DS M280 the highest capture of bacteria was achieved in a lysozyme-independent, unspecific adsorption manner by unfunctionalized beads, whereas for all the other types of beads used, the functionalization with the protein LysE35Q attained the highest values for capture of bacteria. The unfunctionalized M-PVA SAV2 beads did not capture a detectable amount of bacteria. The initial bacteria concentrations were 5.8×10^3 cells ml⁻¹ in capture experiments with M-PVA SAV2, 6.5×10^3 cells ml⁻¹ in capture experiments with DS M270 and DS M280 capture experiments, and 5.5×10^4 cells ml⁻¹ in capture experiments with DSM C1 and DSM T1.

Table 10: Captured bacteria numbers from lettuce, approach A

Approach A	M-PVA SAV2	DS M270	DS M280	DMS C1	DMS T1
unfunctionalized (cells $\mu\text{g}^{-1} \text{ml}^{-1}$)	0	10	3.9	2.2	1.4
Lyswt (cells $\mu\text{g}^{-1} \text{ml}^{-1}$)	8.2	5.7	0.6	5.8	4.4
LysE35A (cells $\mu\text{g}^{-1} \text{ml}^{-1}$)	4.2	5.4	3	5.6	0.8
LysE35Q (cells $\mu\text{g}^{-1} \text{ml}^{-1}$)	3.5	1.8	1.8	4.4	2.6

Table 11: Captured bacteria numbers from lettuce, approach B

Approach B	M-PVA SAV2	DS M270	DS M280	DMS C1	DMS T1
unfunctionalized (cells $\mu\text{g}^{-1} \text{ml}^{-1}$)	0	0.5	1.4	16	14
Lyswt (cells $\mu\text{g}^{-1} \text{ml}^{-1}$)	2.6	0	0	44	31
LysE35A (cells $\mu\text{g}^{-1} \text{ml}^{-1}$)	6.7	1	1	35	19
LysE35Q (cells $\mu\text{g}^{-1} \text{ml}^{-1}$)	6.7	4	0.8	104	20

3.9.4.5 Influence of spacer length on capture of *E. faecalis* from lettuce

All of the results shown thitherto were performed with purified recombinant lysozymes that were biotinylated with EZ-Link® Sulfo-NHS-Biotin, which provides a spacer with a length of 13.5 Å between the lysozyme and the biotin molecule. The specific *E. faecalis* capture experiments from lettuce with DS M270 and DS M280 in approach A as well as DS M280 in approach B failed with this biotinylation as the unfunctionalized beads captured a higher amount of bacteria than the functionalized ones (Figure 3.45).

In order to determine the influence of spacer length onto the bacteria sorption properties of the functionalization, the purified recombinant lysozymes were biotinylated with EZ-Link® NHS-PEG₁₂-Biotin, which provided a spacer length of

56 Å. The biotinylated lysozymes were then immobilized on DS M270 and DS M280. These beads were used to capture *E. faecalis* from artificially contaminated lettuce in the same way as described in Figure 3.43. Figure 3.47 shows the recoveries of the capture experiments obtained from the approaches A and B. The initial cell concentrations were 10^5 cells ml⁻¹ (A) and 5.5×10^4 cells ml⁻¹ (B) (determined by qPCR). The highest capture yield was achieved by unfunctionalized DS M280 (A 280-0) in approach A (57.1%) and unfunctionalized DS M270 and DS M280 in approach B (B 270-0 and B 280-0). The spacer length did not influence the specific capture of bacteria.

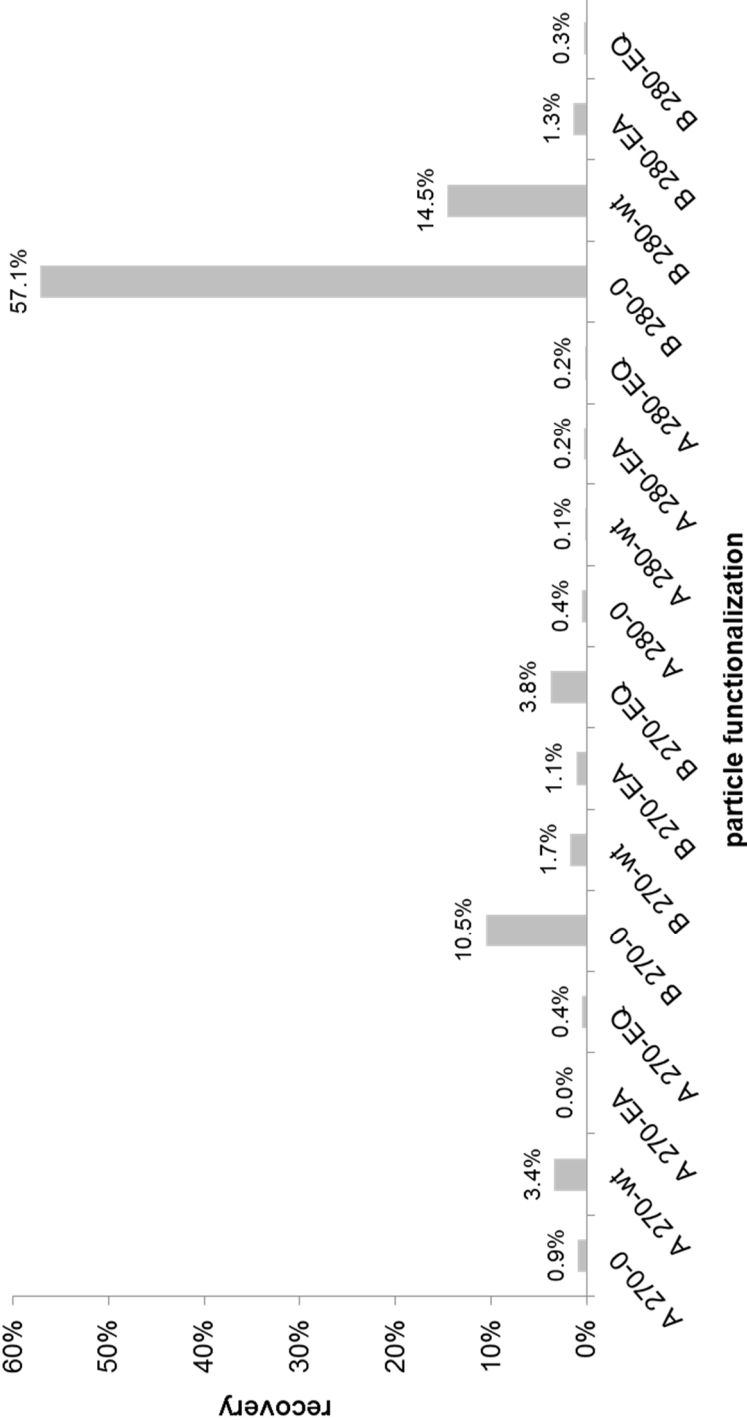


Figure 3.47: *E. faecalis* recovery with Dynabeads® M-270 Streptavidin and Dynabeads® M-280 Streptavidin with spacer lengths of 56.5 Å from lettuce. Initial bacteria amounts were 1×10^5 cells ml^{-1} (A) and 5.5×10^4 cells ml^{-1} (B).

3.9.5 Influence of the immobilization of HEWL onto its bacteriolytic activity

In order to determine the influence of the immobilization of lysozyme onto its activity, turbidity assays were performed with active, commercial, wild-type hen egg white (HEWL), immobilized on magnetic beads. Activity of HEWL was declared to be $100 \text{ U } \mu\text{g}^{-1}$ by its supplier (Sigma Aldrich). The HEWL was biotinylated with EZ-Link® Sulfo-NHS-Biotin in the same way like the recombinant lysozymes described in chapter 3.6.

The influence of the biotinylation on the activity was checked with $1 \mu\text{g ml}^{-1}$ biotinylated HEWL (HEWL-Biotin) and compared to the activity of $1 \mu\text{g ml}^{-1}$ unbiotinylated HEWL. In Figure 3.48 the decrease of the turbidity for HEWL-Biotin and unbiotinylated HEWL are compared. The rate of turbidity decrease caused by biotin-free HEWL, which is an indication of bacteriolysis, was faster than the turbidity decrease caused by biotinylated HEWL. The biotinylation lowered the bacteriolytic activity but did not completely diminish it.

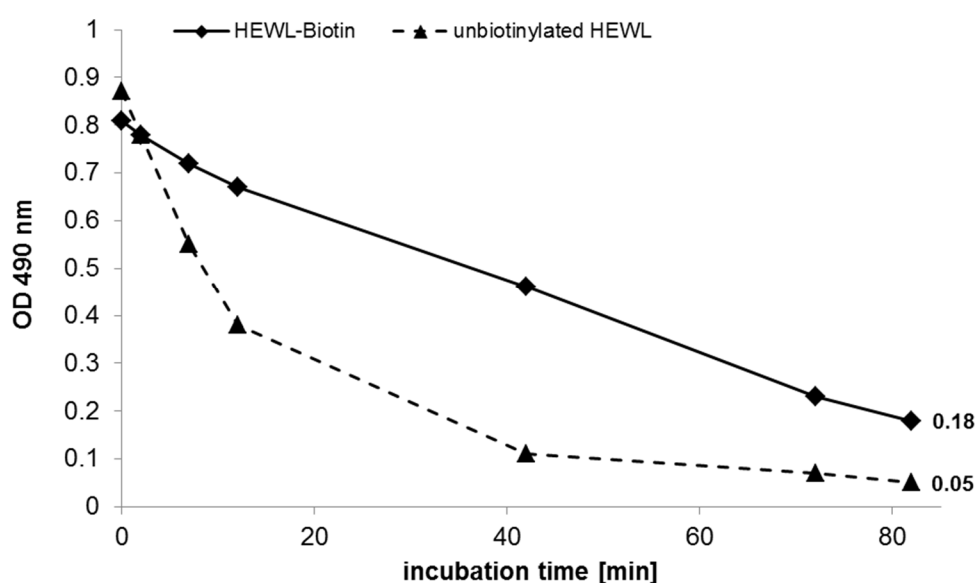


Figure 3.48: *M. luteus* turbidity assay with biotinylated hen egg white lysozyme (HEWL) compared to unbiotinylated HEWL.

After determination of the influence of biotinylation on lysozyme activity, the influence of biotin-streptavidin based immobilization of HEWL to the magnetic beads DS M270, DS M280, DMS C1, and DMS T1 (M270-HEWL, M280-HEWL, C1-HEWL, T1-HEWL) was investigated. The turbidity assay was performed with duplicates of $500 \mu\text{g ml}^{-1}$ of each type of functionalized bead. The results are shown in Figure 3.51. It can be seen that the adsorption decrease after 24 hours of incubation with *M. luteus* suspension is very low, indicating that the immobilization affected the bacteriolytic activity of the HEWL. The second series of HEWL immobilized on DMS T1 (T1-HEWL 2) led to a significant decrease of adsorption after 24 hours. The positive control, $1 \mu\text{g ml}^{-1}$ free HEWL, showed a nearly complete adsorption decrease after 24 hours (Figure 3.49), indicating that activity decrease was caused by immobilization.

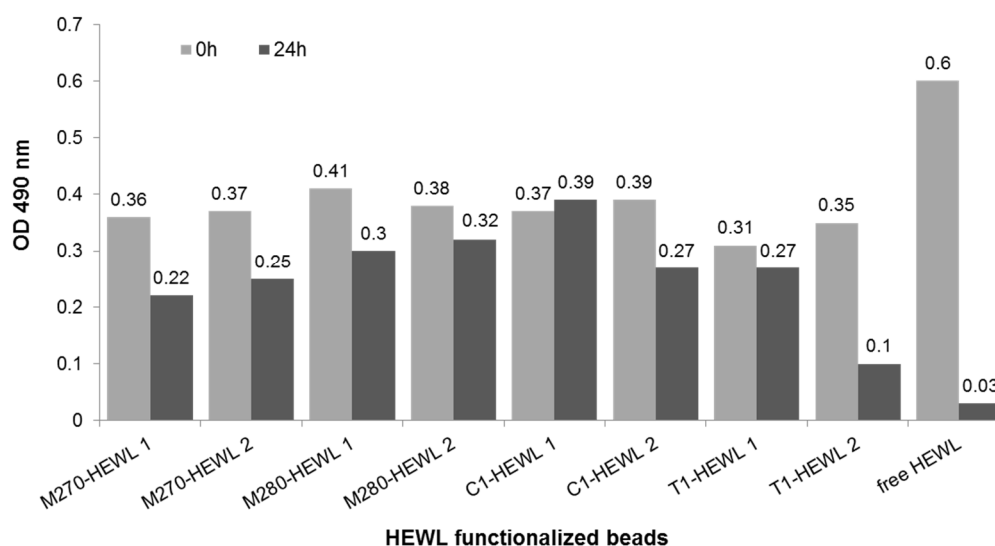


Figure 3.49: Turbidity assay of hen egg white lysozyme immobilized on Dynabeads®.

3.9.6 Summary of chapter 3.9

After verification of the success of lysozyme functionalized beads in specific, capture of bacteria from solutions by fluorescence microscopy, the bacteria recoveries achieved by magnetic separation were determined. Two methods were evaluated for quantification of the bacteria capture yield 1) molecular biological, DNA based Real-Time PCR (qPCR), and 2) cultivation based colony counting after plating the bead-bacteria construct on nutrient agar. Therefore, duplicates of DS M270 functionalized with recombinant wild-type lysozymes (Lyswt) in concentrations ranging from

100 $\mu\text{g ml}^{-1}$ to 700 $\mu\text{g ml}^{-1}$ were incubated with *E. faecalis* suspensions. The initial concentration of bacteria determined in the suspension was 4000 cells ml^{-1} by qPCR and to 1000 CFU ml^{-1} by cultivation based colony counting for the same suspension. The qPCR based determination of the captured bacteria exhibited a good reproducibility between the duplicates and also a correlation between the concentration of applied beads and *E. faecalis* DNA detected. The duplicates of the cultivation based method differ from each other and a correlation between detected bacteria amount and bead amount was not seen. Therefore, qPCR was confirmed to be a more reliable method for the determination of the recovery of the bacteria.

The detection threshold of lysozyme functionalized magnetic beads DS M270 and DS M280 for *E. faecalis* was determined by incubating 250 $\mu\text{g ml}^{-1}$ of the lysozyme functionalized beads (270-Lyswt, 270-LysE35A, 270-LysE35Q, 280-Lyswt, 280-LysE35A, and 280-LysE35Q) in suspensions of *E. faecalis* cells ranging from 10 to 10^4 cells ml^{-1} . The beads 270-LysE35Q and 280-LysE35A could recover 70% and 60%, from the suspension with initial bacteria concentration of 10 cells, respectively. All beads could recover cells out of a suspension with an initial cell concentration of 100 cells with rates up to 16%.

The specific yields of the capture of the functionalized and unfunctionalized beads M-PVA SAV2, DS M270, DS M280, DMS C1, and DMS T1 in *E. faecalis* suspensions were determined and quantified by qPCR. In all cases, one type functionalized beads, predominantly LysE35Q, had a significantly higher capture recovery than unfunctionalized beads. DS M270 beads functionalized with LysE35Q could recover 86.4% from a suspension with an initial bacteria concentration of 4.6×10^4 cells ml^{-1} (Chapter 3.9.3). DMS C1 beads functionalized with LysE35Q captured 2053 cells $\mu\text{g}^{-1} \text{ml}^{-1}$, whereas same beads did not capture any bacteria in an unfunctionalized condition. The DMS T1 beads that were functionalized with LysE35Q could capture 1213 cells $\mu\text{g}^{-1} \text{ml}^{-1}$, whereas unfunctionalized DMS T1 beads did not capture any bacteria.

After verifying the specific capture success of the beads in *E. faecalis* enrichment from suspensions, the beads were applied to artificially contaminated lettuce. Two routes for sample preparation were tested. In the first approach (A) the lettuce was

washed after contamination and then subject to incubation with detergent containing buffer for eluting the bacteria from the lettuce. This elution buffer was used for the capture of bacteria after removal of the lettuce. In a second approach (B), the lettuce that was incubated in detergent containing elution buffer was homogenized in this buffer and filtered. The filtered suspension of homogenized lettuce was incubated with the functionalized beads as well as their unfunctionalized counterparts. The lysozyme functionalized M-PVA SAV2 beads provided recoveries ranging from 17.7% to 57.5%, whereas unfunctionalized beads did not capture a detectable amount of bacteria.

The magnetic beads DS M270 and DS M280 failed in specific separation of bacteria from lettuce. Bacteria adsorption yields with unfunctionalized beads were higher than those from the capture with functionalized beads. The attempt of improvement of the separation efficiency by introducing an elongated spacer arm also failed in specific capture with these kinds of beads. This indicated that spacer length did not influence capture specificity.

The standardization of the yields of the bacteria recovery revealed that the highest bacteria capture from lettuce was achieved with LysE35Q functionalized DMS C1. These beads could capture 94.6% from 5.5×10^4 cells ml^{-1} , which corresponds to 104 cells $\mu\text{g}^{-1} \text{ml}^{-1}$. The unspecific capture of this approach was only 14.9% (16 cells $\mu\text{g}^{-1} \text{ml}^{-1}$).

Besides DS M270 and DS M280 all applied beads were successful in specific and high bacteria recovery from lettuce.

In order to investigate the influence of the immobilization on bacteria binding, an activity assay was performed with fully active commercial wild-type lysozyme molecules that were immobilized on the Dynabeads®. Duplicates of each type of bead were used for activity determination and the results varied especially between the two assays performed with lysozyme functionalized DMS T1. This assay showed that even with the same type of functionalization different lysis efficiencies were obtained, probably due to the random biotinylation of the lysozymes and hence their random orientation on the beads.

4 Discussion

For the maintenance of high hygienic standards in the food industry and in water conditioning, establishment of cultivation-independent detection methods for bacterial pathogens according to the Hazard Analysis and Critical Control Point (HACCP) determination is essential [109, 110]. High quality standards are set for drinking water in industrialized countries and it is dictated that no pathogens should be detectable. The gold standard for the contamination control is the cultivation based detection of bacteria. Such methods fail in detection of bacteria that are in the viable but non-cultivable (VBNC) state, which can be caused by sublethal environmental stress factors like starvation, oxygen concentration, exposure to white light, pasteurisation [103], chlorination [104], and shift in temperature [105, 106]. Hence, the number and diversity of microbes in water is underestimated by the standard cultivation based assays. The VBNC bacteria can be identified as viable by the direct viable count procedure [102, 107]. A lot of human pathogens like *E. coli* (including EHEC) and several *Salmonella* spp. are known to enter the VBNC state. Such bacteria can spread e.g. across the production lines of the food industries or drinking water distribution systems and are able to recover their proliferation depending on changes within the habitats [108]. Insufficient pathogen detection may have severe impacts on the public health [17, 102].

Rapid, cultivation independent detection methods like denaturing gradient gel electrophoresis (DGGE) [38], or quantitative PCR (qPCR) [29] allow the detection of food-borne pathogens without waiting several days like with conventional, microbiologic isolation and detection. But, due to the low bacteria concentrations in tap water, the application of techniques like DGGE or qPCR to the detection of bacteria requires a previous concentration of bacteria by e.g. filtration or centrifugation. Besides the concentration of bacterial cells, these unspecific concentration methods also cause the accumulation of sample components that would interfere with the detection methods [28]. Some components of homogenized eukaryotic matrices like food or human tissues and the components used in DNA extraction like detergents or alcohols also inhibit the PCR based detection of bacteria, leading to false negative results for contamination [30]. Additionally, eukaryotic DNA present in complex matrices can cause a high noise level, interfering

with the sensitive and specific detection of bacterial DNA. Therefore, low amplification volumes compared to sample volumes, inhibitory components of the complex matrices, low contamination levels, and the eukaryotic DNA present in the matrices, require the specific separation and enrichment of bacteria previous to the molecular biological, nucleic acid targeting detection of bacteria [39, 40].

A specific separation of bacteria from food matrices is provided by the method called immunomagnetic separation (IMS). For this method, antibodies, specific for surface antigens of bacterial species can be immobilized on the surface of superparamagnetic beads for the specific capture of the bacteria in food or water by the antibody-antigen interactions and subsequent separation of the magnetic bead-bacteria complex by magnetic forces [47-58]. The IMS has the disadvantage of being specific for a species and hence, comprehensive pathogen detection is not provided by the use of one kind of beads. This species specificity only allows the directed separation of known bacteria. A broad range contamination analysis would necessitate a combination of magnetic particles with different species specific antibodies. A technical approach of the IMS would be too expensive due to the high costs of antibodies. Furthermore, new pathogens, which are not expected in water distribution systems or known as typical food pathogens, could not be detected.

Therefore in this project, the antibodies were replaced by recombinantly expressed hen egg white lysozyme (HEWL) (chicken c-type lysozyme), which binds to peptidoglycan components in bacterial cell walls and thus, provides a broad range of bacteria detection in samples. The outer membrane of Gram negative bacteria protects their cell walls from lysozyme binding, but addition of 10 mM EDTA disrupted the outer membrane and hence enabled the binding of Gram negative bacteria by lysozyme. To inhibit the lysis of bound bacteria, point mutations were introduced to the HEWL cDNA. These mutations resulted in proteins that bound to the bacterial cell walls but did not subsequently lyse them. The lysozymes were immobilized on μ -scaled, magnetic beads, producing lysozyme-bead constructs, which bound to the bacteria and were then separated from the matrices an external magnetic field. This magnetic based separation could remove the bacteria from solid matrix components without the need of standard concentration steps that did not work on separation of bacteria from solid matrices. A further advantage of this method was the separation of only intact bacterial cells. Free nucleic acids of lysed bacteria were not detected

and thus did not lead to false positive results. Nevertheless, the method is not suited for discrimination of intact dead bacteria from live bacteria. But application of methods like live/dead staining subsequent to bacteria separation can enable the determination of the ratio of live and death bacteria. Nevertheless, the separation of opportunistic bacteria whether dead or alive, shows a contamination in the food production lines or the water distribution systems. Therefore, the bacteria separation method, developed in this study, is a suitable tool for the HACCP concept.

As a model organism, for evaluation of the applicability of the lysozyme based magnetic separation method of bacteria, the Gram positive *E. faecalis* was chosen. This bacterium is a member of the human and animal intestine and serves as an indicator organism for faecal contamination in monitoring the water microbiology [18].

4.1 Mutation of lysozyme and its recombinant expression in *P. pastoris*

In its wild-type form, hen egg white lysozyme binds to bacterial cell walls and causes their lysis by hydrolysing the β -(1,4)- glycosidic bond between peptidoglycan components N- acetylmuramic acid (NAM) and N- acetylglucosamin (NAG) [62]. To prevent the lysis of the bacteria, wild-type HEWL cDNA was mutated by site-directed connection PCR [96], which introduces a point mutation into the catalytic centre of the protein. By this method, two cDNA derivatives were generated: the exchange of catalytic glutamic acid 35 by a) alanine (LysE35A) and b) glutamine (LysE35Q). The essential role of the amino acid glutamic acid 35 in cell wall lysis was determined by Malcolm et al. by replacing this amino acid with glutamine resulting in a residual lytic activity of 0.1% in respect to wild-type HEWL. The dissociation constant of this mutant with chitotriose was determined to be 13.3 μ M, whereas wild-type lysozyme has a dissociation constant of 8.6 μ M [66]. The mutation of glutamic acid 35 to glutamine did not diminish the affinity of lysozyme for chitotriose. Therefore in this study the assumption was made that the affinity of the mutant protein for bacterial peptidoglycan could also be at the same range like wild-type lysozyme.

The mutated derivatives LysE35A and LysE35Q and also the wild-type protein Lyswt were successfully expressed in *P. pastoris*.

This methylotropic yeast was chosen as expression organism because in *E. coli* the translation process is initiated with addition of N-terminal methionine to the proteins. This methionine is successfully removed from host proteins but it is hardly removed from recombinant proteins by the *E. coli* proteinases [70, 71, 112]. Another reason for the selection of *P. pastoris* was the possibility that recombinant lysozyme can form complexes with the peptidoglycan layer of the bacterial host during protein purification. By using the expression vector pPic9, a methanol dependent expression and secretion of the recombinant proteins into the cell environment was possible. Laboratory-scale batch fermentations resulted in recombinant protein concentrations between 2 and 30 mg l⁻¹.

The oxygen supply to *P. pastoris* cells is essential for recombinant protein expression. High cell density fed-batch fermentation of *P. pastoris* can cause an up to 10-fold higher protein yield due to controlled oxygen supply than batch fermentation [73]. The lysozyme yields achieved in this study are in good accordance with published values for different types of lysozymes, like 25 mg l⁻¹ human lysozyme with MF- α Prepro secretion signal in shake flasks [115], or 34.5 mg l⁻¹ hen egg white lysozyme [116]. The published *P. pastoris* fed-batch fermentation of lysozymes report about yields of 300 mg l⁻¹ human lysozyme with extra residues Glu-Ala-Glu-Ala at the N-terminal end [117], 250 mg l⁻¹ bovine lysozyme in 1 litre fermentation broth and 325 mg l⁻¹ (Mut⁻ strains) and 450 mg l⁻¹ (Mut⁺ strain) in 10 litre fermentation [118]. Compared to these results, the expression system used in this study consisting of integrated pPic9 vector with recombinant hen egg white lysozyme (mutants LysE35A and LysE35Q and wild-type Lyswt) downstream to the α -factor secretion signal, revealed good yields for the lab-scale batch fermentation in 100 ml expression broth.

4.2 Purification of recombinant lysozyme derivatives from expression broth

Besides recombinant lysozyme, other proteins were also present in expression medium. Initially, chromatographic purification was applied to gain pure lysozyme. These attempts failed due to the low concentration of the target protein. Therefore protein enrichment previous to purification was necessary. A standard enrichment protocol for the precipitation of the proteins employed 2 M ammonium sulphate and centrifugation. This method failed. The pellet included only 0.16-0.6 mg ml⁻¹

recombinant lysozyme because most of the lysozyme did not precipitate as expected but remained soluble in the supernatant. A further increase of ammonium sulphate concentration was not possible due to solubility problems.

Alternatively the nano-scaled cation exchanger particles MagPrepSO₃ were used for purification and enrichment. These particles were functionalized with sulfonate groups, which provide a negative charge at a broad pH range and hence bind to positively charged molecules.

Previous to bead based enrichment, the pH of the cell-free expression medium was adjusted to 8.5. Most of the undesired proteins agglomerated due to their lower pI values whereas lysozyme, which has an average pI of 11 [62], remained predominantly in solution. Only 5%-15% of lysozyme was lost due to co-precipitation. A further purification was achieved with MagPrepSO₃ particles. The lysozyme was bound to the particles, supernatant was subsequently removed, the particles were washed with phosphate buffer and finally, the lysozyme was re-eluted.

To describe the binding properties of the proteins to the magnetic particles, adsorption isotherms of lysozyme binding to the MagPrepSO₃ particles were determined. First, as a reference, single-component adsorption of commercial HEWL from 0.1 M phosphate buffer with neutral pH was recorded. Then the adsorption isotherms of Lyswt and of the mutant LysE35A from expression medium with pH value of 8.5 were determined. The adsorption parameters q_{\max} and K_L were calculated from non-linear regression using the Software SigmaPlot® 10.0. These non-linear regressions resulted in a q_{\max} value of 64.4 mg g⁻¹ and a dissociation constant K_L of 10.2 mg l⁻¹ (700 nM) for single-component adsorption of commercial HEWL. The parameters of the other adsorption were designated as $q_{\max, \text{app}}$ and $K_{L, \text{app}}$, where app means apparent, because it is not known if the adsorption was not conducted in with single components in expression broth. Purification analysis were made with silver staining and despite this method revealed a pure lysozyme, it is possible that proteins, which were not stained by silver ions, also remained in the supernatant despite pH increase. The $q_{\max, \text{app}}$ of Lyswt adsorption was determined to be 254 µg g⁻¹ and thereby is only 0.4% of the single component adsorption of HEWL. This lower binding capacity can be caused by the higher salt concentration present in expression broth compared to 0.1 M phosphate buffer. The dissociation constant was determined as 10.25 µg l⁻¹ (700 pM). This value shows that the affinity of the

MagPrepSO₃ is thousand fold higher for the recombinant wild-type adsorption in alkaline expression broth than for wild-type hen-egg white lysozyme single-component adsorption of in phosphate buffer at pH 7. The cDNA for the Lyswt protein was the same as for commercial hen egg white lysozyme used for single protein adsorption. It is expected that both proteins should have the same structure. Despite same amino acid sequence, expression in *P. pastoris* could cause posttranslational modifications of the lysozymes, which were not detected by methods used in this study. Besides differences in adsorption terms, this modification could also be a reason for the difference in particle adsorption behaviour.

The LysE35A adsorption isotherm also showed a lower binding capacity of the beads for the protein. The $q_{\max, \text{app}}$ was 751 $\mu\text{g g}^{-1}$. This value was nearly threefold higher than Lyswt adsorption, which was exhibited at the same conditions, but only 1.2% of single component HEWL adsorption in phosphate buffer pH7. The $K_{L, \text{app}}$ for LysE35A was determined to be 79 $\mu\text{g l}^{-1}$ (5.4 nM), indicating a 130-fold higher affinity of MagPrepSO₃ particles for LysE35A in expression broth than for HEWL in neutral buffer. The differences between LysE35A adsorption and Lyswt adsorption under same purification conditions are probably a result of the amino acid exchange, which causes the replacement of an amino acid with a carboxyl group in its side chain by an alanine. The carboxyl group would be negatively charged under the chosen conditions for the purification of the proteins and hence, the adsorption to cation exchanger particles would be decreased.

In general, the purification parameters showed an ineffective purification process for recombinant lysozymes from expression broth at alkaline pH values, probably caused by other proteins and components present in the expression broth that were competitive for the binding to the beads or high salt amount of expression broth. Considering that column chromatography based recombinant lysozyme purification was not successful and that recombinant lysozyme enrichment from expression broth by ammonium phosphate precipitation resulted in loss of high amounts of lysozyme, purification and concentration of lysozyme by means of superparamagnetic cation exchange particles was considered successful. Eluates with lysozyme concentrations of up to 250 mg l^{-1} were gained by MagPrepSO₃ purification and enrichment.

4.3 Determination of lysozyme activity with Gram positive and negative bacteria

To determine the activity of the recombinant lysozyme variants, turbidity assays with *M. luteus* cells were performed. In order to check if secretion and protein purification influences the native structure of the target proteins, the wild-type lysozyme (Lyswt), expected to exhibit bacteriolytic activity, was also expressed by *P. pastoris*, and as expected, it caused a significant decrease in optical density of the bacteria suspension, proving that the protein was active. This indicated that the expression, secretion, and purification steps did not denature the protein and the native structure of the protein was retained. The mutated proteins on the other hand did not cause an optical density decrease of *M. luteus* cells, indicating that by the incorporation of the mutations the bacteriolytic activity of the lysozymes was successfully eliminated.

As a Gram negative reference *P. putida* was used for turbidity assays. By adding 10 mM EDTA to the lysozyme bacteria mixture, decrease in adsorption was achieved with Lyswt and commercial HEWL, whereas no bacteriolytic activity was achieved by mutated derivatives.

4.4 Immobilization of recombinant lysozyme to magnetic beads

After turbidity measurements the recombinant proteins were immobilized on commercial μ -scale magnetic streptavidin beads. For immobilization the streptavidin-biotin interaction was employed, known to be the strongest non-covalent interaction with a dissociation constant of 4×10^{-14} M [123]. The purified recombinant lysozymes Lyswt, LysE35A, and LysE35Q were biotinylated with commercial biotinylation kits. The used kind of biotin molecule coupled to the lysozymes had a spacer length of 13.5 Å. It must be mentioned however, that these biotynilations provide rather nonspecific than directed coupling mechanism: In average 2-4 biotynilations occur on each lysozyme (personal communication with Annika Rieder). The biotinylated lysozymes were used for immobilization on the streptavidin-functionalized beads M-PVA SAV2, Dynabeads® M270 and M280 Streptavidin (DS M270 and DS M280), Dynabeads® Myone™ Streptavidin C1 and T1 (DMS C1 and DMS T1).

4.5 Proof of principle by means of fluorescence microscopy

The aim of this study was the specific capture of bacteria for enrichment from fluids with low contamination levels and separations from complex matrices like food by specific bacteria capture using non-lysing lysozyme as ligand. The proof of principle for specific bacteria separation by lysozyme functionalized magnetic beads was based on fluorescence microscopy. Streptavidin-functionalized M-PVA SAV2 beads were labelled with fluorescent dye previous to lysozyme immobilisation. These constructs were subsequently used for capture of Syto® 9 labelled Gram positive *M. luteus* cells from solutions. All constructs, beads functionalized with Lyswt, LysE35A, and LysE35Q, succeeded in bacteria capture, whereas unfunctionalized beads showed a very low, unspecific bacteria capture. This result was a rapid proof of principle that capture was predominantly lysozyme based instead of unspecific bacteria adsorption to bead surface.

The functionalized beads were also used for the capture of labelled Gram negative *P. putida* cells. The *P. putida* cells were labelled with Syto® 9. The fluorescence microscopy showed that capture of the gram negative bacteria was successful and based on lysozyme-peptidoglycan interaction. So, this method succeeded in capturing Gram positive and Gram negative reference bacteria from suspension.

4.6 Application of lysozyme functionalized magnetic beads for bacteria detection in tap water and detection by means of DGGE

After fluorescence microscopy based verification of bacteria capture by lysozyme functionalized magnetic beads, 300 µg of the M-PVA SAV2 beads, each without functionalization and functionalized with the recombinant lysozymes Lyswt, LysE35A, and LysE35Q were applied to bacteria enrichment from tap water. The beads were incubated with 500 ml of tap water from the laboratory, washed with sterile, nucleic acid-free water and then resuspended in 50 µl polyA containing water, leading to a 10⁴-fold concentration. Additionally, a sample of tap water was concentrated 10⁴-fold by centrifugation. This sample served as reference for comparing the concentration efficiency of centrifugation and bead-based enrichment. Additionally, unconcentrated tap water was used as reference. The bacterial DNA of the samples was delivered by

freeze-thaw lysis and the bead free supernatants used as templates for PCR based DNA amplification with the universal primer pair GC27F/GC517R. The PCR products were then subject to species specific fragment separation by DGGE. Samples concentrated by centrifugation and magnetic beads revealed the same DNA pattern. The comparison of the DNA pattern of the concentrated samples with unconcentrated tap water showed that a concentration step is essential to encompass the whole bacterial diversity of the samples. This method revealed that without concentration, the bacteria content of tap water would be underestimated and in the case of pathogen contamination, false negative results could have fatal consequences to public health. In comparison, the magnetic beads based capture pattern of lysozyme functionalized beads with the unfunctionalized bead pattern showed that the same bacterial diversity was determined in all samples. This is a hint for unspecific, bacteria adsorption to the bead surface. Previous to DGGE, the samples were subject to PCR amplification, which is a method that can theoretically multiply only one single DNA molecule. Therefore statement about the significance of the unspecific, lysozyme-independent adsorption of bacteria to bead surface from a conventional PCR based method is not possible. Due to the semi-quantitative nature of the DGGE the quantitative evaluation of capture efficiencies of the functionalized and unfunctionalized beads was hindered.

4.7 Determination of bacteria capture yields of lysozyme functionalized magnetic beads

4.7.1 Comparison of cultivation based quantification and quantitative PCR results

For the quantitative determination of the bacteria recovery achieved by bead based capture and for evaluating if the capture is predominantly due to unspecific bacteria adsorption to bead surface instead being lysozyme-peptidoglycan interaction based, *E. faecalis* enrichment experiments were executed. For the quantification step subsequent to bacteria capture two quantitative methods were benchmarked. One was the cultivation based colony counting method. As the fluorescence microscopy figures showed, each bead can capture more than one CFU which were densely

packed and hence build up one colony. From these figures it was shown that the cultivation based bacteria quantification did not provide reliable results.

The other method for the quantification of the capture efficiency is the application of qPCR. For the capture sample, the initial value for bacteria cells was determined by qPCR to 4000 cells ml⁻¹ or 1000 CFU ml⁻¹ by cultivation on agar plates. The reason for the difference obtained for the two methods could be the agglomeration of the cells which resulted in colonies formed by more than one cell or the induced VBNC state of *E. faecalis* [20, 21]. To determine the lysozyme-bead based capture, aliquots of the cell suspensions, each containing the same amount of initial bacteria, were incubated with 100 µg ml⁻¹ to 700 µg ml⁻¹ recombinant wild-type lysozyme (Lyswt) functionalized DS M270 beads. After washing the beads with detergent containing buffer, the cells were resuspended in 1 ml. As verification that cultivation based bacteria quantification is unreliable, 100 µl of the samples were plated on nutrient agar for colony counting. Portions of 100 µl were used for freeze-thaw cell lysis and subsequent quantification by qPCR. The latter method revealed a positive correlation between used particle amount and captured bacteria, whereas colony counting showed no correlation and even the duplicates had a very large deviation. This experiment verified that molecular biologic methods are more reliable in bacteria detection.

The influence of different contamination analysis methods to the detection of the contamination was previously also shown by Wadud et al. Different kind of food matrices (turkey roast, mixed vegetables, soft cheese, potato-egg salad, smoked salmon, and beef roast) were contaminated with *Listeria monocytogenes* cells. At an inoculum level of 15-25 CFU per 25 g food, 100% of the samples from the used six food matrices were detected to be positive for the bacterium by standard cultivation method, as well as IMS-ALOA (Agar Listeria according to Ottaviani and Agosti) and PCR. With a lower inoculum level of 1-5 CFU per 25 g food, in vegetable salad, 90% of the inoculated samples were detected to be positive for Listeria by IMS-ALOA, 90% were positive by standard cultivation method, and 96% were positive by PCR [48].

Another study verifying the importance of the analytical method was obtained for detection of *Yersinia spp.* in meat by the use of the four different methods cold enrichment in trypticase soy broth, enrichment in modified Rappaport broth at 25°C,

IMS, and nested PCR. The bacteria detection of the first three enrichment methods was performed by plating of the samples on cefsulodin-irgasan-novobiocin agar and Mac Conkey agar. Best results were obtained by PCR (positive score of 39%), whereas the IMS-plating method had a positive score of 2%. The study verifies the efficiency of PCR and better suitability of the DNA based method for bacteria detection. Unspecific capture of beads that were not functionalized was not shown in their publication [51].

In the current study also low recovery values were obtained for cultivation based quantification of bacteria after lysozyme-magnetic bead based separation. Therefore, for an effective recovery, in this study, magnetic bead based separation was combined with quantitative PCR.

4.7.2 Determination of functionalized beads threshold for the capture of bacteria

To determine the capture threshold of lysozyme functionalized beads, $250 \mu\text{g ml}^{-1}$ ($1.5\text{-}1.75 \times 10^7$ beads) of Lyswt, LysE35A, and LysE35Q functionalized magnetic beads DS M270 and DS M280 were used. These beads were incubated with 10-fold dilutions of *E. faecalis* suspension ranging from 10 cells ml^{-1} to $10^4 \text{ cells ml}^{-1}$. The DS M270 beads functionalized with LysE35Q succeeded in capturing 70% from initial value of 10 cells ml^{-1} and LysE35A functionalized M280 beads could capture 60% after incubation in bacteria suspension of 10 cells ml^{-1} . All functionalized beads succeeded in capturing bacteria from solutions with $100 \text{ cells ml}^{-1}$. In these cases, the recoveries were between 6% and 16%. These results show that the lysozyme functionalized beads have a high sensitivity. Two out of six kinds of beads succeeded in bacteria detection at the lowest cell amount. A correlation between the amount of beads applied and bacteria capture efficiency was shown, hence the use of a higher amount of functionalized beads would increase the capture success of the method even at lower bacteria contamination levels.

A lot of research groups evaluate their magnetic separation efficiencies by means of cultivation based methods resulting in low sensitivity of the used separation method. Kretzer et al. employed cell wall binding domain (CBD) of bacteriophage endolysin for *L. monocytogenes* capture from bacteria solution with 10^4 CFU ml^{-1} initial bacteria. With 1.5×10^5 CBD functionalized Ni-nitrilotriacetic acid agarose beads and

initial bacteria amount of 10^4 cells in a volume of 200 μl a recovery of 60% was achieved. The recovery was enhanced to about 100% if 2.7×10^7 M270 Epoxy Dynabeads® were used. The CBD-MS recovery values varied for different *Listeria* strains [60]. Comparing the endolysin based method with the sensitivity of lysozyme-magnetic beads based method developed in the current study shows that lysozyme based capture had a lower capacity (maximal recovery of 1070 cells with $1.5\text{-}1.75 \times 10^7$ particles from suspension with 10^4 cells in 1 ml volume of capture of bacteria) but it is more sensitive as demonstrated from the capture of 70% of the cells from a total cell amount of 10 cells in 1 ml. Taking in consideration that tap water should contain low levels of bacteria, the lysozyme functionalized beads promise a good suitability to technical application in water conditioning.

Another enrichment example study, verifying the high sensitivity of the developed lysozyme-magnetic bead based capture in this study, is IMS coupled with conventional PCR analysis for detection of *H. pylori*. The analytical method was rather qualitative than quantitative. The method was only successful if an initial bacteria level of 10^5 to 10^6 cells/ml were present in capture suspension and 10^7 cells ml^{-1} from stool were needed for bacteria detection by conventional PCR [113].

Compared to the above mentioned published capture sensitivities, the capture efficiencies received with lysozyme functionalized DS M270 and DS M280 in this study are highly sensitive. Two kinds of beads out of six succeeded in capturing 70% and 60% from 10 bacteria cells in 1 ml.

4.7.3 Enrichment of bacteria from suspensions

Most of the published studies about IMS did not employ a negative control with unfunctionalized magnetic beads to check the specificity of capture of bacteria. In contrary, in this study, the unspecific capture yields of bacteria enrichment from *E. faecalis* suspensions were also determined. Therefore, particle functionalizations with Lyswt, its mutated derivatives LysE35A and LysE35Q, also unfunctionalized beads were used in capture experiments. High initial bacteria amounts were used to increase the chance of unspecific adsorption of bacteria. This condition was chosen to achieve more reliable results. The beads were first applied to bacteria enrichment

from liquids and then applied to bacteria separation from artificially contaminated food.

With 600 μg M-PVA SAV2 beads a maximum recovery was achieved by Lyswt functionalization. 27% out of 3×10^4 cells were captured. In comparison, the unfunctionalized beads had a recovery of 13%. This shows that besides specific lysozyme based capture; unspecific bacteria adsorption on the surface of M-PVA SAV2 occurs.

For DS M270 the highest recovery rate of 86.4% was achieved by LysE35Q functionalized beads (270-EQ) after incubation with 4.5×10^4 cells/ml. 270-wt and 280-EQ yielded in approximately 10% recovery. The unfunctionalized DS M280 beads did not capture a detectable amount, whereas the unfunctionalized DS M270 beads (270-0) had a capture of 3%. In summary these beads succeeded in high specific, lysozyme-peptidoglycan interaction based recovery of *E. faecalis* cells from bacteria suspensions.

For DSM C1 and DSM T1 LysE35Q functionalization resulted in recovery values of 4.4% and 2.6% from initial bacteria amounts of 7×10^6 cells ml^{-1} and a bead amount of $150 \mu\text{g ml}^{-1}$. These efficiencies seem to be low but considering the high initial bacteria values, the recoveries correspond to captured cell amounts of $3.1 \times 10^5 \text{ ml}^{-1}$ and 1.9×10^5 cells ml^{-1} . The cells captured by unfunctionalized beads (C1-0 and T1-0) were less than 0.05%. The adsorption of bacteria to unfunctionalized beads was insignificant even with high initial bacteria amounts.

4.7.3.1 Comparison of the yield for capture of bacteria of different kinds of beads

For an evaluation of the success of capture of bacteria achieved by the different kinds of magnetic beads used for enrichment of bacteria, the captured cell amounts were standardized to $1 \mu\text{g ml}^{-1}$ of different beads. This standardization revealed that DSM C1 and DSM T1 beads with a LysE35Q functionalization succeeded in capture of high amounts of bacteria, 2053 and 1213 cells $\mu\text{g}^{-1} \text{ml}^{-1}$, whereas their unfunctionalized counterparts did not capture a detectable amount of bacteria, despite the presence of a high bacteria amount. Comparing the capture yields in table 9, it can be concluded that the DSM C1 and DSM T1 beads were the most

appropriate beads for specific capture of bacteria after lysozyme functionalization. But one must consider that the DMS beads have a diameter of 1 μm , which means a higher specific surface than DS M270 and DS M280 beads. The latter have a diameter of nearly 3 μm and their binding capacity for biotinylated IgG was determined to be 25% to 50% of the binding capacity of DMS C1 and DMS T1.

A statement about the influence of surface properties of the magnetic beads to unspecific capture of bacteria is not possible from this study. Whereas the unfunctionalized hydrophilic M-PVA SAV2 and DS M270 beads showed a lysozyme-independent capture of bacteria, the hydrophilic DMS C1 did not, even in a capture suspension with an initial amount of bacteria, which was 233% and 152% of the other capture experiments with M-PVA SAV2 and DS M270, respectively.

4.7.3.2 Comparison of the lysozyme functionalizations

In most of the performed capture experiments, the LysE35Q lead to a significantly higher capture than the unfunctionalized beads. As discussed above, with LysE35Q functionalized DSM C1 and DSM T1 beads, very high bacteria recoveries from a suspension with an initial bacteria value of 7×10^6 cells ml^{-1} were achieved, whereas no bacteria capture was achieved with unfunctionalized beads, indicating that the bacteria capture was a specific process based on the interaction of lysozyme with the peptidoglycan cell wall of bacteria and not an unspecific adsorption of bacteria to the magnetic beads surface.

In some capture approaches, the unfunctionalized beads had a higher or equal recovery than one or two of the functionalized beads. But for each kind of bead, at least one type of functionalization, most often LysE35Q, had a significantly higher recovery than the unfunctionalized beads. The turbidity assay with recombinant lysozymes verified the bacteria lysis ability and hence the binding of the Lyswt to bacteria cells. But despite verifying this binding ability, the yields for capture of bacteria with Lyswt functionalized beads were low in most cases, except for M-PVA SAV2.

The reason for this is assumed to be the random biotinylation and hence the random orientation of the Lyswt and the other recombinant lysozymes, LysE35A and LysE35Q, at the magnetic bead surface. The biotinylation reaction occurs at primary amines. Additionally to the N-terminal primary amine of its peptide bond, the wild-type

hen egg white lysozyme contains six lysines, eleven arginines, three glutamines, and thirteen asparagines. All these amino acids provide primary amines at their side chains that can be biotinylated if steric access of biotin is possible.

The influence of protein orientation on signal intensity in antibody microarrays was shown by Peluso et al.. The specific orientation of capture agents increases the analyte-binding capacity of surfaces up to 10-fold compared to surfaces with randomly oriented capture agents. Fab' fragment orientation was found to be much denser in specifically oriented manner caused by site-specific carbobiotinylation of IgGs and had a higher activity compared to random orientation due to random biotinylation with NHS- activated biotins [120]. And this is also true for the lysozyme orientations in this study.

If the catalytic centre, which is also the binding cleft of the lysozyme, is not oriented to the environment of the particle, an access to the bacterial cell wall is not possible and therefore, no specific bacteria capture occurs.

To check these considerations, active, commercial hen egg white lysozyme was a) biotinylated and b) biotinylated and immobilized on Dynabeads®. First the lytic activity of biotinylated HEWL was compared to unbiotinylated HEWL by turbidity assay with *M. luteus* cells. Both HEWLs caused a significant absorption decrease, indicating that enzyme is active. The unbiotinylated HEWL showed a faster and improved lysis rate than the biotinylated one. This could be due to a steric hindrance of the binding of bacteria to the modified HEWL caused by the biotinylation close to the active site of the enzyme or even complete blocking of the active site. But the biotinylated HEWL exhibited sufficient lysis activity and thus it was immobilized on DS M270, DS M280, DMS C1 and DMS T1. The turbidity assay was performed again with duplicates of each type of the different beads with HEWL immobilizations. Irreproducible fluctuations resulted in terms of final OD for both, different particle types and even for the same particles applied in duplicates, indicating that the orientation of the lysozyme molecules on magnetic beads surface is determining the binding to the bacteria cells.

The same considerations are also true for the mutant proteins, especially LysE35Q. The dissociation constant of LysE35Q was determined as 13.3 μM and the dissociation constant of HEWL as 8.6 μM in respect to binding of chitotriose by

Malcolm et al. [66]. Therefore, bacteria binding by LysE35Q could also be assumed to be at the same range like wild-type lysozyme. This must be the reason why the capture experiments resulted often in specific binding of cells and highest values of recovery by LysE35Q. But the same orientation problems discussed above for Lyswt protein also holds for LysE35Q. This is probably the explanation for inefficiency of LysE35Q functionalized M-PVA SAV2 beads in bacteria capture. Nevertheless, a trend is clearly visible from the capture experiments with DS M270, DS M280, DMS C1, and DMS T1. In all these cases the LysE35Q functionalization achieved the highest capture efficiency, being significantly higher than the capture with unfunctionalized beads.

4.7.4 Separation of bacteria from lettuce

After successful, specific enrichment of bacteria from suspensions, the constructs were applied to food matrices that were artificially contaminated with *E. faecalis*. Lettuce was chosen as model matrix for application of magnetic beads to capture of bacteria. Two approaches were performed.

For each approach six gram lettuce was incubated for several hours with tap water that was contaminated with *E. faecalis* cells. Then the lettuce was washed twice with water and then the bacteria were eluted by incubating the lettuce with detergent containing phosphate buffer.

For the first approach, designated as A, only detergent containing elution buffer was incubated with functionalized and unfunctionalized beads, after removal of the lettuce for capture.

For the second approach, designated as B, lettuce was homogenized in elution buffer and then filtered through Whatmann paper. This filtrate was then subject to capture of bacteria with beads. The capture efficiencies were determined by qPCR.

First M-PVA SA2 particles were used for capture from lettuce. For both approaches no bacteria capture was detected with unfunctionalized beads. The beads functionalized with Lyswt, LysE35A, and LysE35Q all captured bacteria. By approach A an initial amount of 10^4 cells ml⁻¹ were obtained. The highest yield was achieved with Lyswt functionalized beads: 40.9 % of the initially applied bacteria.

In approach B, the initial bacteria amount was in $5840 \text{ cells ml}^{-1}$. LysE35A and LysE35Q functionalized beads captured 57.4% of these bacteria, whereas the unfunctionalized beads did not capture bacteria in detectable amounts from lettuce.

The M-PVA SAV2 beads did not cause an unspecific binding of bacteria cells but the recoveries of the lysozyme functionalized M-PVA SAV2 beads of 57.4% were low compared to the high levels published for IMS capture of bacteria, which reached recovery levels to up to 100%. The M-PVA SAV2 particles have a binding capacity of only 30 pmol mg^{-1} biotinylated proteins whereas the Dynabeads M280, which are most often used in published IMS experiments, have a binding capacity of 70 pmol mg^{-1} . Therefore, this lower amount can be attributed to the lower lysozyme density on the surface of the magnetic particles. Hence, one can expect that a higher density of the immobilized lysozyme proteins on the surface of the magnetic particles would improve the bacteria binding capacity. Therefore, other streptavidin functionalized, magnetic particles with higher biotinylated protein binding capacities were used.

The next particles used for determination of *E. faecalis* capture efficiency from food were DMS C1. In approach A, the highest recovery was 2.9% achieved with Lyswt functionalization. The lowest capture was achieved with unfunctionalized DMS C1, but this recovery value was 1.1% and hence the difference between specific and unspecific capture of bacteria was low. In approach B, LysE35Q functionalized DMS C1 captured 94.6% of the initial bacteria ($5.5 \times 10^4 \text{ cells ml}^{-1}$). The unfunctionalized beads had a much lower capture yield of 14%.

The DMS T1 capture yields in approach A showed the same low recovery values as with DMS C1 beads in approach A. In approach B, highest yield was achieved with Lywt functionalized beads (27.8% of $5.5 \times 10^4 \text{ cells ml}^{-1}$) but the unspecific capture was not significantly lower (13%).

With DS M270 and DS M280 beads, highest recovery was achieved with unfunctionalized beads in approach A (45% and 17% of $1.1 \times 10^4 \text{ cells ml}^{-1}$). In approach B, the DS M270 beads that were functionalized with LysE35Q had the highest capture of bacteria (31.3% of $6.5 \times 10^3 \text{ cells ml}^{-1}$). The unspecific capture yield was 4%. DS 280 beads did not succeed in specific capture of bacteria from lettuce.

After high unspecific capture yields of bacteria achieved with DS M270 and DS M280 magnetic beads the influence of spacer length to specific capture of bacteria was investigated. The biotin molecules used till then had a spacer length of 13.5 Å. Then biotins with a spacer length of 56 Å were used for recombinant lysozyme immobilization on DS M270 and DS M280. The increase of the spacer length did not change the capture efficiencies. The highest yields of capture of bacteria were again achieved with unfunctionalized beads. These findings are in agreement with the results of Sun et al. They used spacers with lengths of 30.5 Å, 22.4 Å, and 13.5 Å for the biotinylation of antibodies for capture of bacteria. No general trend was observed for the influence of the spacer length on the efficiency of the capture of *E.coli* O157:H7 [114].

4.7.4.1 Comparison of the yield for capture of bacteria of different kinds of beads

The capture yields of bacteria from lettuce by the different kinds of beads were much lower than the capture yields achieved from bacteria suspensions. It is assumed that this is caused by additional components in food and also the Tween20 contained in elution buffer. They hindered an efficient capture of bacteria by beads. The highest capture of 8 cells $\mu\text{g}^{-1} \text{ml}^{-1}$ in approach A was achieved by Lyswt functionalized M-PVA SAV2 beads. With these beads, no detectable amount of bacteria was recovered with unfunctionalized beads from an initial cell value of 10^4ml^{-1} . In approach B, the M-PVA SAV2 beads functionalized with LysE35A and LysE35Q had recovery values of 6.7 cells $\mu\text{g}^{-1} \text{ml}^{-1}$. Again, no unspecific bacteria adsorption to M-PVA SAV2 surface was detected, indicating the suitability of these beads for bacteria capture from complex matrices.

With DMS C1 beads, in approach A, highest recovery of 5.8 cells $\mu\text{g}^{-1} \text{ml}^{-1}$ was achieved with Lyswt functionalization. In approach B, LysE35Q functionalized DMS C1 beads achieved a recovery of 104 cells $\mu\text{g}^{-1} \text{ml}^{-1}$, whereas the unspecific capture in this approach was 16 cells $\mu\text{g}^{-1} \text{ml}^{-1}$.

In summary, the highest cell capture values were achieved with LysE35Q functionalized DMS C1 beads. But these beads showed also an unspecific, lysozyme-independent adsorption of 15% of bacteria to their surface. Whereas M-PVA SAV2 beads had a lower value of bacteria capture but were not subject to unspecific bacteria adsorption to their surface. But the initial cell values for the beads

were different. For DMS C1 beads, a 10-fold higher initial amount of bacteria per ml of capture volume was used than for M-PVA SAV2.

4.7.4.2 Comparison of the lysozyme functionalizations

Most of the used beads were successful in specific lysozyme based bacteria separation from lettuce. But as discussed for the bacteria enrichment from suspension, the random biotinylation of the recombinantly expressed lysozyme molecules and hence their random orientation on the beads seem to influence the capture efficiencies. The reproducibility of the capture yields of bacteria were hindered by these orientations, which were a matter of coincidence. And hence, in some cases LysE35Q functionalization, and in other cases the Lyswt functionalization recovered the highest amount of bacteria. With DS M270 and DS M280, highest recoveries were achieved with unfunctionalized beads. Probably a wrong orientation of the lysozyme on the surface of the beads does not only inhibit specific capture, it furthermore inhibits also unspecific adsorption to the surface of the beads.

5 Conclusion and Outlook

In this work a new method based on lysozyme coupled to magnetic particles for the separation of bacteria was developed. The method was applied for the enrichment of reference bacteria from suspensions and for separation of reference bacteria from artificially contaminated food matrix.

The hen egg white lysozyme (HEWL) used in this study was mutated by exchanging the catalytic amino acid glutamate 35 with alanine (LysE35A) or glutamine (LysE35Q) by means of site-directed PCR. As a result, the bacteriolytic activity of the enzyme was diminished. The mutated derivatives and wild-type lysozyme, which served as reference, were expressed in *P. pastoris* at laboratory batch scale in a secretional manner. Parameter optimization resulted in concentrations of the recombinant lysozymes of up to 30 mg l⁻¹. However considering the large-scale application of the lysozyme based bacteria separation assay, a higher amount of lysozyme is required. Therefore a large- scale expression with controlled carbon source feeding and controlled oxygen supply is necessary.

Conventional purification of the recombinant lysozymes based on column chromatography directly from expression broth failed probably due to low lysozyme concentrations but the use of cation exchange MagPrepSO₃ nanoparticles for protein purification was successful in lab-scale.

An increase of the pH to 8.5 of the expression broth after removal of the *P. pastoris* cells caused agglomeration and precipitation of undesired proteins with lower pI values. This step caused a lysozyme loss of 5-15%. A subsequent incubation of the expression broth with MagPrepSO₃ beads resulted in lysozyme binding and separation due to magnetic forces. Subsequent elution with high salt buffer caused a further purification. The binding capacity of lysozymes to nano- scaled beads was determined as 254 µg g⁻¹ for Lyswt and 751 µg g⁻¹ for LysE35A in alkaline expression broth. These low values were compensated by the reuse of same beads and same high- salt elution buffer for up to 15 times, which caused up to 12.5- fold protein enrichment in the elutate. These values met the practical demands of lab-scale recombinant lysozyme expression.

An assay investigating the ability of the recombinant wild-type lysozyme to lyse *M. luteus* cells confirmed that the lysozyme still kept its bacteriolytic activity after expression and purification with nano-scaled MagPrepSO₃ beads. Therefore, it can be concluded that the recombinant expression and purification did not influence the native protein structure and hence were suitable for the achievement of pure recombinant lysozymes.

But for a large-scale protein expression, the method of protein purification by nano-scaled magnetic cation exchange particles would be too expensive and elaborative. Therefore, the scale-up of protein expression level requires either a higher loading capacity of the magnetic beads or the establishment of another strategy for protein purification e.g. ultrafiltration or column chromatography.

The immobilization of the lysozymes onto magnetic beads was based on streptavidin-biotin interaction. The NHS- activated biotins used in this study react with primary amino groups of proteins. The wild- type hen egg white lysozyme and the mutated derivative LysE35A possess 33 amino acids that provide primary amines in addition to the N-terminal primary amine. The mutant protein LysE35Q contains 34 amino acids with primary amino groups in their side chains. Assumed no sterical hindrance, every primary amine could have subject to biotinylation. This probably has caused a random orientation of the biotinylated lysozymes bound to the streptavidin-functionalized magnetic beads. As a consequence, the binding cleft can be orientated averted from the bacteria. This prevents the effective capture of bacteria by the immobilized lysozymes. Although the capture results show that every type of lysozyme used in this study (Lyswt, LysE35A, and LysE35Q) succeeded in capturing bacteria, the results achieved with any bead and any functionalization were not reproducible. Recombinant Lyswt, which was proven to maintain bacteriolytic activity, exhibited the same trend. Therefore, site-directed immobilization has to be aspired for technical application of the capture of bacteria based on mutated lysozyme: The lysozyme should be oriented on the solid phase in a manner that allows the orientation of the binding cleft averted from the bead surface for efficient bacteria capture. The comparison of the recovery values for bacteria reached with lysozyme functionalized M-PVA SAV2 beads, which have a biotinylated protein binding capacity of only 30 pmol mg⁻¹, to the Dynabeads, with biotinylated IgG binding capacities of up to 70 pmol mg⁻¹, showed that a higher density of lysozymes provided

a higher capture efficiency to the beads . Therefore, the possibility of achieving high density of functionalization should be considered in generating functionalized constructs.

Expression of C-terminally or N-terminally (His)₆ tagged mutant lysozymes could be an alternative way for site- directed immobilization of the proteins on Ni-nitriloacetic acid (NTA) functionalized surfaces. A drawback of this strategy is the low affinity of the His-tag to the Ni⁺-NTA with a K_d value of 10 μM. A further immobilization strategy could be coupling of ssDNA moieties to the lysozymes which have complementary DNA sequences immobilized onto solid surfaces. DNA-protein conjugates can be achieved by covalent attachment, bifunctional linkers, interaction via streptavidin-biotin bridge, or expressed protein ligation. An advantage of DNA- directed immobilization is high immobilization efficiency and the formation of a rigid, double stranded DNA spacer arm between surface and protein. Additionally, alkaline denaturation of the DNA double helix enables the removal of the immobilized protein. This provides an efficient method for the regeneration of the sorbent. Furthermore, the subsequent detection of bacteria can be performed in absence of interfering particles. Another strategy for covalent site- specific immobilization of the proteins on solid surfaces is “click” chemistry where azide functionalized proteins can be immobilized on alkyne modified surfaces like agarose beads [121]. A third strategy is described by Duckworth et al.: The authors genetically fused a CVIA tetrapeptide tag to the C-terminus of a target protein, which is recognized by the enzyme farnesyltransferase and prenylated by the enzyme with farnesyl diphosphate bearing an azide moiety. The protein was then immobilized on agarose beads by Cu(I)-catalysed cycloaddition reaction [122].

Another drawback of this method considering large-scaled use is difficult separation of solid phase used for immobilization of the proteins in this study. The μ-scaled magnetic particles were easily separated from solid-free solutions but the application to unfiltered, homogenized food was accompanied by particle loss and difficult separation due to sterical hinderance of the magnetic particles by food components. A possible strategy to separate magnetic particles from such suspensions is HGMF, which could be suitable to overcome this difficulty. But the magnetic particles used for bacteria capture are expensive, hindering a commercial application. Therefore other solid materials need to be investigated for functionalization with lysozyme and large-

scale capture of bacteria, like filter materials suitable for lysozyme functionalization. An advantage of this filter would be their simple integration into water pipelines as well as their easy removal for the detection of the contamination level.

In addition to this, filters integrated into the flowpath of the water through a pipe would allow the contact of large volumes, thus making inline detection possible, whereas the use of magnetic particles requires off-line detection.

6 References

1. Skjerve, E., Rørvik, L. M. and Olsvik, O. (1990). "Detection of *Listeria monocytogenes* in foods by immunomagnetic separation." Applied and Environmental Microbiology **56**(11): 3478-3481.
2. Jones, I. G. and Roworth, M. (1996). "An outbreak of *Escherichia coli* 0157 and campylobacteriosis associated with contamination of a drinking water supply." Public Health **110**(5): 277-282.
3. Blaser, M. J. (1997). "Epidemiologic and Clinical Features of *Campylobacter jejuni* Infections." Journal of Infectious Diseases **176**(Supplement 2): S103-S105.
4. Furtado, C., Adak, G. K., Stuart, J. M., Wall, P. G., Evans, H. S. and Casemore, D. P. (1998). "Outbreaks of waterborne infectious intestinal disease in England and Wales, 1992–5." Epidemiology & Infection **121**(01): 109-119.
5. Tholozan, J. L., Cappelier, J. M., Tissier, J. P., Delattre, G. and Federighi, M. (1999). "Physiological Characterization of Viable-but-Nonculturable *Campylobacter jejuni* Cells." Appl. Environ. Microbiol. **65**(3): 1110-1116.
6. Notermans, S. and Hoogenboom-Verdegaal, A. (1992). "Existing and emerging foodborne diseases." International Journal of Food Microbiology **15**(3–4): 197-205.
7. Skirrow, M. B. (1990). Foodborne illness: *Campylobacter*. Lancet **336**:921-923
8. Ferroni, A., Nguyen, L., Pron, B., Quesne, G., Brusset, M. C. and Berche, P. (1998). "Outbreak of nosocomial urinary tract infections due to *Pseudomonas aeruginosa* in a paediatric surgical unit associated with tap-water contamination." Journal of Hospital Infection **39**(4): 301-307.
9. Bert, F., Maubec, E., Bruneau, B., Berry, P. and Lambert-Zechovsky, N. (1998). "Multi-resistant *Pseudomonas aeruginosa* outbreak associated with contaminated tap water in a neurosurgery intensive care unit." Journal of Hospital Infection **39**(1): 53-62.
10. <http://www.rki.de/DE/Content/InfAZ/E/EHEC/EHEC.html>
11. Hulten, K., Enroth, H., Nystrom, T. and Engstrand, L. (1998). "Presence of *Helicobacter* species DNA in Swedish water." Journal of Applied Microbiology **85**(2): 282-286.

12. Hulten, K., Han, S. W., Enroth, H., Klein, P. D., Opekun, A. R., Gilman, R. H., Evans, D. G., Engstrand, L., Graham, D. Y. and El-Zaatari, F. A. (1996). "Helicobacter pylori in the drinking water in Peru." Gastroenterology **110**(4): 1031-1035.
13. McFeters, G. A., Pyle, B. H., Lisle, J. T. and Broadaway, S. C. (1998). "Rapid direct methods for enumeration of specific, active bacteria in water and biofilms." Journal of Applied Microbiology **85**(S1): 193S-200S.
14. Jasson, V., Jacxsens, L., Luning, P., Rajkovic, A. and Uyttendaele, M. (2010). "Alternative microbial methods: An overview and selection criteria." Food Microbiology **27**(6): 710-730.
15. Byrd, J. J., Xu, H. S. and Colwell, R. R. (1991). "Viable but nonculturable bacteria in drinking water." Appl. Environ. Microbiol. **57**(3): 875-878.
16. Colwell, R. R., Brayton, P. R., Grimes, D. J., Roszak, D. B., Huq, S. A. and Palmer, L. M. (1985). "Viable but Non-Culturable Vibrio cholerae and Related Pathogens in the Environment: Implications for Release of Genetically Engineered Microorganisms." Nat Biotech **3**(9): 817-820.
17. Colwell, R. R., Brayton, P., Herrington, D., Tall, B., Huq, A. and Levine, M. M. (1996). "Viable but non-culturable Vibrio cholera O1 revert to a cultivable state in the human intestine." World Journal of Microbiology and Biotechnology **12**(1): 28-31.
18. Toranzos, G. A., McFeters, G. A., Hurst, C. J., Knudsen, G. R., McInerney, M. J., Stetzenbach, L. D., and Walter, M. V. (1997). Detection of indicator microorganisms in environmental freshwaters and drinking waters. *Manual of environmental microbiology.*, 184-194.
19. Heim, S., Del Mar Lleo, M., Bonato, B., Guzman, C. A. and Canepari, P. (2002). "The Viable but Nonculturable State and Starvation Are Different Stress Responses of Enterococcus faecalis, as Determined by Proteome Analysis." J. Bacteriol. **184**(23): 6739-6745.
20. Signoretto, C., del Mar Lleo, M., Tafi, M. C. and Canepari, P. (2000). "Cell Wall Chemical Composition of Enterococcus faecalis in the Viable but Nonculturable State." Appl. Environ. Microbiol. **66**(5): 1953-1959.
21. Signoretto, C., Lleò, M. d. M. and Canepari, P. (2002). "Modification of the Peptidoglycan of Escherichia coli in the Viable But Nonculturable State." Current Microbiology **44**(2): 125-131.

22. Oliver, J. (2005). "The viable but nonculturable state in bacteria." Journal of microbiology (Seoul, Korea) **43 Spec No**: 93-100.
23. Allen, M. J., Edberg, S. C. and Reasoner, D. J. (2004). "Heterotrophic plate count bacteria—what is their significance in drinking water?" International Journal of Food Microbiology **92**(3): 265-274.
24. Wadhwa, S. G., Khaled, G. H. and Edberg, S. C. (2002). "Comparative Microbial Character of Consumed Food and Drinking Water." Critical Reviews in Microbiology **28**(3): 249-279.
25. Swaminathan, B. and Feng, P. (1994). "Rapid Detection of Food-Borne Pathogenic Bacteria." Annual Review of Microbiology **48**(1): 401-426.
26. Clark, J. A. (1980). "The influence of increasing numbers of nonindicator organisms upon the detection of indicator organisms by the membrane filter and presence–absence tests." Canadian Journal of Microbiology **26**(7): 827-832.
27. DuPont, H. L., Levine, M. M., Hornick, R. B. and Formal, S. B. (1989). "Inoculum Size in Shigellosis and Implications for Expected Mode of Transmission." Journal of Infectious Diseases **159**(6): 1126-1128.
28. Varela Villarreal, J., Schwartz, T. and Obst, U. (2010). "Culture-independent techniques applied to food industry water surveillance — A case study." International Journal of Food Microbiology **141**:147-155.
29. Malorny, B., Tassios, P. T., Rådström, P., Cook, N., Wagner, M. and Hoorfar, J. (2003). "Standardization of diagnostic PCR for the detection of foodborne pathogens." International Journal of Food Microbiology **83**(1): 39-48.
30. Rossen, L., Nørskov, P., Holmstrøm, K. and Rasmussen, O. F. (1992). "Inhibition of PCR by components of food samples, microbial diagnostic assays and DNA-extraction solutions." International Journal of Food Microbiology **17**(1): 37-45.
31. Urs, C. (1995). "Polymerase chain reaction in food microbiology." Journal of Microbiological Methods **23**(1): 89-103.
32. Klein, D. (2002). "Quantification using real-time PCR technology: applications and limitations." Trends in Molecular Medicine **8**(6): 257-260.
33. van der Velden, V. H. J., Hochhaus, A., Cazzaniga, G., Szczepanski, T., Gabert, J. and van Dongen, J. J. M. (2003). "Detection of minimal residual

- disease in hematologic malignancies by real-time quantitative PCR: principles, approaches, and laboratory aspects." Leukemia **17**(6): 1013-1034.
34. Hartman P. A., Swaminathan B., Curiale M.S., Firstenberg-Eden R., Sharpe A.N., et al. 1992. Rapid methods and automation. In *Compendium of Methods for the Microbiological Examination of Foods*. ed. C Vanderzant. OF Splittstosser, pp. 665-746. Washington DC: Am. Public Health Assoc.
35. Khastsaev, B. (1996). "Principles of food quality monitoring by impedance bactometers." Biomedical Engineering **30**(5): 293-295.
36. Panicker, G., Call, D. R., Krug, M. J. and Bej, A. K. (2004). "Detection of Pathogenic *Vibrio* spp. in Shellfish by Using Multiplex PCR and DNA Microarrays." Applied and Environmental Microbiology **70**(12): 7436-7444.
37. Muyzer, G., de Waal, E. C. and Uitterlinden, A. G. (1993). "Profiling of complex microbial populations by denaturing gradient gel electrophoresis analysis of polymerase chain reaction-amplified genes coding for 16S rRNA." Applied and Environmental Microbiology **59**(3): 695-700.
38. Ercolini, D. (2004). "PCR-DGGE fingerprinting: novel strategies for detection of microbes in food." Journal of Microbiological Methods **56**(3): 297-314.
39. Stevens, K. A. and Jaykus, L.-A. (2004). "Bacterial Separation and Concentration from Complex Sample Matrices: A Review." Critical Reviews in Microbiology **30**(1): 7-24.
40. Bej, A. K., Steffan, R. J., DiCesare, J., Haff, L. and Atlas, R. M. (1990). "Detection of coliform bacteria in water by polymerase chain reaction and gene probes." Applied and Environmental Microbiology **56**(2): 307-314.
41. Olsvik, O., Popovic, T., Skjerve, E., Cudjoe, K. S., Hornes, E., Ugelstad, J. and Uhlén, M. (1994). "Magnetic separation techniques in diagnostic microbiology." Clinical Microbiology Reviews **7**(1): 43-54.
42. Jiang, J., Alderisio, K. A., Singh, A. and Xiao, L. (2005). "Development of Procedures for Direct Extraction of *Cryptosporidium* DNA from Water Concentrates and for Relief of PCR Inhibitors." Applied and Environmental Microbiology **71**(3): 1135-1141.
43. Loge, F. J., Thompson, D. E. and Call, D. R. (2002). "PCR Detection of Specific Pathogens in Water: A Risk-Based Analysis." Environmental Science & Technology **36**(12): 2754-2759.

44. Haukanes, B.-I. and Kvam, C. (1993). "Application of Magnetic Beads in Bioassays." Nat Biotech **11**(1): 60-63.
45. Lea, T., Vartdal, F., Davies, C. and Ugelstad, J. (1985). "Magnetic Monosized Polymer Particles for Fast and Specific Fractionation of Human Mononuclear Cells." Scandinavian Journal of Immunology **22**(2): 207-216.
46. Gaudernack, G., Leivestad, T., Ugelstad, J. and Thorsby, E. (1986). "Isolation of pure functionally active CD8+ T cells positive selection with monoclonal antibodies directly conjugated to monosized magnetic microspheres." Journal of Immunological Methods **90**(2): 179-187.
47. Skjerve, E., Rørvik, L. M. and Olsvik, O. (1990). "Detection of *Listeria monocytogenes* in foods by immunomagnetic separation." Applied and Environmental Microbiology **56**(11): 3478-3481.
48. Wadud, S., Leon-Velarde, C. G., Larson, N. and Odumeru, J. A. (2010). "Evaluation of immunomagnetic separation in combination with ALOA *Listeria* chromogenic agar for the isolation and identification of *Listeria monocytogenes* in ready-to-eat foods." Journal of Microbiological Methods **81**(2): 153-159.
49. Cudjoe, K. S., Thorsen, L. I., Sørensen, T., Reseland, J., Olsvik, Ø. and Granum, P. E. (1991). "Detection of *Clostridium perfringens* type A enterotoxin in faecal and food samples using immunomagnetic separation (IMS)-ELISA." International Journal of Food Microbiology **12**(4): 313-321.
50. Yang, Z.-Y., Shim, W.-B., Kim, K.-Y. and Chung, D.-H. (2010). "Rapid Detection of Enterotoxigenic *Clostridium perfringens* in Meat Samples Using Immunomagnetic Separation Polymerase Chain Reaction (IMS-PCR)." Journal of Agricultural and Food Chemistry **58**(12): 7135-7140.
51. Lucero Estrada, C. S. M., Velázquez, L. d. C., Favier, G. I., Di Genaro, M. S. and Escudero, M. E. (2012). "Detection of *Yersinia* spp. in meat products by enrichment culture, immunomagnetic separation and nested PCR." Food Microbiology **30**(1): 157-163.
52. Liandris, E., Gazouli, M., Andreadou, M., Sechi, L. A., Rosu, V. and Ikonopoulou, J. (2011). "Detection of Pathogenic *Mycobacteria* Based on Functionalized Quantum Dots Coupled with Immunomagnetic Separation." PLoS ONE **6**(5): e20026.
53. Fedio, W. M., Jinneman, K. C., Yoshitomi, K. J., Zapata, R., Wendakoon, C. N., Browning, P. and Weagant, S. D. (2011). "Detection of *E. coli* O157:H7 in raw

- ground beef by Pathatrix™ immunomagnetic-separation, real-time PCR and cultural methods." International Journal of Food Microbiology **148**(2): 87-92.
54. Weagant, S. D., Jinneman, K. C., Yoshitomi, K. J., Zapata, R. and Fedio, W. M. (2011). "Optimization and evaluation of a modified enrichment procedure combined with immunomagnetic separation for detection of E. coli O157:H7 from artificially contaminated alfalfa sprouts." International Journal of Food Microbiology **149**(3): 209-217.
55. Schreier, S., Doungchawee, G., Triampo, D., Wangroongsarb, P., Hartskeerl, R. A. and Triampo, W. (2012). "Development of a magnetic bead fluorescence microscopy immunoassay to detect and quantify *Leptospira* in environmental water samples." Acta Tropica **122**(1): 119-125.
56. Li, A., Zhang, H., Zhang, X., Wang, Q., Tian, J., Li, Y. and Li, J. (2010). "Rapid separation and immunoassay for low levels of *Salmonella* in foods using magnetosome–antibody complex and real-time fluorescence quantitative PCR." Journal of Separation Science **33**(21): 3437-3443.
57. Garbaccio, S. G. and Cataldi, A. A. (2010). "Evaluation of an immunomagnetic capture method followed by PCR to detect *Mycobacterium bovis* in tissue samples from cattle." Revista argentina de microbiología **42**: 247-253.
58. Zhao, Y., Ye, M., Chao, Q., Jia, N., Ge, Y. and Shen, H. (2008). "Simultaneous Detection of Multifood-Borne Pathogenic Bacteria Based on Functionalized Quantum Dots Coupled with Immunomagnetic Separation in Food Samples." Journal of Agricultural and Food Chemistry **57**(2): 517-524.
59. Sun, W., Brovko, L. and Griffiths, M. (2001). "Use of bioluminescent *Salmonella* for assessing the efficiency of constructed phage-based biosorbent." Journal of Industrial Microbiology & Biotechnology **27**(2): 126-128.
60. Kretzer, J. W., Lehmann, R., Schmelcher, M., Banz, M., Kim, K.-P., Korn, C. and Loessner, M. J. (2007). "Use of High-Affinity Cell Wall-Binding Domains of Bacteriophage Endolysins for Immobilization and Separation of Bacterial Cells." Applied and Environmental Microbiology **73**(6): 1992-2000.
61. Fleming, A. (1922). "On a Remarkable Bacteriolytic Element Found in Tissues and Secretions." Proceedings of the Royal Society of London. Series B, Containing Papers of a Biological Character **93**(653): 306-317.
62. Callewaert, L. and Michiels, C. (2010). "Lysozymes in the animal kingdom." Journal of Biosciences **35**(1): 127-160.

63. Blake, C. C. F., Johnson, L. N., Mair, G. A., North, A. C. T., Phillips, D. C. and Sarma, V. R. (1967). "Crystallographic Studies of the Activity of Hen Egg-White Lysozyme." Proceedings of the Royal Society of London. Series B, Biological Sciences **167**(1009): 378-388.
64. Strynadka N.C., James M.N. (1996). "Lysozyme: a model enzyme in protein crystallography." EXS. 75: 185-222
65. Strynadka, N. C. J. and James, M. N. G. (1991). "Lysozyme revisited: Crystallographic evidence for distortion of an N-acetylmuramic acid residue bound in site D." Journal of Molecular Biology **220**(2): 401-424.
66. Malcolm, B. A., Rosenberg, S., Corey, M. J., Allen, J. S., de Baetselier, A. and Kirsch, J. F. (1989). "Site-directed mutagenesis of the catalytic residues Asp-52 and Glu-35 of chicken egg white lysozyme." Proceedings of the National Academy of Sciences **86**(1): 133-137.
67. Matsumura, I. and Kirsch, J. F. (1996). "Is Aspartate 52 Essential for Catalysis by Chicken Egg White Lysozyme? The Role of Natural Substrate-Assisted Hydrolysis." Biochemistry **35**(6): 1881-1889.
68. Phillips, D. C. (1966). "The three-dimensional structure of an enzyme molecule." Scientific American **215**(5): 78-90.
69. Vernon, C. A. (1967). "The mechanisms of hydrolysis of glycosides and their relevance to enzyme-catalysed reactions." Proceedings of the Royal Society of London. Series B, Containing papers of a Biological character. Royal Society (Great Britain) **167**(9): 389-401.
70. Marston, F. A. (1986). "The purification of eukaryotic polypeptides synthesized in *Escherichia coli*." The Biochemical journal **240**(1): 1-12.
71. Makrides, S. C. (1996). "Strategies for achieving high-level expression of genes in *Escherichia coli*." Microbiol. Rev. **60**(3): 512-538.
72. Cregg, J. M., Barringer, K. J., Hessler, A. Y. and Madden, K. R. (1985). "*Pichia pastoris* as a host system for transformations." Mol. Cell. Biol. **5**(12): 3376-3385.
73. Li, P., Anumanthan, A., Gao, X.-G., Ilangovan, K., Suzara, V., Düzgüneş, N. and Renugopalakrishnan, V. (2007). "Expression of Recombinant Proteins in *Pichia Pastoris*." Applied Biochemistry and Biotechnology **142**(2): 105-124.
74. Cregg, J., Cereghino, J., Shi, J. and Higgins, D. (2000). "Recombinant protein expression in *Pichia pastoris*." Molecular Biotechnology **16**(1): 23-52.

75. Cregg, J. M., Vedvick, T. S. and Raschke, W. C. (1993). "Recent Advances in the Expression of Foreign Genes in *Pichia pastoris*." Nat Biotech **11**(8): 905-910.
76. Daly, R. and Hearn, M. T. W. (2005). "Expression of heterologous proteins in *Pichia pastoris*: a useful experimental tool in protein engineering and production." Journal of Molecular Recognition **18**(2): 119-138.
77. Alderton, G. and Fevold, H. L. (1946). "Direct crystallization of lysozyme from egg white and some crystalline salts of lysozyme." The Journal of biological chemistry **164**: 1-5.
78. Muzzarelli, R. A. A., Barontini, G. and Rochetti, R. (1978). "Isolation of lysozyme on chitosan." Biotechnology and Bioengineering **20**(1): 87-94.
79. Hofmeister, F. (1888). "Zur Lehre von der Wirkung der Salze." Naunyn-Schmiedeberg's Archives of Pharmacology **25**(1): 1-30.
80. Shih, Y.-C., Prausnitz, J. M. and Blanch, H. W. (1992). "Some characteristics of protein precipitation by salts." Biotechnology and Bioengineering **40**(10): 1155-1164.
81. Ogez, J. R., Hodgdon, J. C., Beal, M. P. and Builder, S. E. (1989). "Downstream processing of proteins: Recent advances." Biotechnology Advances **7**(4): 467-488.
82. Ming, F., Howell, J., Acosta, F. and Hubble, J. (1993). "Study on separation of conalbumin and lysozyme from high concentration fresh egg white at high flow rates by a novel ion-exchanger." Biotechnology and Bioengineering **42**(9): 1086-1090.
83. Awadé, A. C., Moreau, S., Mollé, D., Brulé, G. and Maubois, J. L. (1994). "Two-step chromatographic procedure for the purification of hen egg white ovomucin, lysozyme, ovotransferrin and ovalbumin and characterization of purified proteins." Journal of Chromatography A **677**(2): 279-288.
84. Ghosh, R. (2003). "Purification of lysozyme by microporous PVDF membrane-based chromatographic process." Biochemical Engineering Journal **14**(2): 109-116.
85. Guérin-Dubiard, C., Pasco, M., Hietanen, A., Quiros del Bosque, A., Nau, F. and Croguennec, T. (2005). "Hen egg white fractionation by ion-exchange chromatography." Journal of Chromatography A **1090**(1-2): 58-67.

86. Franzreb, M., Siemann-Herzberg, M., Hobbey, T. and Thomas, O. (2006). "Protein purification using magnetic adsorbent particles." Applied Microbiology and Biotechnology **70**(5): 505-516.
87. Safarik, I. and Safarikova, M. (2004). "Magnetic techniques for the isolation and purification of proteins and peptides." BioMagnetic Research and Technology **2**(1): 7.
88. Meyer, A., Hansen, D. B., Gomes, C. S. G., Hobbey, T. J., Thomas, O. R. T. and Franzreb, M. (2005). "Demonstration of a Strategy for Product Purification by High-Gradient Magnetic Fishing: Recovery of Superoxide Dismutase from Unconditioned Whey." Biotechnology Progress **21**(1): 244-254.
89. Sontheimer, H., et. al. (1985) adsorptionsverfahren zur Wasserreinigung. Karlsruhe:Engler-Bunte-Institut der Universität Karlsruhe.
90. Sharma, S. and Agarwal, G. P. (2001). "Interactions of Proteins with Immobilized Metal Ions: A Comparative Analysis Using Various Isotherm Models." Analytical Biochemistry **288**(2): 126-140.
91. Scatchard, G. (1949). "Equilibrium in Non-Electrolyte Mixtures." Chemical Reviews **44**(1): 7-35.
92. Tong, X.-D., Xue, B. and Sun, Y. (2001). "A Novel Magnetic Affinity Support for Protein Adsorption and Purification." Biotechnology Progress **17**(1): 134-139.
93. Liao, M.-H. and Chen, D.-H. (2002). "Fast and efficient adsorption/desorption of protein by a novel magnetic nano-adsorbent." Biotechnology Letters **24**(22): 1913-1917.
94. Peng, Z. G., Hidajat, K. and Uddin, M. S. (2004). "Adsorption and desorption of lysozyme on nano-sized magnetic particles and its conformational changes." Colloids and Surfaces B: Biointerfaces **35**(3-4): 169-174.
95. Meyer, A., Berensmeier, S. and Franzreb, M. (2007). "Direct capture of lactoferrin from whey using magnetic micro-ion exchangers in combination with high-gradient magnetic separation." Reactive and Functional Polymers **67**(12): 1577-1588.
96. Ling, M. M. and Robinson, B. H. (1997). "Approaches to DNA Mutagenesis: An Overview." Analytical Biochemistry **254**(2): 157-178.
97. Inoue, H., Nojima, H. and Okayama, H. (1990). "High efficiency transformation of Escherichia coli with plasmids." Gene **96**(1): 23-28.

98. Shugar, D. (1952). "The measurement of lysozyme activity and the ultra-violet inactivation of lysozyme." BBA - Biochimica et Biophysica Acta **8**(C): 302-309.
99. Frahm, E., Heiber, I., Hoffmann, S., Koob, C., Meier, H., Ludwig, W., Amann, R., Schleifer, K. H. and Obst, U. (1998). "Application of 23S rDNA-targeted Oligonucleotide Probes Specific for Enterococci to Water Hygiene Control." Systematic and Applied Microbiology **21**(3): 450-453.
100. Frahm, E. and Obst, U. (2003). "Application of the fluorogenic probe technique (TaqMan PCR) to the detection of Enterococcus spp. and Escherichia coli in water samples." Journal of Microbiological Methods **52**(1): 123-131.
101. Fogel, G. B., Collins, C. R., Li, J. and Brunk, C. F. (1999). "Prokaryotic Genome Size and SSU rDNA Copy Number: Estimation of Microbial Relative Abundance from a Mixed Population." Microbial Ecology **38**(2): 93-113.
102. Byrd, J. J., Xu, H. S. and Colwell, R. R. (1991). "Viable but nonculturable bacteria in drinking water." Appl. Environ. Microbiol. **57**(3): 875-878.
103. Gunasekera, T. S., Sorensen, A., Attfield, P. V., Sorensen, S. J. and Veal, D. A. (2002). "Inducible Gene Expression by Nonculturable Bacteria in Milk after Pasteurization." Appl. Environ. Microbiol. **68**(4): 1988-1993.
104. Oliver, J. D., Dagher, M., and Linden K. (2005). "Induction of Escherichia coli and Salmonella typhimurium into the viable but nonculturable state following chlorination of wastewater." J Water Health **03**(3): 249-257.
105. Wolf, P. W. and Oliver, J. D. (1992). "Temperature effects on the viable but non-culturable state of Vibrio vulnificus." FEMS Microbiology Letters **101**(1): 33-39.
106. Oliver, J. (2005). "The viable but nonculturable state in bacteria." Journal of microbiology (Seoul, Korea) **43**: 93-100.
107. Besnard, V., Federighi, M. and Cappelier, J. M. (2000). "Development of a direct viable count procedure for the investigation of VBNC state in Listeria monocytogenes" Letters in Applied Microbiology **31**(1): 77-81.
108. Allen, M. J., Edberg, S. C. and Reasoner, D. J. (2004). "Heterotrophic plate count bacteria—what is their significance in drinking water?" International Journal of Food Microbiology **92**(3): 265-274.
109. European Union. Guidance Document (2005) Implementation of procedures based on the HACCP principles in certain food business. Brussels.

110. Food and Agriculture Organisation/World Health Organisation (2006). Guidance to governments on the application of HACCP in small and/or less-developed food business. FAO food and nutrition paper 86. ISSN 0254-4725
111. Diler, E., Obst, U., Schmitz, K. and Schwartz, T. (2011). "A lysozyme and magnetic bead based method of separating intact bacteria." Analytical and Bioanalytical Chemistry **401**(1): 253-265.
112. Monsalve, R. I., Lu, G. and King, T. P. (1999). "Expressions of Recombinant Venom Allergen, Antigen 5 of Yellowjacket (*Vespula vulgaris*) and Paper Wasp (*Polistes annularis*), in Bacteria or Yeast." Protein Expression and Purification **16**(3): 410-416.
113. Enroth, H. and Engstrand, L. (1995). "Immunomagnetic separation and PCR for detection of *Helicobacter pylori* in water and stool specimens." J. Clin. Microbiol. **33**(8): 2162-2165.
114. Sun, W., Khosravi, F., Albrechtsen, H., Brovko, L. Y. and Griffiths, M. W. (2002). "Comparison of ATP and in vivobioluminescence for assessing the efficiency of immunomagnetic sorbents for live *Escherichia coli*O157:H7 cells." Journal of Applied Microbiology **92**(6): 1021-1027.
115. Oka, C., Tanaka, M., Muraki, M., Harata, K., Suzuki, K. and Jigami, Y. (1999). "Human Lysozyme Secretion Increased by Alpha-factor Pro-sequence in *Pichia pastoris*." Bioscience, Biotechnology, and Biochemistry **63**(11): 1977-1983.
116. Saito, A., Sako, Y., Usui, M., Azakami, H. and Kato, A. (2003). "Functional Properties of Glycosylated Lysozyme Secreted in *Pichia pastoris*." Bioscience, Biotechnology, and Biochemistry **67**(11): 2334-2343.
117. Goda, S., Takano, K., Yamagata, Y., Katakura, Y. and Yutani, K. (2000). "Effect of extra N-terminal residues on the stability and folding of human lysozyme expressed in *Pichia pastoris*." Protein Engineering **13**(4): 299-307.
118. Brierley, R. A., Bussineau, C., Kosson, R., Melton, A. and Siegel, R. S. (1990). "Fermentation Development of Recombinant *Pichia pastoris* Expressing the Heterologous Gene: Bovine Lysozyme." Annals of the New York Academy of Sciences **589**(1): 350-362.
119. Macauley-Patrick, S., Fazenda, M. L., McNeil, B. and Harvey, L. M. (2005). "Heterologous protein production using the *Pichia pastoris* expression system." Yeast **22**(4): 249-270.

120. Peluso, P., Wilson, D. S., Do, D., Tran, H., Venkatasubbaiah, M., Quincy, D., Heidecker, B., Poindexter, K., Tolani, N., Phelan, M., Witte, K., Jung, L. S., Wagner, P. and Nock, S. (2003). "Optimizing antibody immobilization strategies for the construction of protein microarrays." Analytical Biochemistry **312**(2): 113-124.
121. Rusmini, F., Zhong, Z. and Feijen, J. (2007). "Protein Immobilization Strategies for Protein Biochips." Biomacromolecules **8**(6): 1775-1789.
122. Duckworth, B. P., Xu, J., Taton, T. A., Guo, A. and Distefano, M. D. (2006). "Site-Specific, Covalent Attachment of Proteins to a Solid Surface." Bioconjugate Chemistry **17**(4): 967-974.
123. Holmberg, A., Blomstergren, A., Nord, O., Lukacs, M., Lundeberg, J. and Uhlén, M. (2005). "The biotin-streptavidin interaction can be reversibly broken using water at elevated temperatures." Electrophoresis **26**(3): 501-510.

7 Appendix

```

773 | AOX1 mRNA 5' end (824)
ACAGCAATAT ATAAACAGAA GGAAGCTGCC CTGTCTTAAA CCTTTT TTTT TATCATCATT ATTAGCTTAC

      5' AOX1 Primer Site (855-875)
TTTCATAATT GCGACTGGTT CCAATTGACA AGCTTTTGAT TTTAACGACT TTTAACGACA ACTTGAGAAG

      α-Factor (949-1215)
ATCAAAAAAC AACTAATTAT TCGAAGGATC CAAACG ATG AGA TTT CCT TCA ATT TTT ACT GCA
           Met Arg Phe Pro Ser Ile Phe Thr Ala

GTT TTA TTC GCA GCA TCC TCC GCA TTA GCT GCT CCA GTC AAC ACT ACA ACA GAA GAT
Val Leu Phe Ala Ala Ser Ser Ala Leu Ala Ala Pro Val Asn Thr Thr Thr Glu Asp

GAA ACG GCA CAA ATT CCG GCT GAA GCT GTC ATC GGT TAC TCA GAT TTA GAA GGG GAT
Glu Thr Ala Gln Ile Pro Ala Glu Ala Val Ile Gly Tyr Ser Asp Leu Glu Gly Asp

TTC GAT GTT GCT GTT TTG CCA TTT TCC AAC AGC ACA AAT AAC GGG TTA TTG TTT ATA
Phe Asp Val Ala Val Leu Pro Phe Ser Asn Ser Thr Asn Asn Gly Leu Leu Phe Ile

      α-Factor Primer Site (1152-1172)
AAT ACT ACT ATT GCC AGC ATT GCT GCT AAA GAA GAA GGG GTA TCT CTC GAG AAA AGA
Asn Thr Thr Ile Ala Ser Ile Ala Ala Lys Glu Glu Gly Val Ser Leu Glu Lys Arg
           Xho I

Signal cleavage (1204)
▼ SnaBI EcoRI Avr II Not I
GAG GCT GAA GCT TAC GTA GAA TTC CCT AGG GCG GCC GCG AAT TAA TTCGCCTTAG
Glu Ala Glu Ala Tyr Val Glu Phe Pro Arg Ala Ala Ala Asn ***

ACATGACTGT TCCTCAGTTC AAGTTGGGCA CTTACGAGAA GACCGGTCTT GCTAGATTCT AATCAAGAGG

      3' AOX1 Primer Site (1327-1347)
ATGTCAGAAAT GCCATTTGCC TGAGAGATGC AGGCTTCATT TTTGATACTT TTTTATTTGT AACCTATATA

      AOX1 mRNA 3' end (1418)
GTATAGGATT TTTTTTGCA

```

Figure A1: Multiple cloning site of pPic9

DNA Sequencing results of lysozyme cDNA cloning to the MCS of pPic9:

pPic9LysE35A-1:

AANNAAAAGGGTATCTCTCGNNAANAANNGCTGAAGCTAAAGTTTTCGGTAGGTGCGAATTAGC
CGCCGCAATGAAGCGCCACGGATTGGATAACTATCGTGGATACTCCCTAGGTAAGTGGGTTTGC
GTTGCTAAATTTGCTTCGAACTTTAATACTCAAGCAACCAATCGAAGCACCGACGGGAGCACCGA
CTATGGTATATTGCAGATCAATTCTCGATGGTGGTGAACGATGGCAGAACTCCTGGATCAAGAA
ACTTGTGCAACATTCCCTGTAGTGCTCTGTTATCCTCAGATATCACCTGCATCAGTTAATTGTGCC
AAAAAGATCGTGTCTGACGGAAATGGAATGTCTGCCTGGGTGGCCTTGGAGAAATCGTTGTAAG
GGCACTGATGTACAAGCTTGNATTAGAGGTTGTAGACTTTAGGCGGCCGCGAATTAATTTGCCT
TAGACATGACTGTTCCCTCAGTTCAAGTTGGGCACCTTACGAGAAGACCGGTCTTGCTAGATTCTA
ATCAAGAGGATGTCAGAATGCCATTTGCAANNNN

pPic9LysE35A-2

TANANAAAAGGGTATCTCTCGNNAAGNANAGCTGAAGCTAAAGTTTTCGGTAGGTGCGAATTA
GCCGCCGCAATGAAGCGCCACGGATTGGATAACTATCGTGGATACTCCCTAGGTAAGTGGGTTT
GCGTTGCTAAATTTGCTTCGAACTTTAATACTCAAGCAACCAATCGAAACACCGACGGGAGCAC
GACTATGGTATATTGCAGATCAATTCTCGATGGTGGTGAACGATGGCAGAACTCCTGGATCAAG
AACTTGTGCAACATTCCCTGTAGTGCTCTGTTATCCTCAGATATCACTGCATCAGTTAATTGTGC
CAAAAAGATCGTGTCTGACGGAAATGGAATGTCTGCCTGGGTGGCTTGGAGAAATCGTTGTAAG
GGCACTGATGTACAAGCTTGGATTAGAGGTTGTAGACTTTAGGCGGCCGCGAATTAATTCGCCT
AGACATGACTGTTCCCTCAGTTCAAGTTGGGCACTTACGAGAAGACCGGTCTTGCTAGATTCTAAT
CAGGAGGATGTCAGAATGCCATTTGCAANNNN

pPic9Lyswt

TANANNAANAGGGTATCTCTCGNNAAGNAANGCCTGAAGCTAAAGTTTTCGGTAGGTGCGAATT
AGCCGCCGCAATGAAGCGCCACGGATTGGATAACTATCGTGGATACTCCCTAGGTAAGTGGGTT
TGCGTTGCTAAATTTGAGTCGAACTTTAATACTCAAGCAACCAATCGAAACACCGACGGGAGCAC
CGACTATGGTATATTGCAGATCAATTCTCGATGGTGGTGAACGATGGCAGAACTCCTGGATCAA
GAACTTGTGCAACATTCCCTGTAGTGCTCTGTTATCCTCAGATATCACTGCATCAGTTAATTGTG
CCAAAAGATCGTGTCTGACGGAAATGGAATGTCTGCCTGGGTGGCTTGGAGAAATCGTTGTAAG
GGCACTGATGTACAAGCTTGGATTAGAGGTTGTAGACTTTAGGCGGCCGCGAATTAATTCGCCT
AGACATGACTGTTCCCTCAGTTCAAGTTGGGCACTTACGAGAAGACCGGTCTTGCTAGATTCTAAT
CAAGAGGATGTCAGAATGCCATTTGCANNNNNNNN

pPic9LysE35Q-1

TANAGNAAAAGGGTATNCTCTTCNTANAAAAAAAANCCTGAAGCTAAAGTTTTCGGTAGGTGCG
AATTAGCCGCCGCAATGAAGCGCCACGGATTGGATAACTATCGTGGATACTCCCTAGGTAAGTGG
GTTTGCCTTGTAAATTTGAGTCGAACTTTAATACTCAAGCAACCAATCGAAACACCGACGGGAG
CACCGACTATGGTATATTGCAGATCAATTCTCGATGGTGGTGAACGATGGCAGAACTCCTGGAT
CAAGAACTTGTGCAACATTCCCTGTAGTGCTCTGTTATCCTCAGATATCACTGCATCAGTTAATT
GTGCCAAAAGATCGTGTCTGACGGAAATGGAATGTCTGCCTGGGTGGCTTGGAGAAATCGTTG
TAAGGGCACTGATGTACAAGCTTGGATTAGAGGTTGTAGACTTTAGGCGGCCGCGAATTAATTCG
CCTTAGACATGACTGTTCCCTCAGTTCAAGTTGGGCACTTACGAGAAGACCGGTCTTGCTAGATT
TAATCAAGAGGATGTCANAATGCCATTTGCAANNNNNNC

pPic9LysE35Q-2

GCCNGNCCCAAAAAGNNACAGGGTATNCTCTTCTNNAAGAAANCCTGAAGCTAAAGCTTTTCGG
TAGGTGCGAATTAGCCGCCGCAATGAAGCGCCACGGATTGGATAACTACTCGTGGATACTCCCT
AGGTAAGTGGGTTTTCGTTGCTAAATTTTCAGTCGAACTTTAATACTCAAGCAACCAATCGAAACAC
CGACGGGAGCACCGACTATGGTATATTGCAGATCAATTCTCGATGGTGGTGAACGATGGCAGA
ACTCCTGGATCAAGAACTTGTGCAACATTCCCTGTAGTGCTCTGTTATCCTCAGATATCACTGCA
TCAGTTAATTGTGCCAAAAAGATCGTGTCTGACGGAAATGGAATGTCTGCCTGGGTGGCTTGGAG
AAATCGTTGTAAGGGCACTGATGTACAAGCTTGGATTANAGGTTGTAGACTTTAGCGGCCGCGA
ATTANTTCGCCTTAGACATGACTGTTCCCTANGTTCAAGNTGGGCACTTTACNGACAAGACCGNTC
NTGCTAGATTCTAATCCAGAGGATGTCACAANNGCCCTTTGCATCTCANANCCACCNCCTCNNT
NCNCCNCCCGACTCNANNANNNCNNTCCNCNCGCCNCCCATGCNCCAACCNNCTNANCN
CCTNNCCCCANCNNCCNCTNTCCNACCGTCCCCCTANCCNAACCACCACCNATCNCNCNA
CCCTCCCCCACACTCCACCCNCCNGANCGNCNCCCTTACCAACCACAACGCCACCCACCTNN
CCNCCCNACCCCCCNNTNCTCGCNCGTNCNCACCCACANNAANCGACTNACCTCNCN
NTNACACNAACNCNAAANANCACNCACNCCCCCNACCNTNACCCTCCCTCNCCTCNTAN
CCNCCCGTGCCTNNANCANNCGCCANANACCACCGCCNCGG

pPicLysE35Q-3

TAANNAAGGGTATCTTCTCTANAAAAAANCCTGAAGCTAAAGTTTTTCGGTAGGTGCGAATTAG
CCGCCGCAATGAAGCGCCACGGATTGGATAACTATCGTGGATACTCCCTAGGTAAGTGGGTTTTC
CGTTGCTAAATCTTCAGTCGAACTTTAATACTCAAACAACCAATCGAAACACCGACGGGAGCACC
GACTATGGTATATTGCAGATCAATTCTCGATGGTGGTGAACGATGGCAGAACTCCTGGATCAAG
AACTTGTGCAACATTCCCTGTAGTGCTCTGTTATCCTCAGATATCACTGCATCAGTTAATTGTGC
CAAAAAGATCGTGTCTGACGGAAATGGAATGTCTGCCTGGGTGGCTTGGAGAAATCGTTGTAAG
GGCACCTGATGTACAAGCTTGGATTAGAGGTTGTAGACTTTAGGCCGGCCGCGAATTAATTGCGC
CTTAGACATGACTGTTCCCTCAGNTCANGTTGGGCACTTACGAGAAGACCGGTCNTGCTAGANTCT
AATCNAGAGGATGTCAGAATGCCNTTTCANNNNNNCCNCCN

pPic9LysE35Q -4

NAAANAGCAANAGGGTATTCTCTCGTNGAAANNAACGCCTGAAGCTAAAGTTTTTCGGTAGGTGC
GAATTAGCCGCCGCAATGAAGCGCCACGGATTGGATAACTACTCGTGGATACTCCCTAGGTAAGT
GGTCTGCGTTGCCTAAATTTTCAGTCGAACTTTAATACTCAAGCAACCAATCGAAACACCGACG
GGAGCACCGACTATGGTATATTGCAGATCAATTCTCGATGGTGGTGAACGATGGCAGAACTCCT
GGATCAAGAACTTGTGCAACATTCCCTGTAGTGCTCTGTTATCCTCAGATATCACTGCATCAGTT
AATTGTGCCAAAAAGATCGTGTCTGACGGAAATGGAATGTCTGCCTGGGTGGCTTGGAGAAATCG
TTGTAAGGGCACTGATGTACAAGCTTGGATTAGAGGNTGTAGACTTTAGGCCGGCCGCGAATTA
NTCGCCTTATACATGACNTGTTCCCTTAGTTCAANTTGGGCACTTACGAGAAGACCGNTCCTTGCTA
GATTCTAATCAAAGAGGATGTCCAANTGCCCTTTNCAANNCCCTCNNGACACCTCCNCCCAACC
TNTNACGCCTCCCTACANCNCNTCNCC

pPic9LysE35Q-5

TAAAGNAAAGGGTATCTCTCGNNAAGAAAGCTGAAGCTAAAGTTTTCGGTAGGTGCGAATTAGCC
 GCCGCAATGAAGCGCCACGGATTGGATAACTATCGTGGATACTCCCTAGGTAAGTGGGTTTGCG
 TTGCTAAATTTTCAGTCGAACCTTAATACTCAAACAACCAATCGAAACACCGACGGGAGCACC
 GACTATGGTATATTGCAGATCAATTCTCGATGGTGGTGAACGATGGCAGAACTCCTGGATCAAGAAAC
 TTGTGCAACATTCCCTGTAGTGCTCTGTTATCCTCAGATATCACTGCATCAGTTAATTGTGCCAAA
 AAGATCGTGTCTGACGGAAATGGAATGTCTGCCTGGGTGGCTTGGAGAAATCGTTGTAAGGGCA
 CTGATGTACAAGCTTGGATTAGAGTTGTAGACTTTAGGCGGCCGCGAATTAATTCGCCTTAGAC
 ATGACTGTTCTCAGTTCAAGTTGGGCACTTACGAGAAGACCGGTCTTGCTAGATTCTAATCAAG
 AGGATGTCAGAATGCCATTTGCAANNNNNNNN

Enzymatic activity determination with gram negative reference bacteria *P. putida*

Table A1: *P. putida* cells incubated with lysozymes and EDTA concentration at 10 mM.

time point [h]	HEWL	HEWL +EDTA	EDTA	Lyswt +EDTA	LysE35A +EDTA	LysE35Q +EDTA
0	0.75	0.75	0.77	0.65	0.65	0.66
22	0.63	0.06	0.51	0.07	0.51	0.44

Table A2: *P. putida* cells incubated with lysozymes and EDTA concentration at 25 mM.

time point [h]	HEWL	HEWL +EDTA	EDTA	Lyswt +EDTA	LysE35A +EDTA	LysE35Q +EDTA
0	0.75	0.79	0.8	0.73	0.66	0.71
24	0.55	0.04	0.41	0.07	0.42	0.41

Table A3: *P. putida* cells incubated with lysozymes and EDTA concentration at 50 mM.

time point [h]	HEWL	HEWL +EDTA	EDTA	Lyswt +EDTA	LysE35A +EDTA	LysE35Q +EDTA
0	0.82	0.75	0.81	0.69	0.69	0.71
24	0.55	0.05	0.5	0.2	0.49	0.51

Table A4: *P. putida* cells incubated with lysozymes and EDTA concentration at 100 mM.

time point [h]	HEWL	HEWL +EDTA	EDTA	Lyswt +EDTA	LysE35A +EDTA	LysE35Q +EDTA
0	0.41	0.29	0.4	0.48	0.43	0.45
24	0.3	0.07	0.18	0.08	0.23	0.22

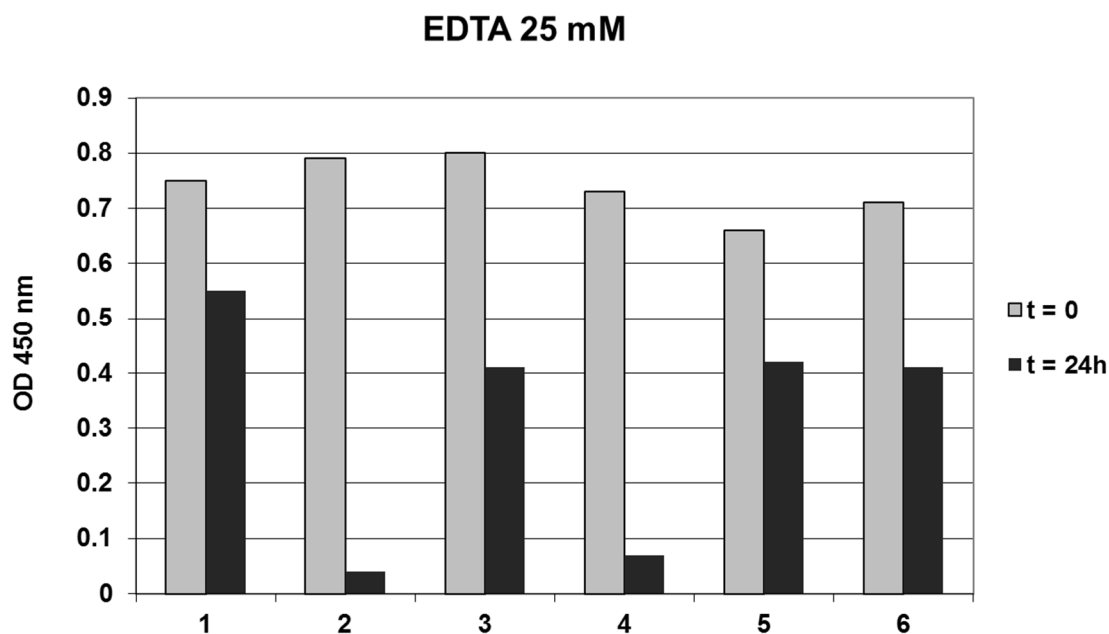


Figure A2: 25 mM EDTA: the adsorption values of *P. putida* cells at 450 nm with lysozyme and 10 mM EDTA at time points 0 and after 22h incubation. The HEWL amount is 5 μ g. 1: HEWL 2: HEWL + EDTA 3: EDTA 4: Lyswt + EDTA 5: LysE35A + EDTA 6: LysE35Q + EDTA

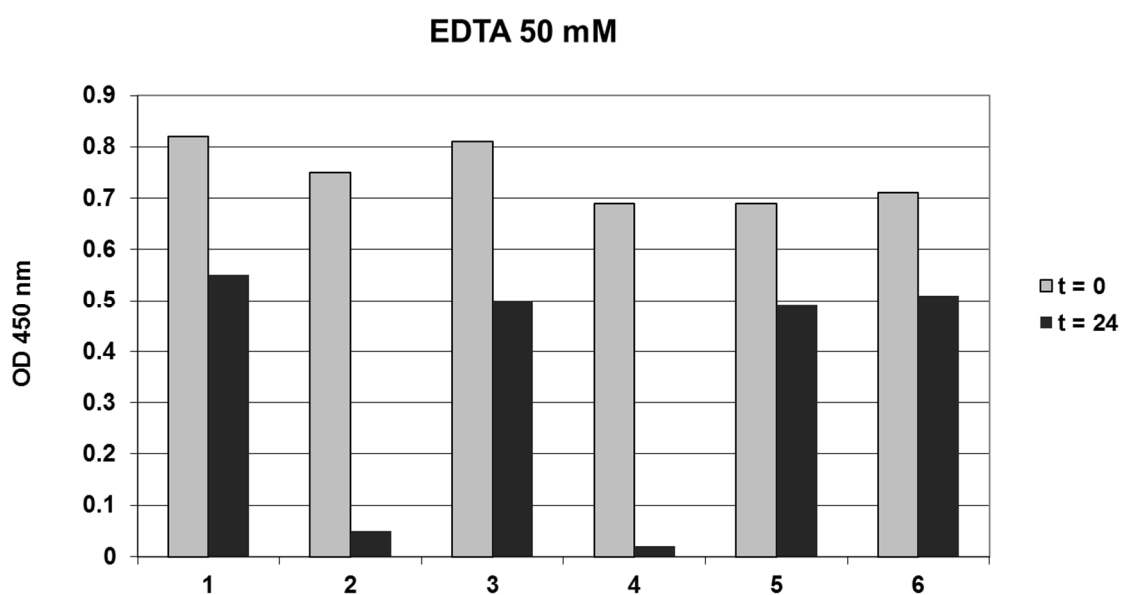


Figure A3: 50 mM EDTA: the adsorption values of *P. putida* cells at 450 nm with lysozyme and 10 mM EDTA at time points 0 and after 22h incubation. The HEWL amount is 5 μ g. 1: HEWL 2: HEWL + EDTA 3: EDTA 4: Lyswt + EDTA 5: LysE35A + EDTA 6: LysE35Q + EDTA

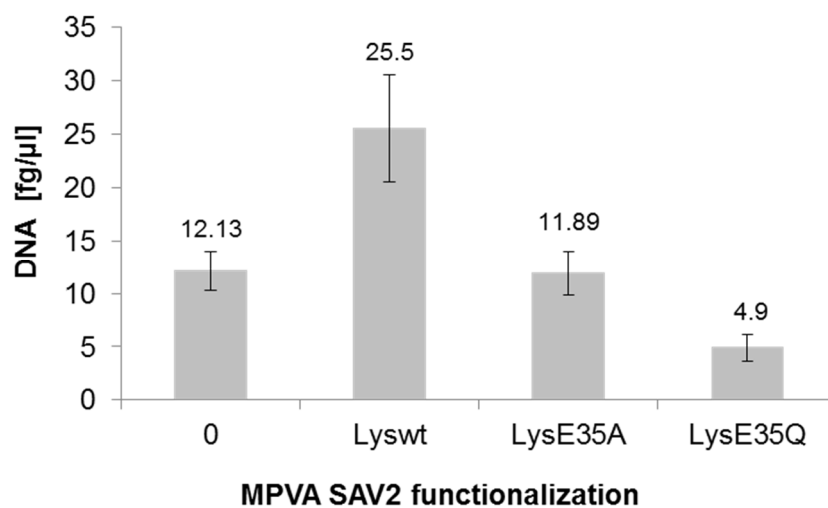


Figure A4: Determined DNA amounts for capture of *E. faecalis* from suspensions with 600 µg M-PVA SAV2 particles

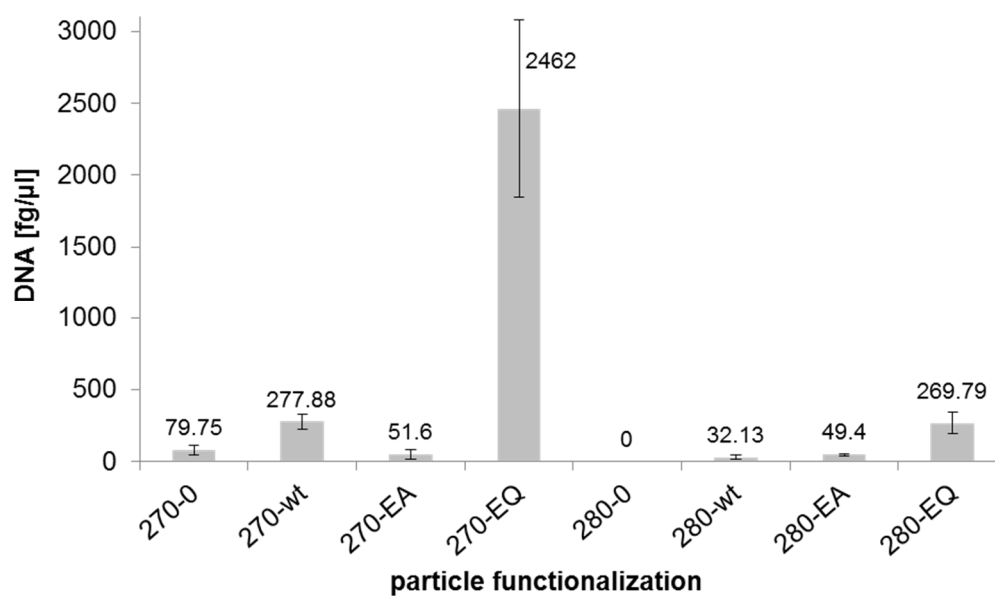


Figure A5: The DNA amounts determined by qPCR in 1 µl of 20-fold concentrated samples after capture of *E. faecalis* from suspension with 150 µg DS M270 and DS M280 beads .

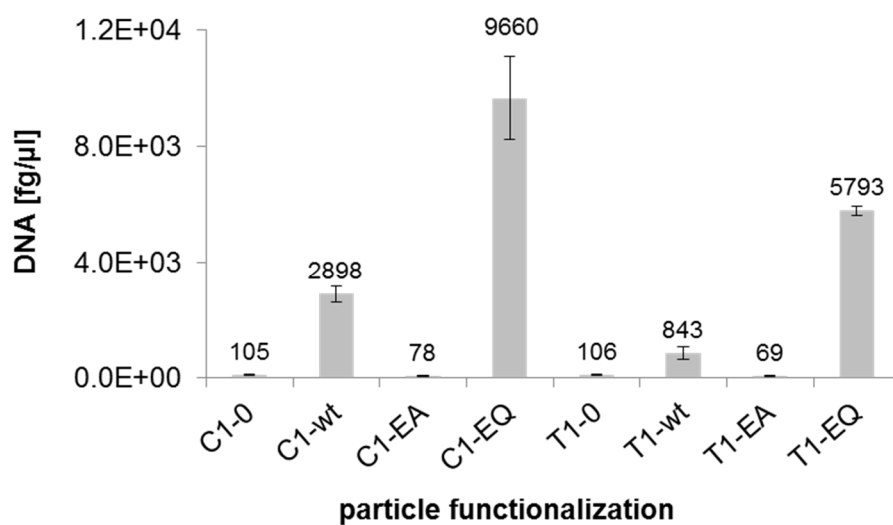


Figure A6: DNA amounts of *E. faecalis* in 1 µl 10-fold concentrated samples after capture of bacteria from suspensions with MyOne™ Streptavidin C1 and MyOne™ Streptavidin T1 beads. Determined by qPCR.

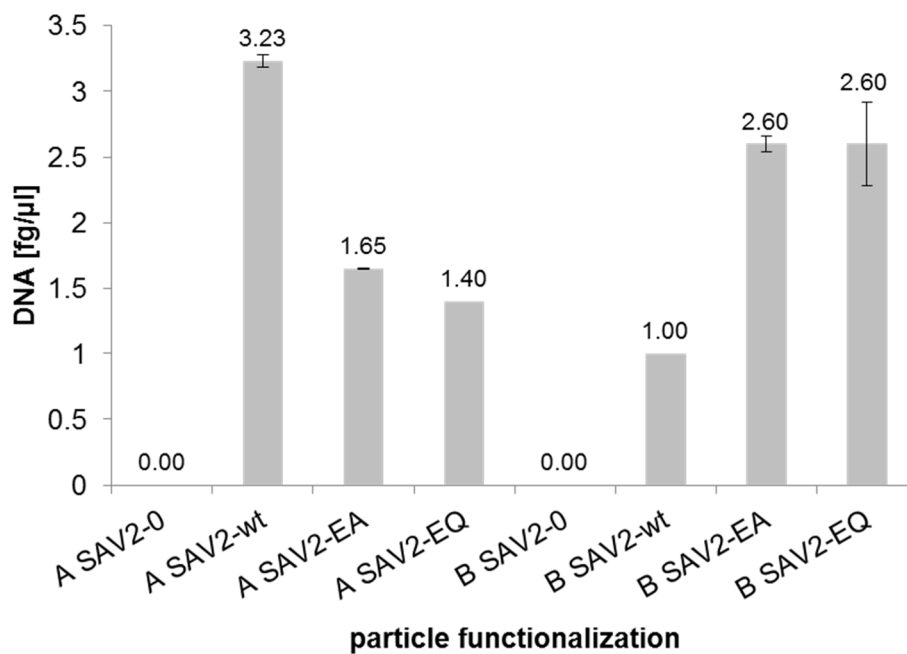


Figure A7: DNA amounts of *E. faecalis* in 1 µl 2.22-fold concentrated samples after capture of bacteria from lettuce with M-PVA SAV2 beads. Determined by qPCR.

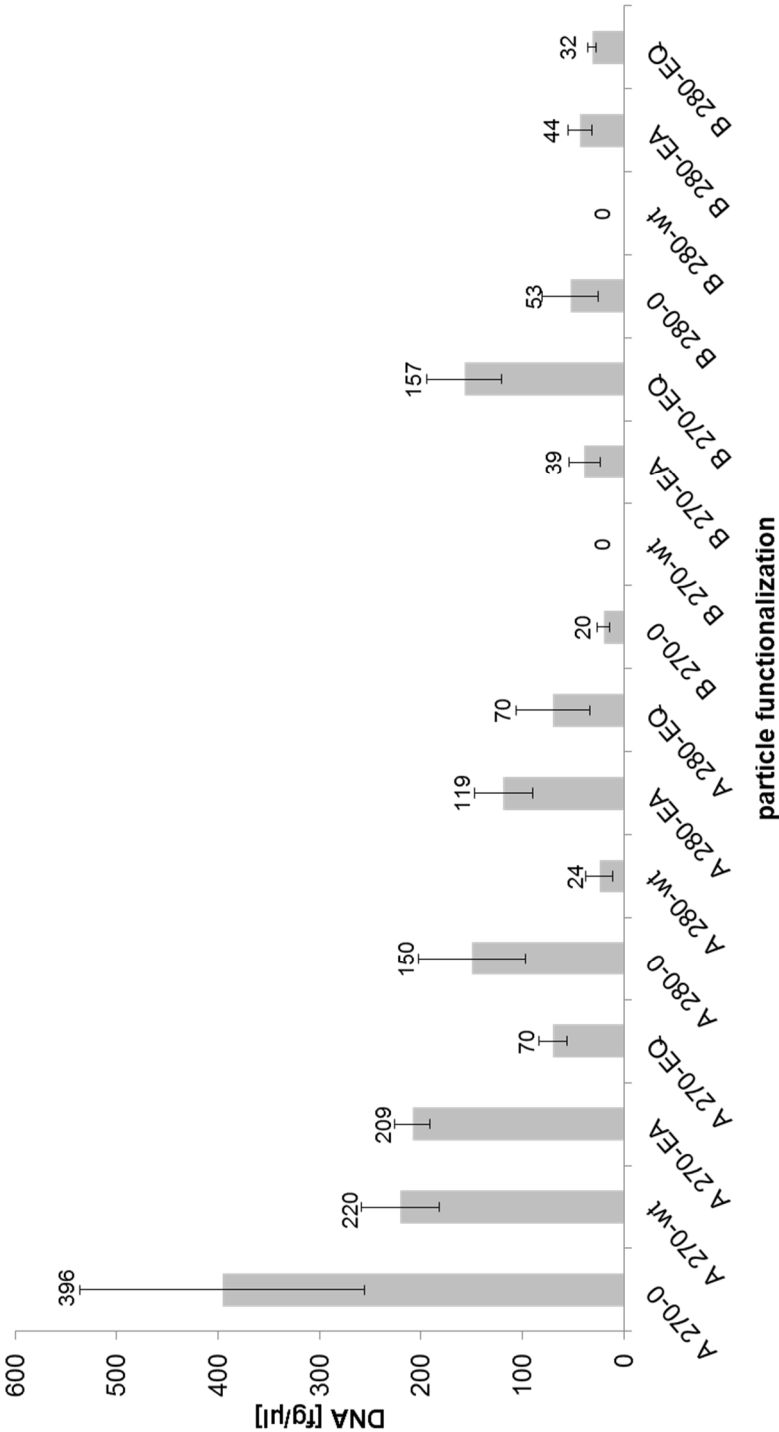


Figure A8: DNA amounts of *E. faecalis* in 1 µl of 50 fold concentrated samples after capture of bacteria from lettuce matrix determined by qPCR.

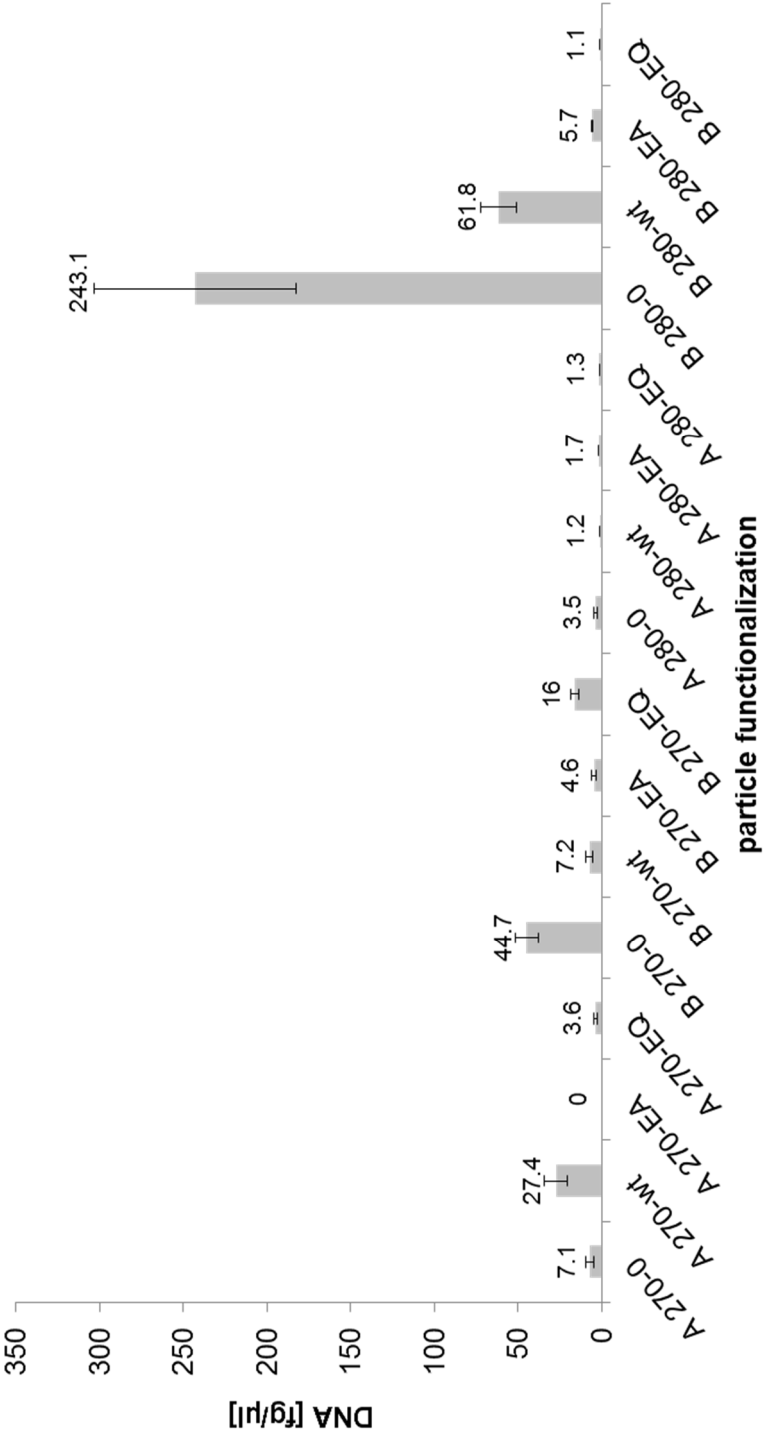


Figure A9: DNA amounts in 1 µl of 5-fold concentrated samples determined by qPCR after capture of bacteria from lettuce.

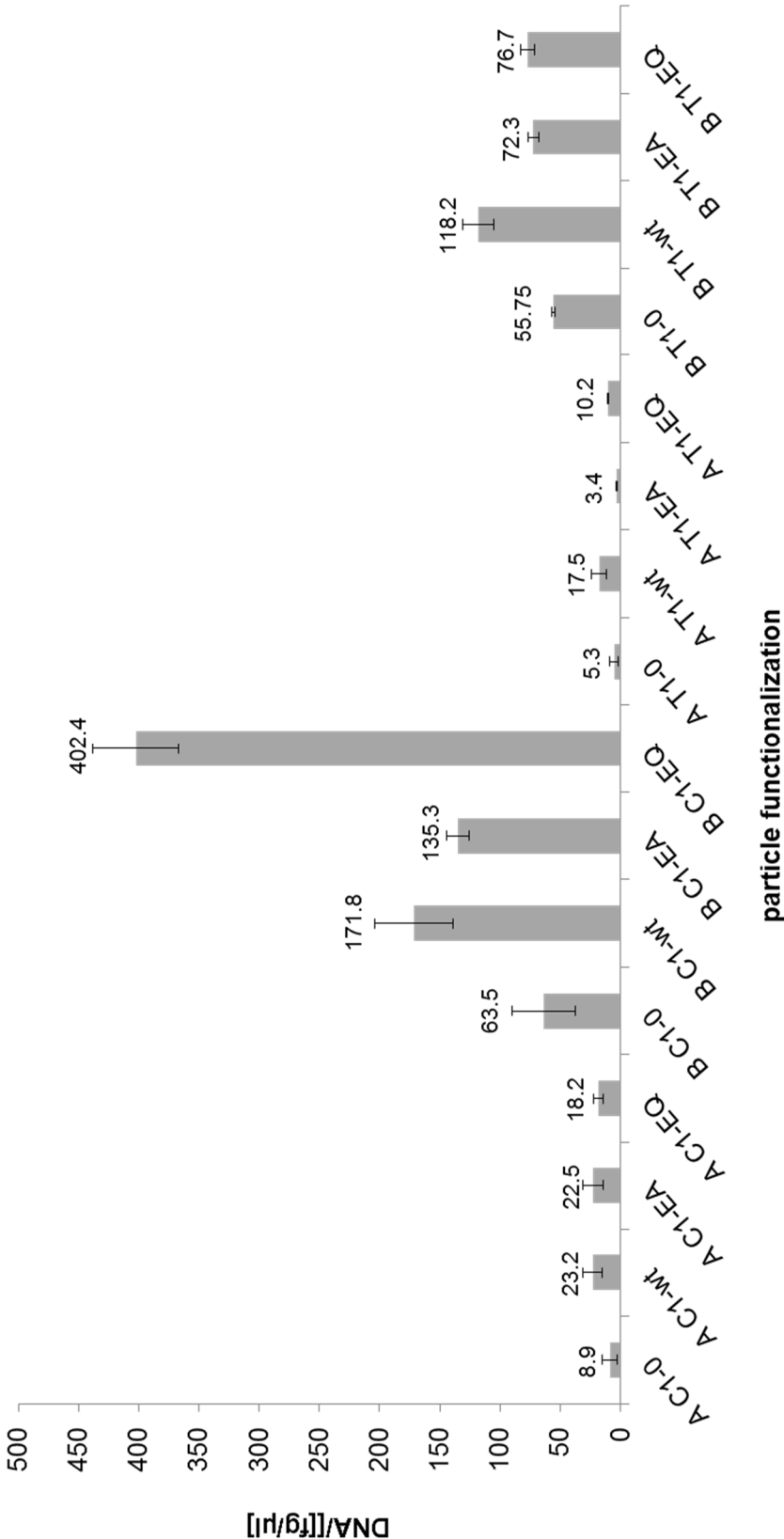


Figure A10: DNA amounts in 1 µl of 5 fold concentrated samples determined by qPCR after capture with lysozyme functionalized DS M280 and DS M270. The spacer length of biotin was 56 Å.

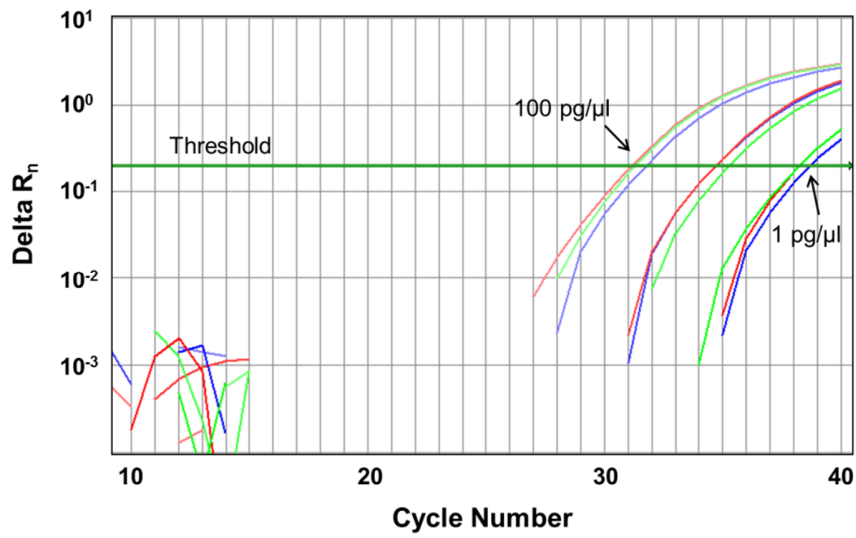


Figure A 11: Amplification plot of 10-fold dilutions of *E. coli* DNA.

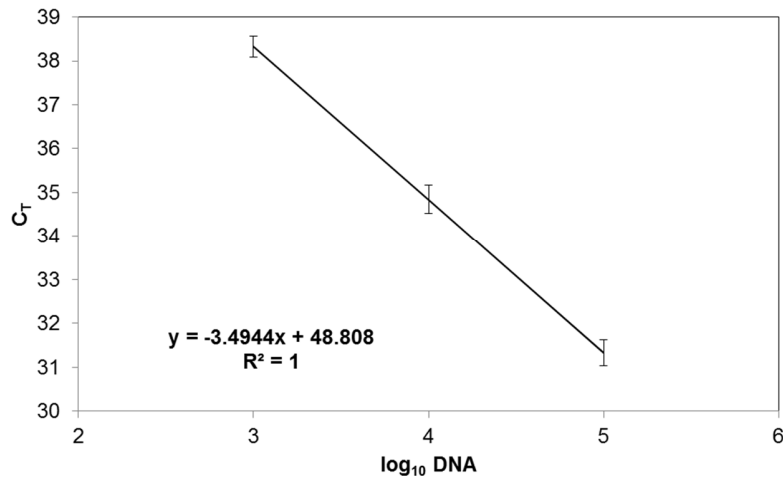


Figure A12: Standard curve for qPCR based DNA quantification *E. coli* samples. The C_T values were the threshold fluorescence is exceeded first is shown as a function of DNA amount.

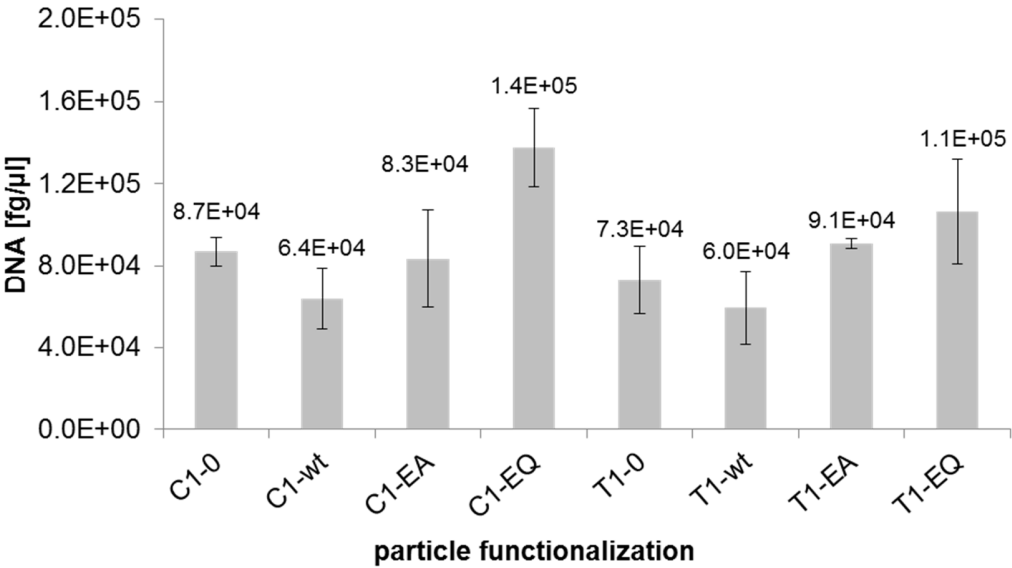


Figure A13: qPCR based DNA quantification of captured *E. coli* cells